The effect of fluconazole on cytochrome P450 1B1, formation of arachidonic acid metabolites, and protection against angiotensin II-induced cardiac hypertrophy

By

Ahmad Hindi M. Alammari

A thesis submitted in partial fulfillment of the requirements for the degree of

Master of Science

In

Pharmaceutical Sciences

Faculty of Pharmacy and Pharmaceutical Sciences

University of Alberta

Abstract

Several studies have elucidated the role of cytochrome P450s (CYPs) and their associated arachidonic acid (AA) metabolites in development of cardiac hypertrophy. CYP1B1 has been reported to have a major role in metabolizing AA into cardiotoxic metabolites, mid-chain hydroxyeicosatetraenoic acid (HETEs). Of particular interest, several studies have demonstrated the role of mid-chain HETEs in the development of cardiac hypertrophy. Recently, fluconazole was shown to inhibit the formation of mid-chain HETEs metabolite. However, whether fluconazole would be able to modulate CYP1B1-mediated AA metabolism in an Ang II-induced cellular hypertrophy model and in rats' heart has never been investigated before. Therefore, the objectives of this study were; 1) to investigate the effect of fluconazole on CYP1B1 mediated AA metabolites and to explore the potential protective effect against Ang II-induced cellular hypertrophy, and 2) to study the effect of fluconazole on CYP1B1 and its associated AA metabolites in vivo in Sprague Dawley rats. Our results demonstrated that fluconazole was able to attenuate Ang-II-induced cellular hypertrophy as evidenced by a significant inhibition of hypertrophic markers, β-myosin heavy chain (MHC)/ α-MHC, BNP as well as cell surface area. The protective effect of fluconazole was associated with a significant decrease in the level of CYP1B1 gene, protein, activity levels and its associated mid-chain HETEs metabolite induced by Ang II. Furthermore, treatment of rats with fluconazole significantly decreased the expression of CYP1B1 enzyme and the formation level of cardiotoxic mid-chain HETEs metabolites in the heart. In conclusion, our results showed that fluconazole protects against Ang II-induced cellular hypertrophy by inhibiting CYP1B1 and its associated mid-chain HETEs metabolites. Our study provides the first evidence that fluconazole may be repurposed as a mid-chain HETEs formation inhibitor for the treatment of cardiac hypertrophy and heart failure.

This work is dedicated to

My father (may he rest in peace), my mother and my love Rand Alobeikan

Acknowledgements

My deepest gratitude goes first to my supervisor, Dr. Ayman El-Kadi for his unconditional trust, consistent support, guidance and mentorship.

I would like to thank my previous lab member Dr. Zaid Alma'ayah for his valuable help and advice throughout my study. My special appreciation is extended to my colleague, Sherif Shoieb for his continuous help and useful discussions.

I would like to thank Qassim University in Saudi Arabia for offering me the scholarship to complete my MSc degree at University of Alberta.

I would like to thank the Canadian Institutes of Health Research (CIHR) for funding this research project.

My appreciation is extended to the Saudi Arabian Cultural Bureau in Canada and my academic advisor at the Bureau, Nancy Jadd.

Lastly, I would like to thank the faculty administrative and support staff for their kind help throughout my study.

Table of contents

List of tables

List of Figures

List of abbreviations

AA	Arachidonic acid
AhR	Aryl hydrocarbon receptor
ANOVA	Analysis of Variance
ANP	Atrial Natriuretic Peptide
Ang II	Angiotensin II
AT1	Angiotensin II receptor type 1
AT2	Angiotensin II receptor type 2
ATP	Adenosine-5'-triphosphate
BNP	B-type natriuretic peptide
BaP	Benzo(a)pyrene
c-AMP	Cyclic adenosine monophosphate
CEE	6-chloroethyl ether
CVD	Cardiovascular Disease
DEPC	Diethylpyrocarbonate
DHE	Dihydroethidium
DMSO	Dimethyl Sulfoxide
DMEM	Dulbecco's modified Eagle's medium
DHET	Dihydroxyeicosatrienoic acid
EET	Epoxyeicosatrienoic acid
ERK	Extracellular-signal regulated kinase
EROD	7-Ethoxyresorufin O-deethylation
Gapdh	Glyceraldehyde-3-phosphate dehydrogenase

HETE	Hydroxyeicosatetraenoic acid
HF	Heart Failure
h	Hours
i.p.	Intraperitoneal
JNK	c-Jun NH2-terminal kinase
LC-ESI-MS	Liquid Chromatography-Electrospray Ionization-Mass Spectromerty
LOX	Lipoxygenase
MAPK	Mitogen-activated protein kinases
MTT	3-(4,5-Dimethylthiazol-2-yl)-2,5-diphenyltetrazolium bromide
NADPH	Nicotinamide adenine dinucleotide phosphate tetrasodium
NFAT	Nuclear factor of activated T cells
NF-κB	Nuclear factor-κB
PAGE	Polyacrylamide gel electrophoresis
PCR	Polymerase Chain Reaction
PG	Prostaglandin
ROS	Reactive oxygen species
SD	Sprague Dawley
SDS	Sodium dodecyl sulfate
sEH	Soluble epoxide hydrolase
TEMED	N,N,N',N'-Tetramethylethylenediamine
VSMC	Vascular Smooth Muscle Cell
α-MHC	α-Myosin heavy chain
β-MHC	β-Myosin heavy chain

Chapter 1: Introduction

1.1 Cardiac hypertrophy and heart failure

Cardiac hypertrophy is considered an independent risk factor for heart failure and it is known to be the most indicative predictor of adverse cardiovascular events (Gradman and Alfayoumi, 2006). It is attributed to more than half a million deaths per year in the United States, and thus poses a major health and economic concern worldwide (Benjamin et al., 2017). It is been reported that number of heart failure patients in the USA is 6.5 million (Benjamin et al., 2017). Recently it was (Public Health Agency of Canada, 2018) reported that 669.600 (3.6%) Canadian adults live with diagnosed heart failure and about 92,900 Canadian adults received a new diagnosis of heart failure every year. Heart failure patients have high rate of hospitalization which mounts to cost more than 500 million dollars annually for inpatient care alone (Tran et al., 2016). Moreover, heart failure patients have a poor prognosis with an average annual mortality rate around 33% (Roger, 2013).

In addition of being a major risk factor of heart failure, cardiac hypertrophy is associated with other cardiovascular diseases (CVDs), such as hypertension and ischemic heart diseases (Ho et al., 1998). The hallmarks of cardiac hypertrophy are an increase in cardiomyocyte size, increased protein synthesis, as well as altered sarcomeric organization (Rohini et al., 2010a). It is defined as a thickening of the ventricular wall and/or septum, leading to alterations in chamber size and geometry, and eventually cardiac remodeling (Braunwald and Bristow, 2000). Cardiac hypertrophy can be considered as a compensatory mechanism in an effort to balances the biochemical stress and optimizes cardiac output; however, prolonged hypertrophy is a major health risk that will lead eventually to sudden death (Carreño et al., 2006).

1.1.1 Pathophysiology of cardiac hypertrophy

Cardiac hypertrophy can be classified as physiological or pathological. Physiological hypertrophy occurs during normal postnatal growth, pregnancy, or chronic exercise (Bernardo et al., 2010). Normal or improved cardiac function, no changes in cardiac gene-expression pattern, and proportional enlargement of cardiac chambers are considered the main manifestations (Fagard, 1997). However, the changes of cardiac energy metabolism in physiological hypertrophy include enhanced fatty acid oxidation (FAO), as well as enhanced glucose utilization (Dyck and Lopaschuk, 2006; Bernardo et al., 2010).

On the other hand, pathological hypertrophy occurs in response to chronic pressure or volume overload in a disease condition, such as hypertension or valvular heart disease (Bernardo et al., 2010). Cardiac dysfunction, fibrosis, cardiomyocyte apoptosis or necrosis and changes in chamber size and geometry are the main manifestations (Weber and Brilla, 1993). At the molecular level, pathological hypertrophy is characterized by reactivation of cardiac fetal gene-expression pattern which include upregulation of atrial natriuretic peptide, B-type natriuretic peptide, b-myosin heavy chain, and a-skeletal actin (Nadal-Ginard et al., 2003). However, the changes of cardiac energy metabolism in pathological hypertrophy include decreased FAO and increased glucose utilization (Dyck and Lopaschuk, 2006; Bernardo et al., 2010).

Cardiac hypertrophy can also be classified morphologically to concentric and eccentric hypertrophy (Bernardo et al., 2010). An increase in the wall thickness and cardiac mass with a small reduction in chamber volume are considered the main manifestations of concentric hypertrophy (Bernardo et al., 2010). Microscopically, it is characterized by the parallel additions of sarcomeres, leading to an increase in cardiomyocyte width more than its length (Gerdes, 2002).

It is usually occurring in response to chronic pressure overload, which may be pathological (e.g., hypertension) or physiological (e.g., strength training) (Bernardo et al., 2010; Rohini et al., 2010b).

On the other hand, eccentric hypertrophy is characterized by an increase in the cardiac mass with an increase in the chamber volume, leading to cardiac dilatation (Bernardo et al., 2010). Microscopically, sarcomeres are added in series, leading to an increase in cardiomyocyte length more than width (Gerdes, 2002). It is usually occurring in response to chronic volume overload, which may be pathological (e.g., valvular heart disease) or physiological (e.g., endurance training) (Bernardo et al., 2010; Rohini et al., 2010b).

1.1.2 Angiotensin II induced cardiac hypertrophy

Angiotensin II (Ang II) is an octapeptide hormone with a well-known sympathetic activity that plays a fundamental role in cardiovascular homeostasis. Ang II is reported to play a major role in elevation of blood pressure through its direct effect which includes vasoconstriction, sympathetic nervous stimulation and a rise in aldosterone biosynthesis (Fyhrquist et al., 1995). Both circulating Ang II and aldosterone are contributors in the fibrosis and resultant changes in tissue structure (Weber and Brilla, 1991). Furthermore, it is been confirmed that despite its vasopressor effect, the vascular hypertrophy induced by Ang II is independent of the pressure induced (Griffin et al., 1991). Mechanistically, (Crowley et al., 2004) established that the increase in blood pressure by Ang II is mediated by Angiotensin II receptor type 1 (AT1) receptors. Importantly, the development of left ventricular hypertrophy and cardiac fibrosis were linked to AT2 receptors. (Ichihara et al., 2001) reported that chronic loss of AT2 by gene targeting diminished left ventricular hypertrophy and cardiac fibrosis in mice with Ang II-induced hypertension. Recently, we reported that Ang II-induced cellular hypertrophy was mediated through the involvement of

reactive oxygen species (ROS), mitogen-activated protein kinase (MAPK) and nuclear factor κB (NF-kB) signaling pathways (Elkhatali et al., 2017).

1.1.3 Signaling pathway involved in cardiac hypertrophy

1.1.3.1 Oxidative stress

Oxidative stress could be broadly defined as an imbalance between oxidant production and the antioxidant capacity of the cell to prevent oxidative injury (Thannickal and Fanburg, 2000). In general, toxic metabolites called reactive oxygen species (ROS) are the end product of the consumption of oxygen (Thannickal and Fanburg, 2000). These ROS are kept in balance within a very low level by different naturally occurring antioxidants. When there is an imbalance, ROS demonstrate a toxic effect named oxidative stress (Thannickal and Fanburg, 2000). Cardiomyocytes are more susceptible to ROS-dependent toxicity because they have low expression levels of the antioxidant enzymes. Furthermore, mitochondria, a source of as well as a target for ROS, comprise about 50% of the cardiomyocyte mass (Lemieux and Hoppel, 2009).

Superoxide anion was implicated in the hypertrophy process through the increase of proto-oncogene factors, such as c-my and c-fos, mediating the linkage of Na+/K+ ATPase to hypertrophy and modulating the activity of MAPK (Wassmann et al., 2001). When these superoxides were treated with antioxidants the hypertrophic response of cardiomyocytes was inhibited (Nakamura et al., 1998) Moreover, overexpression of superoxide dismutase or NADPH oxidase knockdown blunted hypertrophic responses to Ang-II (Welch, 2008). We recently reported that cellular cardiac hypertrophy induced by Ang II was associated with an elevated level of ROS (Elkhatali et al., 2017). The above information suggests that superoxide has a role in the development cardiac hypertrophy.

1.1.3.2 Mitogen Activated Protein Kinases (MAPK)

At the intracellular level, MAPKs are considered as signaling cascades that activate and control different intracellular functions, such as cell proliferation and cell death (Alsaad et al., 2013). Activation of tyrosine kinase receptor usually leads to the activation of Ras (master regulator that activates MAPKs) and Raf (MAPK kinase kinase) (Muslin, 2005). Accordingly, MKK1/2 are activated, which, in turn, activate extracellular signal-related kinase (ERK)1/2. Activated ERK1/2 plays pivotal roles in the regulation of cellular functions of cardiomyocytes and eventually produce cardiac hypertrophy, where they can alter transcriptional activity and can work as amplifiers for signals coming from other receptors (Alsaad et al., 2013). For instance, MAPK/ ERK kinase (MEK)1-ERK1/2 was reported to induce cardiac hypertrophy by promoting the transcriptional activity of the NFAT-signaling cascade (Sanna et al., 2005). On the other hand, other MAPKs, such as p38 and Jun N-terminal kinase (JNK), function as regulators of genes mediating cell proliferation and differentiation (Alsaad et al., 2013). As an independent activation pathway, other stimuli, such as ROS, are shown to be involved in the activation of p38 and JNK (Urano et al., 2000). There are four members of MAPKs that are involved in the development of cardiac hypertrophy, these are ERK1/2, JNK, p38, and ERK5 (Rose et al., 2010).

Simultaneous activation of JNK, ERK, and p38 results in pathological cardiac hypertrophy (Heineke and Molkentin, 2006). Both p38-a and JNK1/2 are involved in pathological cardiac remodeling, where their inhibition was effective to reduce pathological cardiac remodeling and left ventricle dysfunction (See et al., 2004). ERK5 has been shown to be involved in the development of cardiac hypertrophy. Within cardiomyocytes, different stimulus, such as Ang II, is also reported to activate the ERK5-signaling cascade (Ikeda et al., 2005). It has also been shown

that ERK5 is activated in Ang II-induced hypertrophy of human aortic SMCs through the activation of MEF-2C (Zhao et al., 2009).

1.1.3.3 Nuclear factor-kappaB (NF-κB)

NF-kB is a transcription factor having a pivotal role in the regulation of healthy cardiac functions and has been linked to the development of several cardiac diseases (Alsaad et al., 2013). In almost all cells, NF-kB exists in the cytoplasm in the inactive trimeric form. Upon activation, dimeric NF-kB is released by proteases and translocated to the nucleolus to activate the transcription of several genes (Wong and Tergaonkar, 2009). Over the years, the role of NF-kB signaling cascade in the development of cardiac hypertrophy has been discussed extensively. It has been previously reported that NF-kB activation is sufficient to cause hypertrophy in rat neonatal ventricular cardiomyocytes (Purcell et al., 2001; Maayah and El-Kadi, 2016a). Activation of NF-kB was essential to induce the expression of hypertrophic markers, such as atrial natriuretic factor, and to increase the size of cardiomyocytes (Alsaad et al., 2013). In addition, many studies showed that NF-kB is able to control proinflammatory cytokines and induce the expression of immune proteins, such as tumor necrosis factor alpha (TNF-a, which has a depressant effect on the heart leading to heart failure (Gutiérrez et al., 2008). In addition, activation of NF-kB may be attributed to the generation of reactive oxygen species (ROS) and oxidative stress, where NF-kB is known to be a redox-sensitive transcription factor (Kabe et al., 2005).

1.1.3.4 Calcineurin-NFAT signaling

Nuclear factor of activated T cells (NFAT) is a family of transcription factors that have essential roles in the development of the cardiac system (Alsaad et al., 2013). It is considered as a calcium Ca^{+2} -dependent transcription factor, which has a role in nonimmune cells, such as cardiomyocytes (Hill-Eubanks et al., 2003). Calcineurin, a calmodulin-dependent Ca2+-activated phosphatase, is

an effector downstream of Gq-protein coupled receptors and PKC activation that dephosphorylates the NFAT transcription factor. Upon activation by several mechanical and neurohormonal factors, NFAT translocates to the nucleus where it activates GATA-4 transcription factor leading to cardiac hypertrophy and heart failure (Molkentin et al., 1998).Therefore, calcineurin is directly involved in the activation of NFAT and its translocation to the nucleus (Alsaad et al., 2013). Of importance, recent studies have shown that the hypertrophic response of cardiomyocytes is linked to alteration in Ca^{+2} regulation, which, in turn, activates calmodulin-activated calcineurin. Thereafter, calcineurin activates NFAT as a downstream signaling cascade mediating the hypertrophic response through different kinases including glycogen synthase kinase 3b (GSK-3b), c-Jun Nterminal kinase (JNK) and p38 MAP kinases, casein kinase I (CK1), protein kinase A (PKA), and mitogen activated protein kinase kinase kinase 1 (MEKK1) (Wilkins and Molkentin, 2004). Both calcineurin-NFAT and mitogen-activated protein kinase (MAPK)-signaling cascades are shown to be dependent on each other, where they are involved in the hypertrophy response (Molkentin, 2004).

1.2 Cytochrome P450 (CYP)

CYP is a superfamily of heme-thiolate enzymes that are present in almost all biological systems. Their role is significant in the inactivation of a wide array of xenobiotics, in addition to mediating key biological reactions in the cascade of biosynthesis of endogenous compounds (El-Sherbeni and El-Kadi, 2017a). Xenobiotic metabolism is usually divided to phase I and II, where polar function groups are unmasked or introduced in the chemical structure (phase I or activation), followed by the conjugation between this polar group of the xenobiotic and endogenous molecules, notably glucuronic acid, to further improve hydrophilicity (phase II or conjugation) (El-Sherbeni and El-Kadi, 2017a). CYP enzymes dominate the catalysis of phase I metabolism of xenobiotics

(Anzenbacher and Anzenbacherová, 2001). They are all membrane-attached; either attached to the endoplasmic reticulum (microsomal) or attached the mitochondrial inner membrane at the matrix side (mitochondrial). (Aguiar et al., 2005). Structurally, CYP have 45-60 kDa molecular size since they have approximately 500 amino acids in addition to a single heme group coordinated with a cysteine molecule (Poulos, 2005). CYPs are classified, according to the homology in their amino acid sequence, into families and sub-families and comprise of more than 6000 enzymes (Guengerich, 2003). Family members have more than 40% homology in their amino acid sequence whereas enzymes with more than 55% homology in their amino acid sequence are categorized in the same subfamily. Arabic numbers followed by letters are used to designate members of the same family and subfamilies, respectively. An additional Arabic numbers are added to the subfamily to refer to a specific CYP enzyme. CYPs are expressed in the liver as well as extrahepatic tissues such as kidneys, lungs and heart (Zordoky and El-Kadi, 2008a).

1.2.1 Cardiac expression of CYP

CYP isoenzymes have been detected in cardiac tissue in vivo and reported by several studies (Geetha et al., 1991; McCallum et al., 1993; Fulton et al., 1995). Moreover, it is well documented that CYP genes are expressed in cultured cardiomyocytes, cardiac-derived H9c2 cells (Thum and Borlak, 2000; Zordoky and El-Kadi, 2007) and RL-14 cells (Maayah et al., 2015b).

1.2.2 CYP1 family

CYP1A1 and CYP1B1 messenger RNAs (mRNAs) have been detected in rat left-ventricular tissue (Thum and Borlak, 2002). In humans, the expression of CYP1A1 mRNA has been reported in the right ventricle and the left atrium of patients with dilated cardiomyopathy and in the left ventricle of healthy subjects (Thum and Borlak, 2002). In another study, CYP1A1 mRNA was detected in the left-ventricular tissue of explanted human hearts (Michaud et al., 2010). In explanted human

hearts, CYP1B1 has been shown to be the second most abundantly expressed CYP gene (Bièche et al., 2007). Also, it was expressed at a higher basal level than CYP1A1 in human cardiac fibroblasts (Dubey et al., 2005). In another study, it has been shown that concentrated ambient particles induce CYP1B1 mRNA in rat hearts (Ito et al., 2008). Furthermore, benzo(a)pyrene (BaP), a compound found in cigarettes, has been shown to induce both CYP1A1 and CYP1B1 in rat heart (Aboutabl et al., 2009). Interestingly, CYP1B1 has been shown to be constitutively expressed in the hearts of both control and aryl hydrocarbon receptor (AhR)-deficient mice, which suggests parallel pathways that regulate the expression of cardiac CYP1B1 (Shimada et al., 2003). CYP1A1 was detected in the pulmonary aorta (Thum and Borlak, 2002). Also, CYP1A1 was detected in smooth muscle cells of human coronary arteries (Dubey et al., 2004). CYP1B1 is expressed in vascular smooth muscle cells (VSMCs) (Kerzee and Ramos, 2001). In humans, CYP1B1 was detected in veins (Bertrand-Thiebault et al., 2004). In mice, CYP1B1 protein was detected in endothelial cells (ECs) and aortic SMCs (Alsaad et al., 2013).

1.2.3 CYP2 family

In the cardiovascular system, the CYP2 subfamily is widely expressed. However, the main CYP2 isozymes responsible for expoxygenase activity in cardiac tissue are CYP2C, and CYP2J2. These isoforms are constitutively expressed in the healthy human heart, with CYP2J2 being the most highly expressed enzyme (Thum and Borlak, 2002; Bièche et al., 2007). Significant levels of CYP2J2 expression were observed in healthy hearts, with levels 1000 times higher than CYP2C8 and CYP2C9 (Delozier et al., 2007a). However, there are limited data on the cardiac expression of other CYP2 subfamilies. For instance, CYP2B6/7 has been reported in the right ventricle and aorta of patients with dilated cardiomyopathy (Thum and Borlak, 2002). In rats, CYP2C23 and CYP2J3 were identified in ventricular tissues (Imaoka et al., 2005a). In vitro studies have shown

that CYP2J3 were also expressed in H9c2 cells at comparable levels to those expressed in rat heart tissues (Zordoky and El-Kadi, 2007).

1.2.4 CYP3 family

The CYP3 subfamily consists of CYP3A4, CYP3A5, CYP3A7 and CYP3A43. (Martínez-Jiménez et al., 2007) reported that CYP3A4 is the most predominantly expressed and is responsible for 60% of the hepatic CYP-mediated metabolism of drugs in humans. The expression of CYP3A4 in cardiovascular tissue has been detected in the endothelium, endocardium and coronary vessels (Minamiyama et al., 1999). Another report (Thum and Borlak, 2000) have detected CYP3A mRNA and protein in isolated cardiomyocytes.

1.2.5 CYP4 family

CYP4A and CYP4F are the most important members of CYP4 family and they are responsible for the fatty acid omega-hydroxylation (Okita and Okita, 2001). With respect to the expression of CYP4 family in the cardiovascular system, it has been demonstrated that CYP4 is mainly expressed in freshly isolated cardiomyocytes of control animals and adult human cardiomyocytes (Thum and Borlak, 2000; Chaudhary et al., 2009) .Furthermore, CYP4A and CYP4F were found in the failing human heart whereas, CYP4A has been shown to be induced in hypertrophied human hearts (Thum and Borlak, 2000; Elbekai and El-Kadi, 2006).

1.3. CYP-mediated arachidonic acid metabolism

Arachidonic acid (AA) is a polyunsaturated omega 6 fatty acid comprised of a 20-carbon atom chain and four double bonds. AA is bound to plasma membrane and is released by the activity of phospholipases, most prominently cPLA2 (Tacconelli and Patrignani, 2014) which is released by several stimuli including Ang II (Zafari et al., 1999). Once AA is released from the membrane, free AA can then be metabolized into a number of biologically active eicosanoid metabolites

(Choudhary et al., 2004a) through three different pathways (i) cyclooxygenase (COX) pathway that produces prostanoids, (ii) lipoxygenase (LOX) pathway that produces leukotrienes, lipoxins and mid-chain hydroxyeicosatetraenoic acids (HETEs) or (iii) cytochrome P450 (CYP) pathway that mediates the metabolism of AA to epoxyeicosatrienoic acids (EETs) and HETEs (Figure 1).

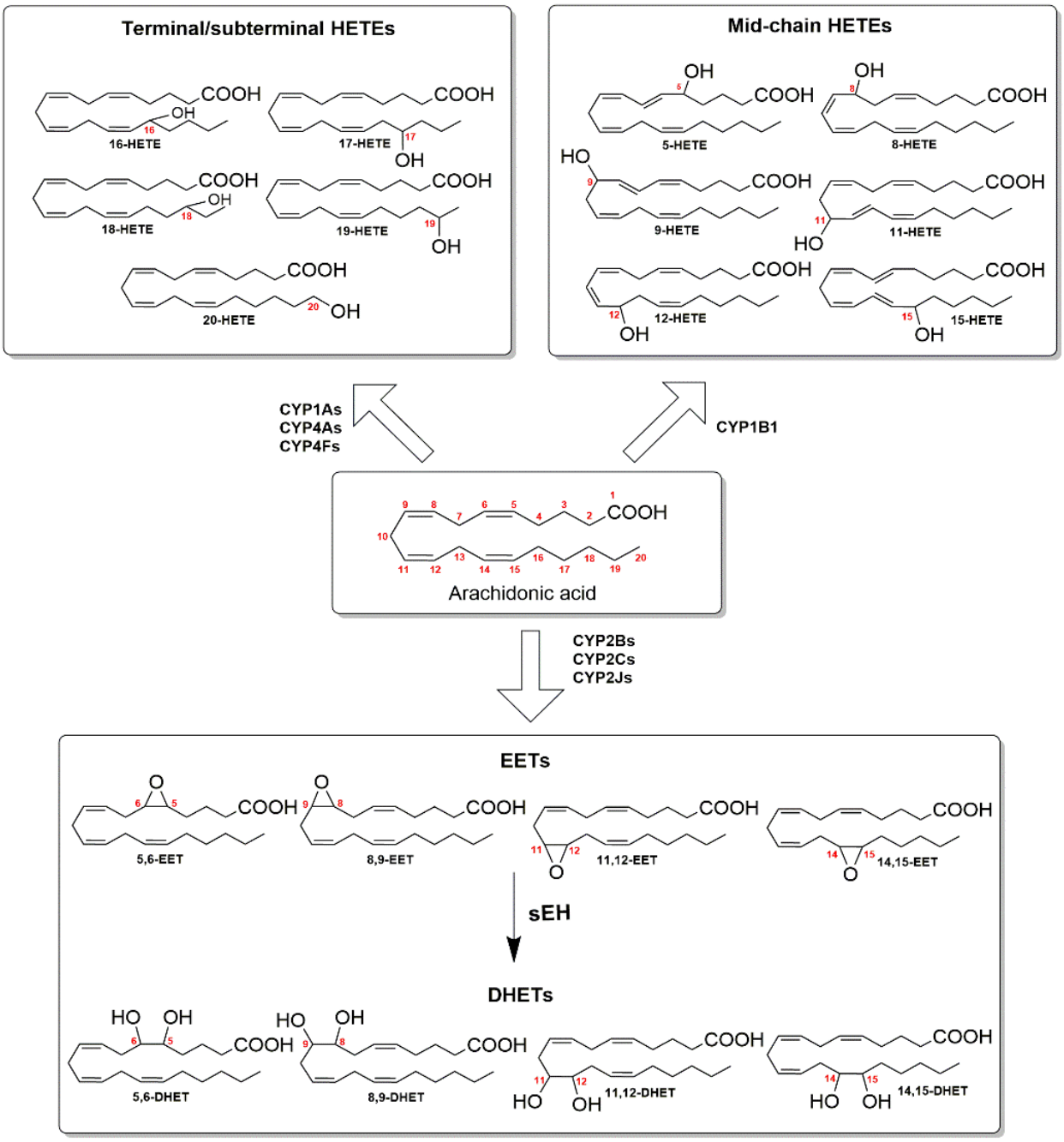

Figure 1. CYP-mediated arachidonic acid metabolism.

Arachidonic acid is released following activation of phospholipase A2 and subsequent metabolism by CYP pathways. These enzymes insert oxygen at different positions in AA to generate a major family of biologically active mediators called eicosanoids.

1.3.1 Mid-chain HETEs

Mid-chain HETEs, namely 5-, 12-, and 15-HETE, are biologically active eicosanoids that result from the metabolism of AA by CYP-catalyzed bis-allylic oxidation reaction. Several lines of evidence support the role of mid-chain HETEs in the development of cardiac hypertrophy, for example, the formation of mid-chain HETEs was shown to increase during pressure overload-induced cardiac hypertrophy (El-Sherbeni and El-Kadi, 2014a). Of particular interest in this model, the generation of mid-chain HETEs was accompanied by the induction of CYP1B1 protein expression levels, implicating CYP1B1 enzyme as a crucial generator of mid-chain HETEs. The role of CYP1B1 in the formation of mid-chain HETEs was further confirmed by the ability of the recombinant CYP1B1 enzyme to catalyze the formation of mid-chain HETEs (Choudhary et al., 2004a; El-Sherbeni and El-Kadi, 2014b). 15-HETE has been shown to increase the sensitivity of the ISO-mediated β-adrenergic response in cardiomyocytes and has been proposed to be implicated in heart failure by induction of cardiac fibrosis (Levick et al., 2007; Zhang et al., 2014). Moreover, it has been shown that norepinephrine induced its hypertrophic effect through the induction of 12- and 15-HETE (Parmentier et al., 2001). 8-, 9-, and 11-HETE are considered non-LOX mid-chain HETE metabolites as they are produced by auto-oxidation reaction in addition to CYP1B1 (Maayah and El-Kadi, 2016c). While 9- and 11-HETE have minimal or no physiological functions (Honn et al., 1992), 8-HETE has been reported to have a proliferator and pro-inflammatory action. This is supported by a previous observation that 8-HETE directly stimulates human neutrophil chemotaxis in vitro (Hunter et al., 1985). 8-HETE is formed as a minor metabolite in human neutrophils and human tracheal epithelial cells (Hunter et al., 1985). In humans, 8-HETE is most probably not the product of 8-LOX since this enzyme has not been detected in human tissues. Instead, 8-HETE may be either formed by non-enzymatic lipid

peroxidation or by CYP1B1-catalyzed AA metabolism (Choudhary et al., 2004a). 5-HETE has been shown to participate in the pathogenesis of Ang-II-induced hypertrophy in which blocking 5-LOX inhibited Ang-II-induced hypertrophy in ApoE-/- mice (Revermann et al., 2011).

1.3.2 Epoxyeicosatrienoic acids (EETs)

EETs were shown to play an important role in modulating different pathophysiological conditions such as inflammation, hypertension, cardiac hypertrophy, ischemic heart diseases and atherosclerosis (Imig, 2012). CYP2Cs are considered the major contributors to EET production (Roman, 2002). Several studies have highlighted the cardioprotective properties of EETs in cardiac hypertrophy and heart failure. For example, EETs treatment was shown to have protective effects against the cellular hypertrophy induced by Ang II and isoproterenol in primary neonatal cardiomyocytes (Xu et al., 2006) and the H9c2 cell line (Tse et al., 2013a), respectively. Recently, CYP2J2 overexpression or EET treatment was shown to protect against cardiac dysfunction, hypertrophy, and fibrosis in response to Ang II treatment (He et al., 2015). Moreover, it has been recently reported that cardiac specific overexpression of CYP2J2 provides cardioprotection against heart failure induced by Ang II and isoproterenol (Wang et al., 2014). Additionally, overexpression of CYP2J2 was shown to protect against electrical remodelling induced in response to pathological hypertrophy (Westphal et al., 2013). EETs were shown to have cytoprotective effects through their anti-apoptotic and antioxidant properties (Imig, 2012). Recently, treatment with EETs was shown to abolish the induced endoplasmic stress and apoptotic response in cardiomyocytes mediated by Ang II (Wang et al., 2014). EETs are known to be metabolized by soluble epoxide hydrolase (sEH) into their corresponding degradation products dihydroxyeicosatrienoic acids (DHETs) which diminishes their cardioprotective effects (Imig, 2012). Importantly, hypertrophied heart induced

by Ang-II and ISO has demonstrated a high mRNA and protein expression level of sEH (Althurwi et al., 2013b; El-Sherbeni and El-Kadi, 2014d).

1.3.3 20- Hydroxyeicosatetraenoic acids (20-HETE)

The formation of CYP-mediated AA metabolite 20-HETE is mainly mediated through the CYP4A and CYP4F subfamilies (Alsaad et al., 2013). 20-HETE is a potent vasoconstrictor mainly synthesized in the vasculature, kidney and lung. 20-HETEs' vasoconstrictive effect is by blocking calcium-activated K^+ channels, consequently leading to the depolarization of the VSMCs, and leading to an increase of intracellular K+ levels with subsequent activation of voltage-gated Ca^{2+} channels. 20-HETE plays a role during ischemic reperfusion injury as the levels of 20-HETE are found to increase and the inhibition of CYP4A and CYP4F causes a reduction in infarct size (Gross et al., 2004). Chronic selective blockade of 20-HETE and soluble epoxide hydrolase production provided protection against the development of hypertension and its associated cardiac hypertrophy in young pre-hypertensive Ren-2 renin transgenic rats (Certíková Chábová et al., 2010). Moreover, the cardiotoxic effect of 20-HETE may be mediated through a direct effect on the cardiac muscle in addition to the blood vessels (Elshenawy et al., 2013a). It is been reported that 20-HETE exerts a direct hypertophic effect on rat cardiomyoblasts, H9c2 cells, and promotes the apoptotic effect of Ang-II in primary cultured neonatal rat ventricular myocytes (Tse et al., 2013a). Moreover, the biosynthesis of 20-HETE was increased in isoproterenol-induced cardiac hypertrophy in rats (Zordoky et al., 2008).

1.4 Fluconazole

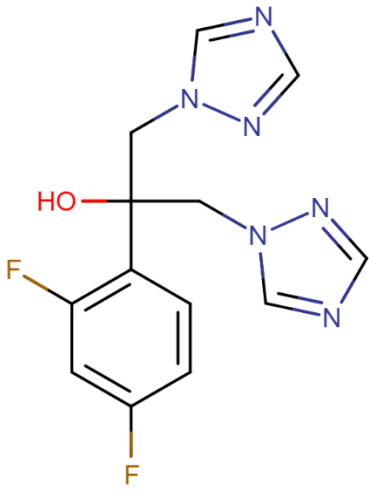

Figure 2. Chemical structure of Fluconazole.

Fluconazole (Figure 2) is a synthetic triazole antifungal agent widely used to treat systemic and superficial fungal infections. The mechanism of action of fluconazole is to interact with 14-α demethylase, a cytochrome P450 enzyme necessary to convert lanosterol to ergosterol. As ergosterol is an essential component of the fungal cell membrane, inhibition of its synthesis results in increased cellular permeability causing leakage of cellular contents. Fluconazole may also inhibit endogenous respiration, interact with membrane phospholipids, inhibit the transformation of yeasts to mycelial forms, inhibit purine uptake, and impair triglyceride and/or phospholipid biosynthesis. Upon absorption fluconazole is distributed in all body tissues and fluids with a half-life of 30 h (range 20-50 h). Fluconazole is poorly metabolized with only 11.4% of the administered dose is not recovered in the urine. Only 3 metabolites have been isolated: a 1,2,4-triazole compound and 2 N-dealkylated products resulting from loss of the triazole. The t_{max} after a single 100 mg oral dose administration is 2.4 to 3.7 h. The mean (± SD) C_{max} calculated is 2.0 ± 0.2 mg/L with reported low binding to plasma protein 11 to 12% (Debruyne, 1997).

Of special interest on the effect of fluconazole on CYPs, it been reported that fluconazole has an inhibitory effect on CYP2Cs. In fact, fluconazole is recommended in regulatory guidance as a prototype inhibitor to assess potential Drug-Drug Interactions by CYP2Cs inhibition (USFDA, 2013). It has been previously reported that fluconazole modulate CYP2B and CYP3A enzymes in rat liver and Cyp2b and Cyp3a families of isoforms in mouse liver (Sun et al., 2006). Recently, data from our lab demonstrated that fluconazole inhibits the formation of mid-chain HETEs metabolites in human microsomes (El-Sherbeni and El-Kadi, 2016a).

1.5. Rationale, Hypotheses, and Objectives

1.5.1 Rationale

The mechanisms involved in the development of cardiac hypertrophy have been the center of recent investigation recently. Of interest, CYPs mediated AA metabolism have been shown to play an important role in the prevention or the development of cardiac hypertrophy through the metabolism of AA into cardioprotective EETs and cardiotoxic HETEs (Zordoky and El-Kadi, 2008a). CYP1B1 has been reported to contribute to the pathogenesis of cardiovascular diseases such as ischemic heart diseases, myocardial infarction, hypertension, atherosclerosis, cardiac hypertrophy, and heart failure (Korashy and El-Kadi, 2006a; Malik et al., 2012a).

The cardiotoxic role of CYP1B1 could be mediated through the metabolism of AA into mid-chain HETEs (Choudhary et al., 2004b). Several studies have established the role of mid-chain HETEs, 5-, 8-, 12-, and 15-HETE, in the development of cardiovascular diseases (Nozawa et al., 1990; Cyrus et al., 1999). 5- and 12-HETEs play a broad spectrum of biological actions with potent effects on recruitment and activation of inflammatory effectors and the induction of cellular hypertrophy (Burhop et al., 1988a; Wen et al., 2003). 15-HETE has been proposed to be implicated in heart failure by induction of cardiac fibrosis (Kayama et al., 2009). Moreover, mid-chain HETEs

has been linked to the development of cardiac cellular hypertrophy (Maayah et al., 2015a) and their toxic role were diminished by modulation of CYP1B1 in rats cardiac hypertrophic model (Maayah et al., 2017). However, targeting mid-chain HETEs by FDA- approved drugs that shows capacity to modulate CYPs and their associated AA metabolites has never been investigated.

Interestingly human recombinant CYP1B1 and CYP2C8 showed the highest midchain HETE-forming activities, as well as human liver and kidney microsomes. Moreover, fluconazole shows an inhibitory effect on mid-chain HETEs levels. However, the effect of fluconazole on CYP1B1 has never been studied before. This raise the question whether fluconazole could inhibit CYP1B1 and their associated mid-chain HETEs metabolites in the heart and confer cardioprotection against Ang II-induced cellular hypertrophy.

1.5.2 Hypotheses

Hypothesis 1: Administration of fluconazole exerts a cardioprotective effect against Ang II-induced cellular hypertrophy in vitro

Hypothesis 2: Fluconazole inhibit CYP1B1 and their associated midchain HETE metabolites in vitro in H9c2 and RL-14 cells

Hypothesis 3: Administration of fluconazole to rats inhibit CYP1B1 and their associated mid-chain HETEs metabolites in the heart.

1.5.3 Objectives

The specific objectives of this study are:

1) To examine the effect of fluconazole against Ang II-induced cellular hypertrophy in H9c2 and RL-14 cells.
2) To determine the effect of fluconazole on CYPs gene and protein expression as well as activity levels in presence and absence of Ang II
3) To investigate the effect of fluconazole on AA metabolites in the presence and absence of hypertrophic agent, Ang II in H9c2 and RL-14 cells.
4) To determine the effect of fluconazole on cardiac CYPs gene and protein expression and activity and thereafter investigate the consequent alteration on AA metabolites in vivo.

Chapter 2: Materials and methods

2.1 Chemicals and materials

Arachidonic acid, angiotensin II, fluconazole, nicotinamide adenine dinucleotide phosphate tetrasodium (NADPH), Dulbecco's modified Eagle's medium/F-12 (DMEM/F-12), and anti-goat IgG secondary antibody were purchased from Sigma-Aldrich Chemical Co (St Louis, MO). 100X Antibiotic–antimycotic (10,000 units/ml of penicillin, 10,000 μg/ml of streptomycin, and 25 μg/ml of amphotericin B, L-glutamine, fetal bovine serum (FBS) and TRIzol reagent were purchased from Invitrogen (Carlsbad, CA). High-capacity cDNA Reverse Transcription Kit, SYBR Green SuperMix were purchased from Applied Biosystems (Foster City, CA). Real-time PCR primers were synthesized by Integrated DNA Technologies Incorporation (San Diego, CA) according to previously published sequences. AA metabolite standards (15-HETE, 12-HETE,11-HETE,9-HETE, 8-HETE, 5-HETE, 5,6-EET, 8,9-EET, 11,12-EET, 14,15-EET, 5,6-DHET, 8,9-DHET, 11,12-DHET, 14,15-DHET, 20-HETE, and 14(15)-DHETE-d11) were obtained from Cayman Chemical (Ann Arbor, MI). Acrylamide, N′N′-bismethylene- acrylamide, β-mercaptoethanol, ammonium persulfate, glycine, bromphenol blue, pure nitrocellulose membrane (0.45 mm) and N,N,N′,N′-tetramethylethylenediamine (TEMED) were purchased from Bio-Rad Laboratories (Hercules, CA). Chemiluminescent Western blotting detection reagents were purchased from GE Healthcare Life Sciences (Piscataway, NJ). Reagents used for liquid chromatographic-electrospray ionization-mass spectrometry (LC-ESI-MS) were at HPLC-grade. Acetonitrile and water (HPLC grade) were purchased from EM Scientific (Gibbstawn, NJ). Rabbit anti-rat CYP1B1 polyclonal (sc-32882) was purchased from Santa Cruz Biotechnology, Inc. (Santa Cruz, CA). Rabbit anti–rat CYP2C23 polyclonal (ab53944) was purchased from Abcam (Cambridge, United Kingdom). All other chemicals were purchased from Fisher Scientific Co (Toronto, ON, Canada).

2.2 Cell culture

Rattus norvegicus cardiomyoblast H9c2 cells (American Type Culture Collection, Manassas, VA) were maintained in DMEM, without phenol red, supplemented with 0.45% glucose, 0.15% sodium bicarbonate, 0.11% sodium pyruvate, 10% fetal bovine serum, 20 (μM L-glutamine, 50 μg/ml gentamicin sulfate, 100 IU/ml penicillin, 10 μg/ml streptomycin, and 25 ng/ml amphotericin B. Cells were grown in 75-cm tissue culture flasks at 37°C in a 5% CO_2 humidified incubator.

Human cardiomyocyte RL-14 cells (American Type Cell Culture Patent Deposit Designation No. PTA-1499, Manassas, VA) were maintained in DMEM/F-12, with phenol red supplemented with 12.5% fetal bovine serum, 20 μM L-glutamine, 100 IU/ml penicillin G and 100 μg/ml streptomycin. Cells were grown in 75 cm2 tissue culture flasks at 37 °C under a 5% CO2 humidified environment. In all experiments, the cells were washed with phosphate-buffered saline (PBS) and then treated for the indicated time intervals in serum-free media with test compounds as indicated.

2.3 Chemical treatments

Both H9c2 and RL-14 cells were seeded in different culturing flasks were use in this study. For the determination of AA metabolites, H9c2 and RL-14 cells were seeded at a petri dish in flat bottom with low evaporation lid petri dish. For RNA assay, cells were grown in 12-well cell culture plates in a DMEM culture media. For protein assay, cells were seeded at a cell density of $1.5*10^6$ cells/well in six-well cell culture plates and plated at a cell density of $7.5*10^4$ cells/well in 96-well cell culture plates for CYP1B1 enzyme activity assay. Upon 70-80% confluence (2-3 days), the cells were treated in serum-free media with fluconazole 50 μM for 24 h in the presence and absence of Ang II 10 μM.

2.4. Measurement of cell viability

The effect of the tested chemical on cell viability was determined by measuring the capacity of reducing enzymes in viable cells to convert 3-[4,5-dimethylthiazol-2-yl]-2,5-diphenyltetrazolium bromide (MTT) to formazan crystals as described previously (Liu et al., 1997). Briefly, the tested chemical was incubated in H9c2 and RL-14 cells for 24 h in a 96-well plate at 37°C under a 5% CO2 humidified incubator. The medium was then removed and replaced with 100 µl of serum-free medium containing 1.2 mM of MTT dissolved in PBS, pH 7.2. The plate was then re-incubated at 37°C under a 5% CO2 humidified incubator for 2 h. The medium was then decanted off by inverting the plate, and 100 µl of isopropyl alcohol was added to each well with shaking for 1 h to dissolve the formazan crystals. The color intensity in each well was measured at wavelength of 550 nm using a Synergy H1 hybrid multi-mode microplate reader (Biotek Instruments Inc., VT, USA).

2.5. Measurement of cell surface area and volume

Relative changes in cell surface area, as an indicator for cellular hypertrophy in response to treatments, were measured using phase contrast imaging, which was taken with a Zeiss Axio Observer Z1 inverted microscope using the 20X objective lens as described previously(Tse et al., 2013b). Briefly, H9c2 and RL-14 cells were treated with test compounds for 24 h; thereafter, phase contrast images were taken with Zeiss Axio Observer Z1 inverted microscope using the 20X objective lens. Surface area was then quantified by imaging to the complete boundary of individual cells with Zeiss AxioVision Software (Carl Zeiss Imaging Solutions). Six different images have been taken and fifty cells were counted for each treatment group.

2.6. Arachidonic Acid incubation in vitro

H9c2 and RL-14 cells were treated with tested compounds, and then the cells were incubated with 50 μM AA for 3 h. AA metabolites were extracted with 1 ml ethyl acetate and dried using speed vacuum (Savant, Farmingdale, NY). Extracted AA metabolites were analyzed using liquid chromatography–electrospray ionization mass spectrometry (LC–ESI–MS) (Micromass ZQ 4000 spectrometer; Waters, Milford, MA) method (Section 2.17).

2.7. Measurement of CYP1B1 enzymatic activity

CYP1B1-dependent 7-ethoxyresorufin O-deethylase (EROD) activity was performed on intact living H9c2 and RL-14 cells (Kennedy et al., 1993; Lo et al., 2013). After incubation of the cells with test compounds, 100 μl of 2 μM 7-ethoxyresorufin in assay buffer (0.05 M Tris, 0.1 M NaCl, pH 7.8), were then added to each well. Immediately, an initial fluorescence measurement (t=0) at excitation/emission (545 /575 nm) followed by an additional set of fluorescence measurements of the samples were recorded every 5 min for a 40 min interval using the Bio-Tek Synergy H1Hybrid Multi-Mode Microplate Readers (Bio-Tek Instruments, Winooski, VT, USA). The amount of resorufin formed in each sample was determined by comparison with the control. In vivo, microsomes from heart of various treatments (1 mg protein/ml) were incubated in the incubation buffer (0.1 M potassium phosphate buffer, pH 7.4) with 100 μM of luciferin 6'-chloroethyl ether (luciferin-CEE) in a shaking water bath at 37 ºC (10 min) and then the reaction started after the addition of 2 mM NADPH. After incubation at 37 ºC (30 min), the luciferin detection reagent was added followed by 10 min incubation at room temperature. Immediately, an initial luminescence measurement (t=0) at integration time (0.25-1 sec) followed by an additional set of measurements of the samples were recorded every 5 min for a 40 min interval using the Bio-Tek Synergy

H1Hybrid Multi-Mode Microplate Readers (Bio-Tek Instruments, Winooski, VT, USA). The amount of light formed in each sample was determined by comparison with the control.

2.8. Determination of CYP1B1-inhibition kinetics by fluconazole

The O-dealkylation rate of 7-ethoxyresorufin by (EROD) recombinant human CYP1B1 was measured in the absence and presence of fluconazole. Briefly, 96-well solid black polystyrene microplates were used to carry out the florescent assay. The reaction mixture containing 100 mM potassium phosphate (pH 7.4) buffer supplemented with 5 mM magnesium chloride hexahydrate and 1 pmol of human CYP1B1, was incubated with 10-100 nM of EROD. In addition, 0, 20, 40, 80, 120 or 240 nM of fluconazole was added to the reaction mixture. The volume of the reaction mixture was 100 µL. The reaction was initiated by the addition of 100 µL of 2 mM NADPH, the fluorescent signal related to the formation of resorufin was measured every one minute (excitation and emission wavelengths of 550 and 585 nm, respectively) for 30 min at 37°C using a BioTek Synergy H1 Hybrid Reader (BioTek Instruments, Inc.). The quantity of formed resorufin was measured by the construction of standard curve of 0-200 nM of resorufin dissolved in the same incubation buffer. The formation rate of resorufin in each well was determined over the first 4-min period using linear regression. The formation rates of resorufin at different EROD concentrations were fitted to Michaelis-Menten equation; while, fluconazole-CYP1B1 inhibition rates were fitted to competitive, noncompetitive, uncompetitive, and mixed models of enzyme inhibition. The most probable enzyme inhibition model was selected according to Akaike information criteria (AIC). The fitting was carried out using GraphPad Prism (version 5.01; GraphPad Software, Inc., La Jolla, CA).

2.9. Animals

The protocol of this study was approved by the University of Alberta Health Sciences Animal Policy and Welfare Committee. Male Sprague-Dawley rats, weighing 200–250 g, were purchased from Charles River Canada (St. Constant, QC, Canada). All animals were housed in cages under controlled environmental condition, a 12-hour light/dark cycle, and had free access to food and water available ad libitum.

2.10. Treatment protocol

To determine the changes in CYP and their associated AA metabolites following fluconazole treatment, the rats were randomly segregated into two groups. The first group (n= 6) consisted of control rats that received saline intraperitoneally (i.p.). The second group (n= 6) consisted of fluconazole-treated rats that received fluconazole (20 mg/kg for 24 h i.p.). Thereafter, animals were euthanized under isoflurane anesthesia after 24 h exactly, and hearts, livers, kidneys, lungs and brains were excised, rinsed, blotted dry and then flash-frozen in liquid nitrogen. The frozen hearts were stored at -80 °C for further analysis.

2.11. RNA extraction and cDNA synthesis

Total RNA from frozen tissues or treated H9c2 and RL-14 cells was isolated using TRIzol reagent (Invitrogen®) according to the manufacturer's instructions. Briefly, approximately 0.6 to 1 ml of TRIzol reagent was added to each twelve-well cell culture plate to lyse cells or 0.2 g tissue. Cell lysates or tissue homogenates were then collected into 1.5 ml tubes and mixed with 0.2 ml of chloroform followed by shaking for 15 seconds and then centrifugation at 12,000 x g for 15 min at 4 °C. The aqueous phase which contains RNA was then transferred to new Eppendorf tube and 0.3 ml isopropyl alcohol was then added to each tube to precipitate the RNA by freezing the samples at – 20 °C for 2 h. Following centrifugation at 12,000 x g for 10 min at 2 °C, the RNA

pellet was washed once with 75% ethanol in diethylpyrocarbonate (DEPC)-treated water and followed by centrifugation at 12,000 x g for 5 min at 4 °C then the supernatant was removed and the pellet was allowed to dry for 10 min. Pellets were then dissolved in DEPC-treated water and incubated at 55 – 60 °C for 10 minute to ensure total re-suspension. Total RNA was quantified by measuring the absorbance at 260 nm and the purity of RNA was determined by measuring 260/280 ratio. Thereafter, first strand cDNA synthesis was performed using the High-Capacity cDNA reverse transcription kit (Applied Biosystems), according to the manufacturer's instructions. Briefly, 1.5 µg of total RNA from each sample was mixed with high capacity cDNA reverse transcription reagents as following: 2.0 µl of 10x reverse transcriptase buffer, 0.8 µl of 25x dNTP mix (100 mM), 2.0 µl of 10x reverse transcriptase random primers, 1.0 µl of MultiScribe reverse transcriptase, and 4.2 µl of nuclease-free water (DEPC-treated water). The total volume in each microcentrifuge tube was 20 µl. The final reaction mix was kept at 25 °C for 10 min, heated to 37 °C for 120 min, heated for 85 °C for 5 s, and finally cooled to 4 °C.

2.12. Quantification by real time-polymerase chain reaction (PCR)

Quantitative analysis of specific mRNA expression was performed by real time-PCR by subjecting the resulting cDNA to PCR amplification using 96-well optical reaction plates in the ABI Prism 7500 System (Applied Biosystems). Each 25 µl reaction mix contained 0.1 µl of 10 µM forward primer and 0.1 µl of 10 µM reverse primer (40 nM final concentration of each primer), 12.5 µl of SYBR Green Universal Mastermix, 11.05 µl of nuclease free water, and 1.25 µl of cDNA sample. Human and rat primer sequences and probes for CYP1A1, 1A2, 1B1, 2C11, 2C23, 2J2, 2J3, 3A4, 4F2, 4F11, α-myocin heavy chain (α-MHC), β-myocin heavy chain (β-MHC), brain natriuretic peptide (BNP), EPHX2 and human β-actin are listed in Table 1. No template controls were incorporated onto the same plate to test for the contamination of any assay reagents. After sealing

the plate with an optical adhesive cover, the thermocycling conditions were initiated at 95°C for 10 min, followed by 40 PCR cycles of denaturation at 95°C for 15 seconds, and annealing/extension at 60°C for 1 min. Melting curve (dissociation stage) was performed by the end to ascertain the specificity of the primers and the purity of the final PCR product.

2.13. Real time-PCR data analysis

The real-time PCR data were analyzed using the relative gene expression i.e. (2- ΔΔCT) method as described in Applied Biosystems User Bulletin No.2 and explained further by Livak et al (Livak and Schmittgen, 2001). Briefly, the data are presented as the fold change in gene expression normalized to the endogenous reference gene, glyceraldehyde-3-phosphate dehydrogenase (GAPDH) or β-actin and relative to a calibrator. The untreated control was used as the calibrator when the change of gene expression by the treatment was studied.

Table 1. Primer sequences used for real time- PCR reactions.

Gene	species	Forward primer	Reverse primer
a-MHC	Human	GCCCTTTGACATTCGCACTG	GGTTTCAGCAATGACCTTGCC
β-MHC	Human	TCACCAACAACCCCTACGATT	CTCCTCAGCGTCATCAATGGA
BNP	Human	CAGAAGCTGCTGGAGCTGATAAG	TGTAGGGCCTTGGTCCTTTG
CYP1A1	Human	CCAAACGAGTTCCGGCCT	TGCCCAAACCAAAGAGAATGA
CYP1B1	Human	CAGAAGCTGCTGGAGCTGATAAG	TGTAGGGCCTTGGTCCTTTG
CYP2C11	Human	GCCTGAAACCCATAGTGGTG	GGGGCTGCTCAAAATCTTGATG
CYP2J3	Human	GAGCTTAGAGGAACGCATTCAG	GAAATGAGGGTCAAAAGGCTGT
CYP3A4	Human	CCATCCCCATTGCACGACTT	CAGGTAGACAAGCAGGTAGGG
CYP4F2	Human	GAGGGTAGTGCCTGTTTGGAT	CAGGAGGATCTCATGGTGTCTT
EPHX2	Human	GTGCCACTACCCGGCTTATG	GGCAGACTTTAGCGGTCTCG
β-actin	Human	ACCAGTTCCTGAATGGCTGC	GGC TGCACTCCACCATTTCT
a-MHC	Rat	CAGCTGGCCTTCCTCAGACT	TGCTGTTTTTGCAGTGGTATGTAA
β-MHC	Rat	ACCTGCAAGACCATCGACATG	CGAGCCTTAGTTTGGACAGGAT
BNP	Rat	ACAGAGTGCTTCGTGCCTGAT	CGAATTTCGGAGGGTTCTGC
EPHX2	Rat	GATTCTCATCAAGTGGCTGAAGAC	GGACACGCCACTGGCTAAAT
CYP1A2	Rat	GAATGGCTTCTAGTCCCA	TCATCTTCTCACTAAGGGCT
CYP1B1	Rat	CCTGGTTCTGCAACCTCATCA	CTCAACATGACAAGAGGGGCA
CYP2C23	Rat	CGTCCAATCACACGGTCAAGT	TTCGGGCTCCTGCTCCTT
CYP2J2	Rat	GAGCTTAGAGGAACGCATTCAG	GAAATGAGGGTCAAAAGGCTGT
CYP3A4	Rat	CCATCCCTTGATGATCGTACCA	AATTGGGGCAAGATCTGCAAA
CYP4F1	Rat	CAGGTCTGAAGCAGGTAACTAAGC	CCGTCAGGGTGGCACAGAGT
β-actin	Rat	CAAGGTCATCCATGACAACTTTG	GGGCCATCCACAGTCTTCTG

2.14. Protein extraction from H9c2 and RL-14 cells

Twenty-four h after incubation with the fluconazole 50 μM in the presence and absence of Ang II 10 μM, approximately 1.5 x 10^6 cells per six-well culture plate were collected in 100 μl lysis buffer (50 mM HEPES, 0.5 M sodium chloride, 1.5 mM magnesium chloride, 1 mM EDTA, 10% glycerol (v/v), 1% Triton X-100, and 5μl/ml of protease inhibitor cocktail). Total cellular proteins were obtained by incubating the cell lysates on ice for 1 h, with intermittent vortex mixing every 10 min, followed by centrifugation at 12,000x g for 10 min at 4°C.

2.15. Preparation of microsomal proteins

Heart, liver, kidneys, lungs and brain microsomal proteins were prepared by differential centrifugation of homogenized tissues. Briefly, individual tissues were rapidly removed, washed in ice-cold potassium chloride [1.15% (w/v)] and cut in pieces. Thereafter, cold sucrose solution (1 g of tissue in 5 ml of 0.25 M sucrose) was used to homogenize tissues pieces. The homogenate was spun at 10,000g for 20 min, and the resulting supernatant was spun once again at 100,000g for 60 min to obtain the microsomal pellet. The final pellets were dissolved in cold sucrose and stored at -80^o C. Thereafter, the Lowry method (LOWRY et al., 1951) with bovine serum albumin as a standard was used to determine microsomal protein concentrations.

2.16. Western blot analysis

Western blot analysis under denaturing and reducing conditions was performed using a previously described method (Liu et al., 1997). Briefly, proteins from each treated group were diluted with same amount (1:1) of 2X loading buffer (0.1 M tris(hydroxymethyl)aminomethane (Tris)-HCl, pH 6.8, 4% sodium dodecyl sulfate (SDS), 1.5% bromophenol blue, 20% glycerol, 5% β-mercaptoethanol), boiled and loaded onto a 10% SDS-polyacrylamide gel. Samples were electrophoresed at 120 V for 2 h and separated proteins were transferred to Trans-Blot

nitrocellulose membrane (0.45 µm) in a buffer containing 25 mM Tris–HCl, 192 mM glycine, and 20% (v/v) methanol. The membranes were blocked overnight at 4°C in a solution containing 5% skim milk powder, 2% BSA and 0.5% Tween-20 in Tris-buffered saline (TBS) solution (0.15 M NaCl, 3 mM KCl, 25 mM Tris-base). After blocking, the blots were washed 6 times for 1 h with TBS-Tween-20 before being incubated with a primary antibody (0.2 µg/ml) for 2 h at room temperature in TBS solution containing 0.05% (v/v) Tween-20 and 0.02% sodium azide. Incubation with a peroxidase conjugated anti-rabbit or anti-mouse IgG secondary antibody was carried out in blocking solution for 1 h at room temperature. The bands were visualized using the enhanced chemiluminescence method according to the manufacturer's instructions (GE Healthcare, Mississauga, ON). The intensity of protein band was semi-quantified relative to the signals obtained for GAPDH protein, using ImageJ® image processing program (National Institutes of Health, Bethesda, MD, http://rsb.info.nih.gov/ij).

2.17. Microsomal Incubation of Arachidonic acid

Heart microsomes (1 mg protein/ml) were incubated in the incubation buffer (5 mM magnesium chloride hexahydrate dissolved in 0.1 M potassium phosphate buffer pH=7.4) at 37°C in a shaking water bath (50 r.p.m). A pre-equilibration period of 5 min was performed. The reaction was initiated by the addition of 1 mM NADPH. Arachidonic acid was added to a final concentration of 50 µM and incubated for 30 min. The reaction was terminated by the addition of 600 µl ice-cold acetonitrile followed by the internal standard. AA metabolites were extracted twice by 1 ml ethyl acetate and dried using speed vacuum (Thermo Fisher Scientific, Ottawa, ON, Canada).

2.18. Separation of AA Metabolites by LC–ESI–MS

Extracted AA and metabolites were analyzed using LC–ESI–MS (Micromass ZQ 4000 spectrometer; Waters, Milford, MA) method as described previously (Nithipatikom et al., 2001).

Briefly, a gradient separation was performed on a reverse-phase C18 column (Alltima HP, 150 × 2.1 mm; GRACE Davison, Lokeren, Belgium) at 35°C. Mobile phase A consisted of water with 0.01% formic acid and 0.005% triethylamine (v/v), whereas mobile phase B consisted of 8% methanol, 8% isopropanol, and 84% acetonitrile with 0.01% formic acid and 0.005% triethylamine (v/v). Injection volume of 40 µL was used, and the mass spectrometer was run under negative ionization mode with single ion monitoring of AA at m/z= 303, HETEs and EETs at m/z=319, DHETs at m/z=337 and internal standards at m/z=311, m/z=327, m/z=348.2 and m/z=360 for AA-d8, 15-HETE-d8, 14,15-DHET-d11 and PGE2-d9, respectively.

Calibration samples of AA metabolites were prepared in acetonitrile containing 0.001, 0.01, 0.1 and 1.0 µg/ml of each of the AA metabolites. Calibration curves performed on three separate days were analyzed to evaluate the linearity. Accuracy and precision were determined using quality-control samples at four levels in the range of expected concentrations in incubates, 0.001, 0.01, 0.1 and 1.0 µg/ml for AA metabolites. Each quality-control sample (10 µl) was injected in triplicate on three different days to permit an assessment of intraday and interday accuracy and precision. Accuracy was determined by the calculating the concentration of each quality-control sample based on the calibration curve equations. Bias was assessed by calculating percentage of error [%error = $(C_{calculated} - C_{nominal})/C_{nominal} \times 100$] for all injections at each level analyzed. Precision was assessed by calculating the coefficient of variation (%CV = S.D./mean × 100) for all injections at each level analyzed.

2.19. sEH activity assay

sEH activity was measured using the Morisseau and Hammock method with modifications. 14,15-EET was used as the natural substrate (Morisseau and Hammock, 2007). Briefly, the cytosolic fraction was diluted with sodium phosphate buffer (0.076 M, pH 7.4) supplemented with bovine

serum albumin (2.5 mg/ml) to 0.4 mg/ml. The assay was initiated by the addition of 14,15-EET (final concentration, 2 mg/ml). The mixture was incubated at 37°C for 10 min. The reaction was terminated by the addition of 600 µl ice-cold acetonitrile followed by the internal standard. 14,15-EET and its corresponding 14,15-DHET were extracted by ethyl acetate twice, dried using speed vacuum, and analyzed using the LC-ESI-MS method as described previously.

2.20. Statistical Analysis

Data are presented as mean ± standard error of mean (SEM). Student's t test or one-way analysis of variance, followed by a Student–Newman–Keuls post hoc test, was used. A result was considered statistically significant where $p < 0.05$. Analysis was performed using SigmaPlot® for Windows (Systat Software, Inc, CA).

Chapter 3: Results

3.1 Effect of fluconazole on Ang II-induced cellular hypertrophy in H9c2 and RL-14 cells

3.1.1 Effect of fluconazole and Ang II on cell viability

To establish the cytotoxic effect of fluconazole and Ang II, both H9c2 and RL-14 cells were treated with increasing concentrations of fluconazole (6.25, 12.5, 25, 50, 100 μM) and Ang II (1, 2.5, 5, 10 μM). Thereafter, cell viability was assessed using MTT assay as described in the material and methods. The MTT assay showed that fluconazole concentrations ranging from 6.25-100 μM did not significantly affect cell viability compared to control in H9c2 and RL-14 cells (Figures 3A and B). Furthermore, the cytotoxic effect of Ang II at concentration 10 μM in the presence and absence of fluconazole 50 μM was evaluated and the MTT assay showed that the combination did not significantly affect cell viability compared to control in H9c2 and RL-14 cells (Figures 3C and D). Therefore, the observed changes are not due to the direct toxicity of fluconazole and Ang II on the cells.

3.1.2 Effect of fluconazole on cardiac hypertrophy markers

To investigate whether fluconazole has a protective effect on the development of cellular hypertrophy, hypertrophic markers were assessed in H9c2 and RL-14 cells treated with Ang II. Our resulted showed that treatment of H9c2 cells with Ang II 10 μM for 24 h significantly increased the hypertrophic markers β/α MHC and BNP by 55% by 60% and 55%, respectively, compared to control (Figure 4A and B). On the other hand, treatment of H9c2 cells with fluconazole 50 μM was able to reverse the AngII mediated induction of β/α MHC and BNP by 60% and 75%, respectively (Figure 4A and B). In RL-14 cells, treatment of the cells with Ang II 10 μM for 24 h significantly increased the hypertrophic markers β/α MHC and BNP by 47% and 72%, respectively, compared to control (Figure 5A and B). Treatment with fluconazole was able

to protect RL-14 cells and was able to reverse the AngII mediated induction of β/α MHC and BNP by 41% and 56%, respectively (Figure 5A and B).

3.2.3 Effect of fluconazole on cell surface area

To further confirm the changes observed with fluconazole treatment on hypertrophic markers, cell surface area was assessed. Cell size change is response to treatment is an indicator of cellular hypertrophy. For this purpose, both H9c2 and RL-14 cell were treated with fluconazole 50 μM in the presence and absence of Ang II 10 μM for 24 h. Thereafter, cell surface area was measured using phase contrast imaging which was taken with Zeiss Axio Observer Z1 inverted microscope using ×20 objective lens as described in materials and methods. As shown in (Figure 6A), after treatment of H9c2 with Ang II, the cell surface area was significantly increased by 68% compared to control. Interestingly, fluconazole significantly reversed the AngII mediated increase of cell surface area by 63% compared with AngII in H9c2 cells. On the other hand, the same trend of protection was observed with RL-14 cells. Ang II significantly increased cell surface area by 60% compared to control which was significantly decreased by 51% with fluconazole treatment (Figure 6B).

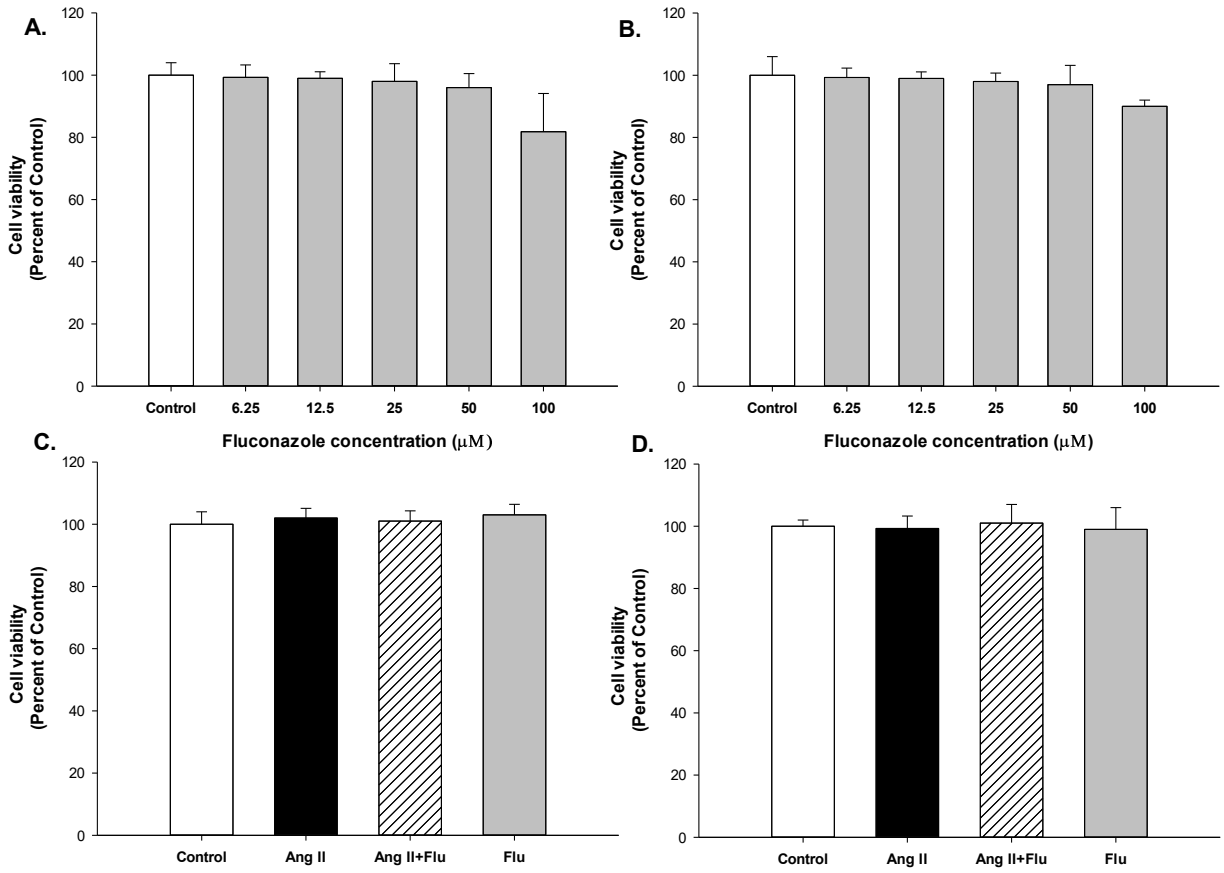

Figure 3: Effect of fluconazole and Ang II on H9c2 and RL-14 cell viability.

H9c2 and RL-14 cells were treated with increasing concentrations of fluconazole (6.25, 12.5, 25, 50, 100 μM) for 24 h (A and B), respectively. H9c2 and RL-14 cells were treated with fluconazole 50 μM in the presence and absence of Ang II 10 μM for 24 h (C and D), respectively. The cell viability was measured by the MTT assay as described in materials and methods. Data are presented as a percentage of control (mean + S.E.M, n=8).

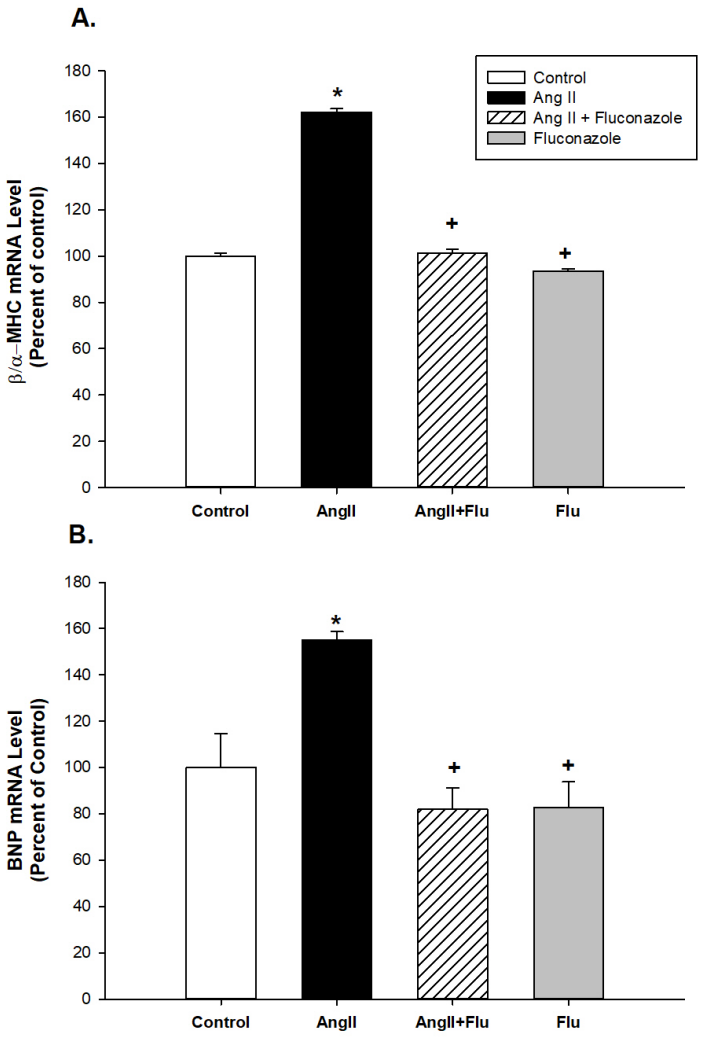

Figure 4: Effect of fluconazole in the presence and absence of Ang II on H9c2 cardiac hypertrophy markers.

H9c2 cells were treated with fluconazole 50 µM in the presence and absence of Ang II 10 µM for 24 h. Thereafter, total RNA was isolated using TRIzol reagent, and the mRNA level of β-MHC/α-MHC (A) and brain natriuretic peptide (B) was quantified using real-time PCR and normalized to β-actin. The results are presented as ± S.E.M. (n = 6). *P < 0.05 compared to control +P <0.05 compared to Ang II alone.

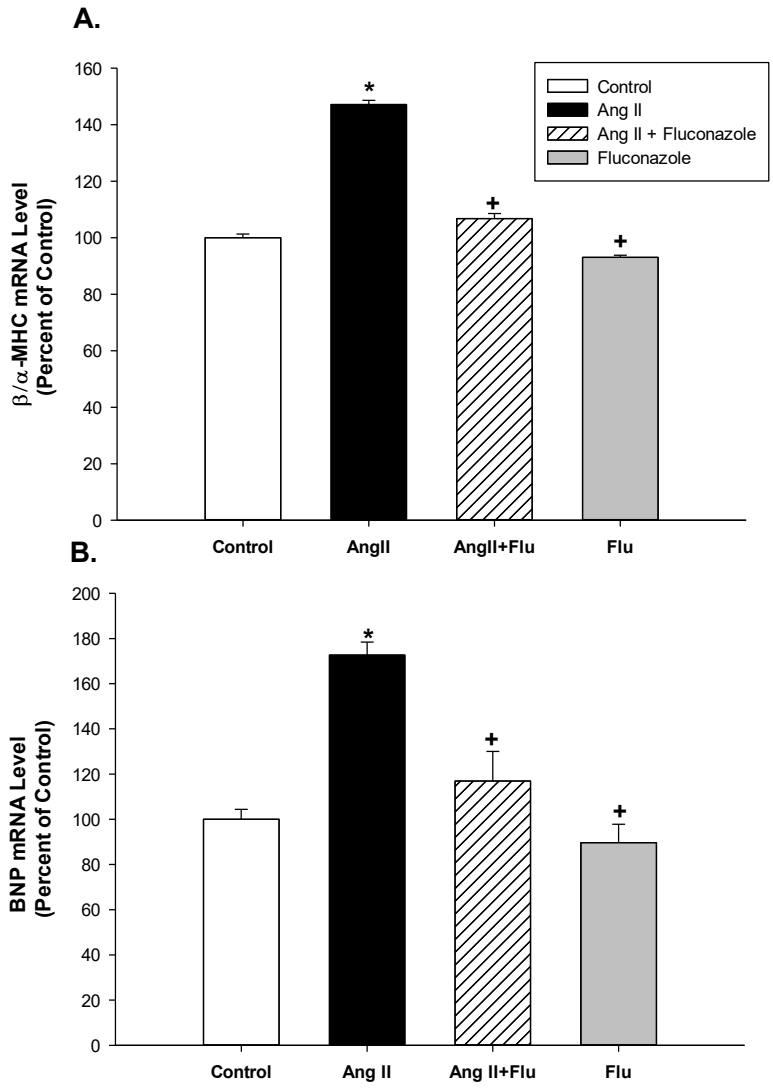

Figure 5: Effect of fluconazole in the presence and absence of Ang II on RL-14 cardiac hypertrophy markers.

RL-14 cells were treated with fluconazole 50 μM in the presence and absence of Ang II 10 μM for 24 h. Thereafter, total RNA was isolated using TRIzol reagent, and the mRNA level of β-MHC/α-MHC (A) and brain natriuretic peptide (B) was quantified using real-time PCR and normalized to β-actin. The results are presented as ± S.E.M. (n = 6). *P < 0.05 compared to control +P <0.05 compared to Ang II alone.

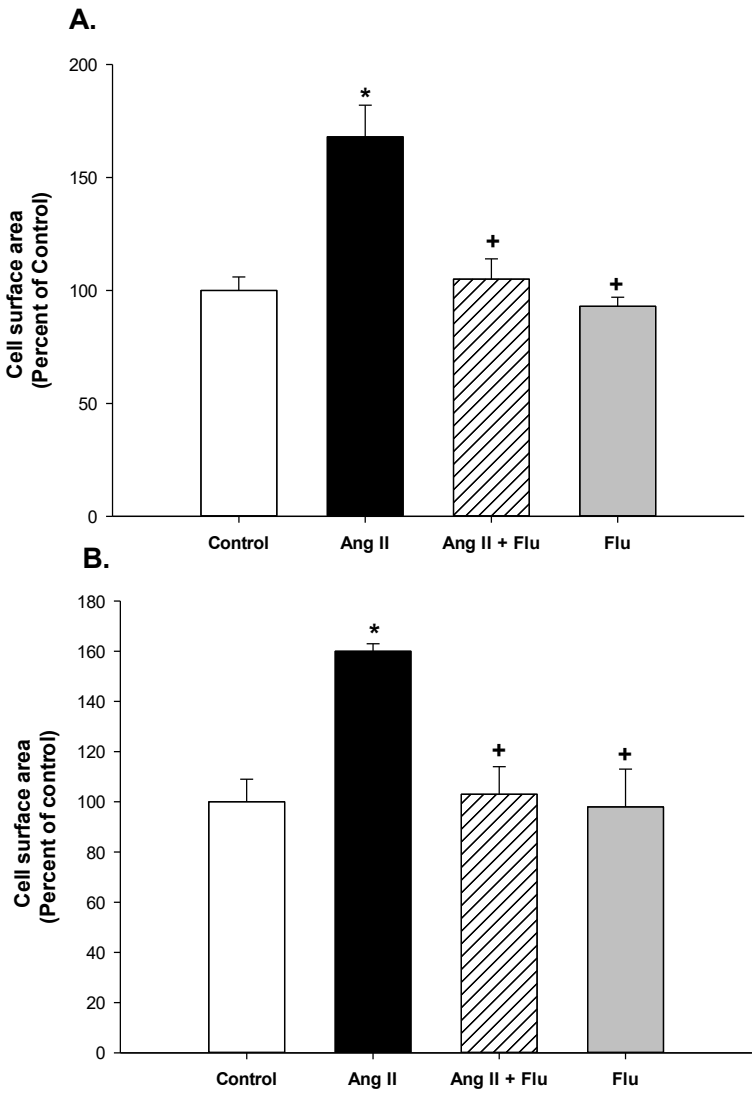

Figure 6: Effect of fluconazole in the presence and absence of Ang II on cell surface area. H9c2 (A) and RL-14 (B) cells were treated with fluconazole 50 μM in the presence and absence of Ang II 10 μM for 24 h. Thereafter, cell surface area was determined by phase contrast images which were taken with Zeiss Axio Observer Z1 inverted microscope using a ×20 objective lens. The values represent mean ± SEM (n=6). *P < 0.05 compared to control +P <0.05 compared to Ang II alone.

3.2 Effect of fluconazole on CYP-mediated AA metabolism in H9c2 and RL-14 cells

3.2.1 Effect of fluconazole on Ang II-mediated AA metabolites formation, mid-chain HETEs

To determine the ability of fluconazole to inhibit the formation of mid-chain HETEs altered by Ang II treatment, AA metabolites were extracted from H9c2 and RL-14 cells. Thereafter, mid-chain HETEs metabolites were measured using LC-ESI-MS as described in the materials and methods. For this purpose, both H9c2 and RL-14 cell were treated with fluconazole 50 μM in the presence and absence of Ang II 10 μM for 24 h. Our results show that in H9c2 cells, Ang II was able to significantly increase the formation levels of 12- and 5-HETEs by 32% and 24%, respectively, compared to control. On the other hand, fluconazole significantly decreased the formation level of 15-,12-,11-,9-,8- and 5-HETEs by 42%, 53%, 31%, 32%, 32% and 39%, respectively, compared to control. Furthermore, fluconazole significantly decreased the formation levels of 12- and 5-HETEs by 42% and 47%, respectively, compared to Ang II (Figure 7). Interestingly, in RL-14 cells, Ang II was able to significantly increase the formation levels of 15-, 12- and 5-HETEs by 29%, 37% and 22%, respectively, compared to control. On the other hand, fluconazole significantly decreased the formation level of 15-,12-,11-,9-,8- and 5-HETEs by 33%, 44%, 40%, 38%, 28% and 48%, respectively, compared to control. Furthermore, fluconazole significantly decreased the formation levels of 15-, 12- and 5-HETEs by 28%, 45% and 33%, respectively, compared to Ang II (Figure 8).

3.2.2 Effect of fluconazole on Ang II-mediated alteration of CYPs gene expression

To investigate the mechanism by which fluconazole decreased the formation of mid-chain HETEs metabolites, the gene expression of different CYPs involved in AA metabolism were determined. Both H9c2 and RL-14 cells were treated with fluconazole 50 μM in the presence and absence of Ang II 10 μM for 24 h. Thereafter, the mRNA expression of different CYPs was analyzed using

real-time PCR as described in the materials and methods. For H9c2, the gene expression of CYP1A2, CYP1B1, CYP2C23, CYP2J3, CYP3A4 and CYP4F1 were determined and only the gene expression of CYP1B1 was altered. Ang II was able to significantly increase the gene expression of CYP1B1 by 36% as compared to control while fluconazole significantly decreased the expression of CYP1B1 by 29% as compared to control. Interestingly, fluconazole significantly decreased the gene expression of CYP1B1 by 37% compared to Ang II (Figure 9). Similarly, in RL-14, the gene expression of CYP1A1, CYP1B1, CYP2C19, CYP2J2, CYP4A3 and CYP4F5 were investigated and only the gene expression of CYP1B1 was altered. Ang II was able to significantly increase the gene expression of CYP1B1 by 29% as compared to control while fluconazole significantly decreased the expression of CYP1B1 by 30% as compared to control. Interestingly, fluconazole significantly decreased the gene expression of CYP1B1 by 29% compared to Ang II (Figure 10).

3.2.3 Effect of fluconazole on Ang II-mediated alteration of CYP1B1 protein expression

Based on the findings observed on the effect of fluconazole on different CYPs genes expression and the fact that only CYP1B1 gene expression was altered by fluconazole, the effect of fluconazole on CYP1B1 protein expression was investigated. Both H9c2 and RL-14 cells were treated with fluconazole 50 μM in the presence and absence of Ang II 10 μM for 24 h. Thereafter, Western blot analysis was performed as described in the materials and methods. In H9c2 cells, Ang II significantly increased the protein expression of CYP1B1 by 55% compared to control. Fluconazole alone significantly decreased the protein expression level by 57% compared to control. Interestingly, fluconazole significantly decreased the protein level of CYP1B1 by 73% compared to Ang II. (Figure 11A). The same trend of modulation was observed in RL-14 cells. Ang II significantly increased the protein expression of CYP1B1 by 53% compared to control.

Also, fluconazole significantly decreased the protein expression level of CYP1B1 by 46% and 40%, respectively, compared to control and Ang II groups (Figure 11B).

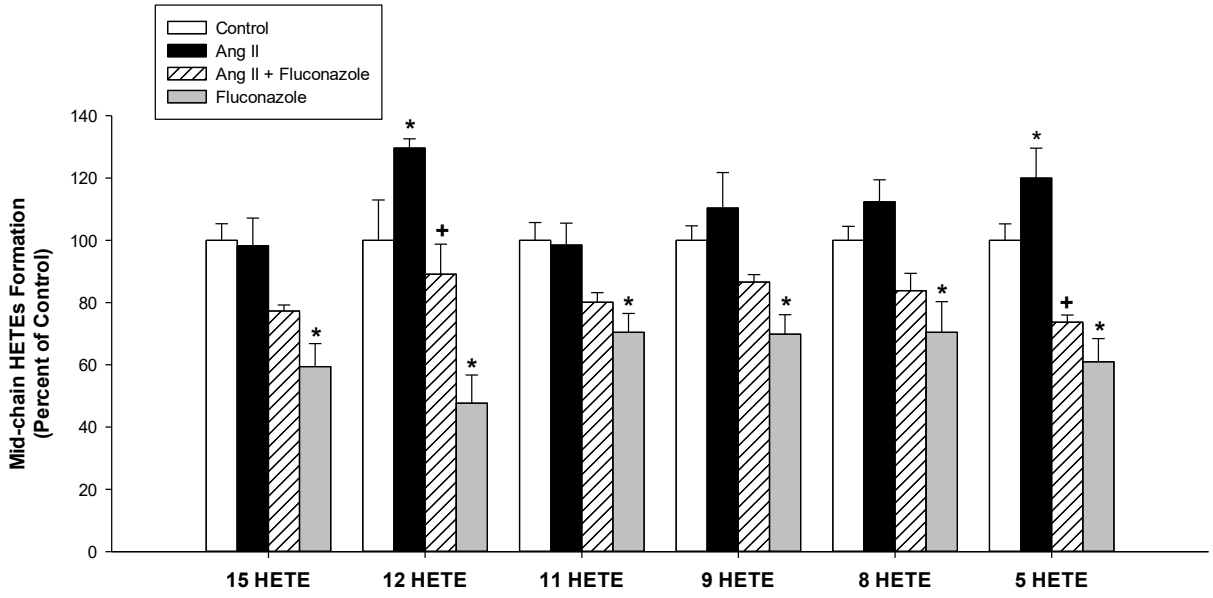

Figure 7: Effect of fluconazole in the presence and absence of Ang II on mid-chain HETEs metabolites formation.

H9c2 cells were treated with fluconazole 50 μM in the presence and absence of Ang II 10 μM for 24 h. Thereafter, mid-chain HETEs were quantified using LC-ESI-MS. The values represent mean ± SEM (n=6). *P < 0.05 compared to control +P <0.05 compared to Ang II alone.

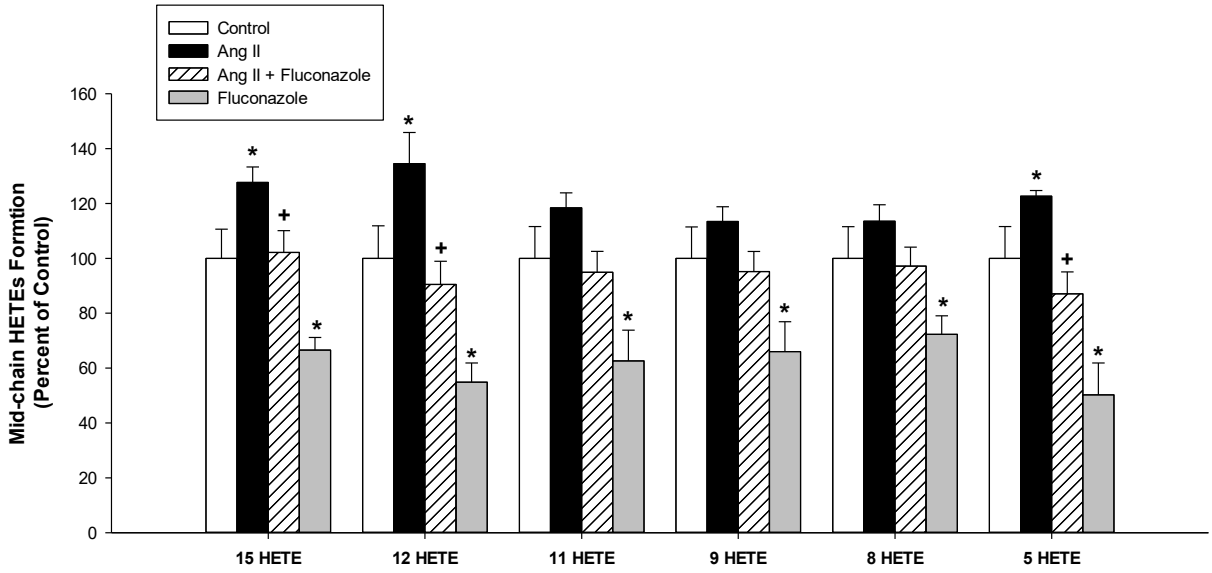

Figure 8: Effect of fluconazole in the presence and absence of Ang II on mid-chain HETEs metabolites formation.

RL-14 cells were treated with fluconazole 50 μM in the presence and absence of Ang II 10 μM for 24 h. Thereafter, mid-chain HETEs were quantified using LC-ESI-MS. The values represent mean ± SEM (n=6). *P < 0.05 compared to control +P <0.05 compared to Ang II alone.

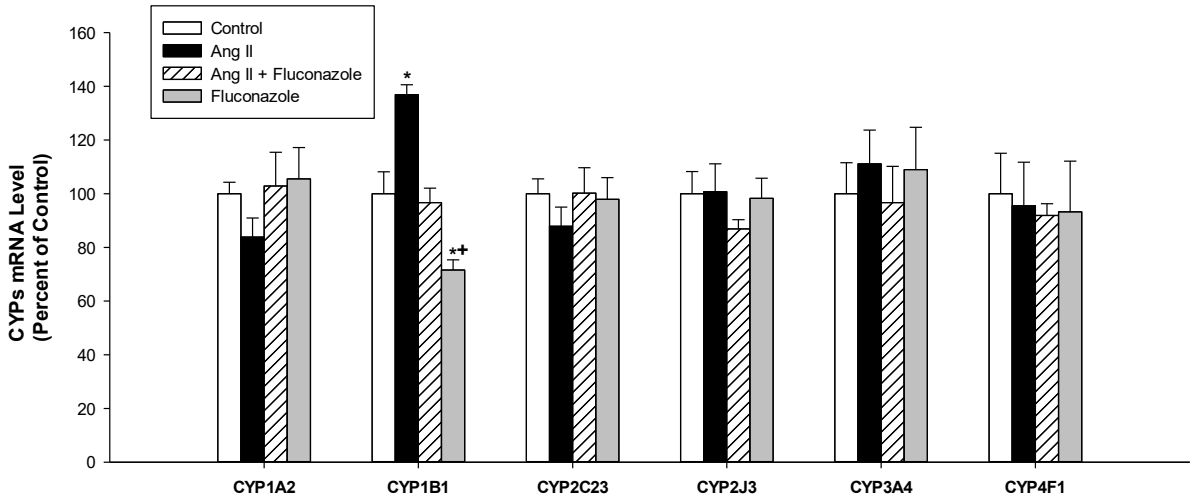

Figure 9: Effect of fluconazole in the presence and absence of Ang II on H9c2 CYP genes expression.

H9c2 cells were treated with fluconazole 50 μM in the presence and absence of Ang II 10 μM for 24 h. Thereafter, mRNA levels of CYP1A2, CYP1B1, CYP2C23, CYP2E1, CYP2J3, CYP3A4 and CYP4F1 were quantified using real time-PCR and normalized to β-actin. The values represent mean ± SEM (n=6). *P < 0.05 compared to control +P <0.05 compared to Ang II alone.

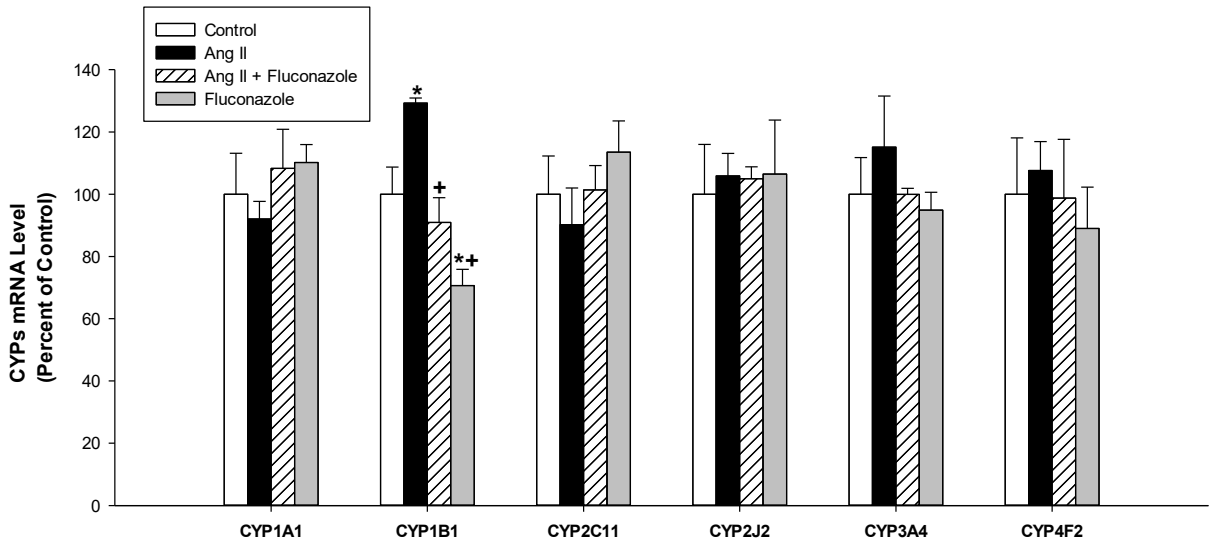

Figure 10: Effect of fluconazole in the presence and absence of Ang II on RL-14 CYP genes expression.

RL-14 cells were treated with fluconazole 50 μM in the presence and absence of Ang II 10 μM for 24 h. Thereafter, mRNA levels of CYP1A1, CYP1B1, CYP2C19, CYP2E1, CYP2J2, CYP4A3 and CYP4F5 were quantified using real time-PCR and normalized to β-actin. The values represent mean ± SEM (n=6). *P < 0.05 compared to control +P <0.05 compared to Ang II alone.

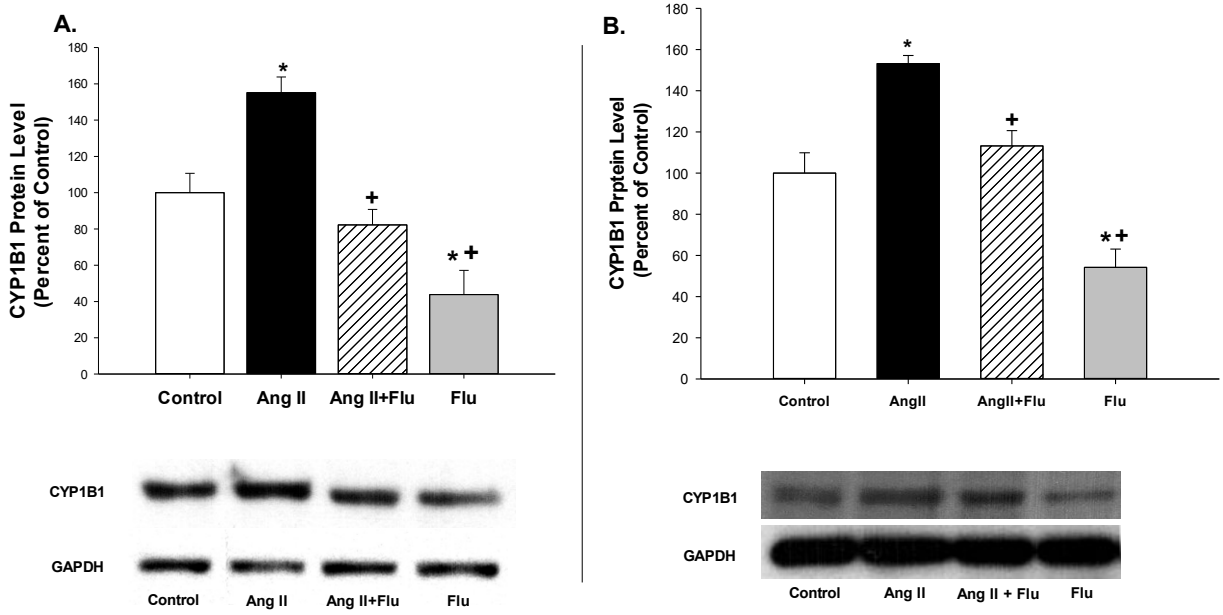

Figure 11: Effect of fluconazole in the presence and absence of Ang II on CYPs protein expression in H9c2 (A) and RL-14 (B).

Cells were treated with fluconazole 50 μM in the presence and absence of Ang II 10 μM for 24 h. Thereafter, protein levels of CYP1B1 were determined by Western blot analysis. Protein levels were detected using the enhanced chemiluminescence method. The intensity of the protein band was normalized to the signals obtained for GAPDH protein and quantified using ImageJ. The results are presented as the mean and S.E.M (n=6) of at least three individual experiments. Data were analyzed using one-way ANOVA followed by Student-Newman-Keuls as post-hoc test. *P < 0.05 compared to control + compared to Ang II alone (P <0.05).

3.3 Effect of fluconazole on CYP1B1 enzyme activity

3.3.1 Effect of fluconazole on CYP1B1 enzyme activity in H9c2 and RL-14 cells

To examine whether the effect of fluconazole on CYP1B1 mRNA and protein level can be translated to activity level, we examined the effect of fluconazole on CYP1B1 activity. Therefore, H9c2 and RL-14 cells were treated with fluconazole 50 μM in the presence and absence of Ang II 10 μM for 24 h. Thereafter, EROD (CYP1B1 substrate) was added and the activity of the enzyme was measured as described in the materials and methods. Our data show that Ang II significantly increased the enzyme activity of CYP1B1 in H9c2 cells by 29% compared to control. Fluconazole significantly decreased the enzyme activity of CYP1B1 by 56% and 60%, respectively, compared to control and Ang II groups (Figure 12A). RL-14 cells showed similar effect where Ang II significantly increase the enzyme activity of CYP1B1 by 74% compared to control. On the other hand, fluconazole significantly decreased the enzyme activity of CYP1B1 by 36% and 107%, respectively, compared to control and Ang II groups (Figure 12B).

3.3.2 Effect of fluconazole on CYP1B1 activity mediated by human recombinant CYP1B1

To confirm the inhibitory effect of fluconazole on CYP1B1 enzyme activity in both H9c2 and RL-14 cells, we examined the effect of fluconazole on EROD activity mediated by human recombinant CYP1B1. The O-dealkylation rate of 7-ethoxyresorufin by recombinant human CYP1B1 was measured in the absence and presence of (20, 40, 80 and 200 nM) of fluconazole. Our data show (Figure 13) that fluconazole at concentration of 120 nM significantly inhibited the human recombinant CYP1B1 by 34% and 52% in comparison to control at 80 nM and 200 nM concentration of the substrate. Moreover, fluconazole at concentration 240 nM significantly inhibited the human recombinant CYP1B1 by 37% and 56% in comparison to control at 80 nM

and 200 nM concentration of the substrate. This finding strongly suggest that fluconazole inhibits the human recombinant CYP1B1 in concentration-dependent manner.

Furthermore, experiments involved the assessment of 7-ER-O-deethylase kinetics by determination of the rate of resorufin formation over time. Based on the nonlinear regression analysis and fitting to Michaelis-Menten model, the maximal EROD activity (V_{max}) was 44.51 pmol resorufin/pmol P450/min (R^2 =0.978) (Table 2). The substrate concentration at which the reaction velocity is equal to one half of the maximal velocity is known as Michaelis-Menten constant (K_m). The K_m value for the current EROD reaction is 196.2 nM (Table 1). Nonlinear regression analysis and comparisons showed that the mode of inhibition for fluconazole is noncompetitive inhibition of CYP1B1 enzyme with Ki values of 130.9 nM, (Table 2).

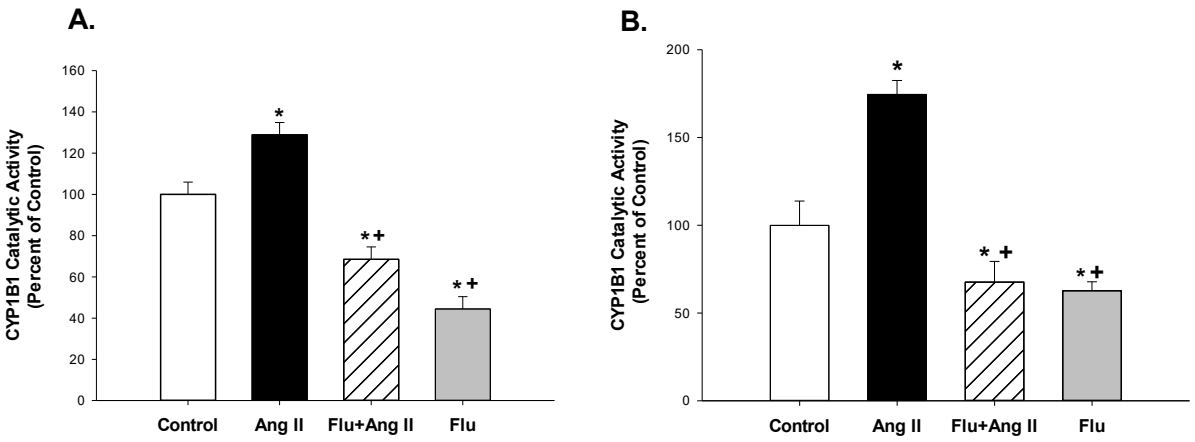

Figure 12: Effect of fluconazole in the presence and absence of Ang II on CYP1B1 catalytic activity in H9c2 (A) and RL-14 (B).

Cells were treated with fluconazole 50 μM in the presence and absence of Ang II 10 μM for 24 h. Thereafter, CYP1B1 catalytic activity level was determined by EROD assay. The values represent mean ± SEM (n=6). *P < 0.05 compared to control +P <0.05 compared to Ang II alone.

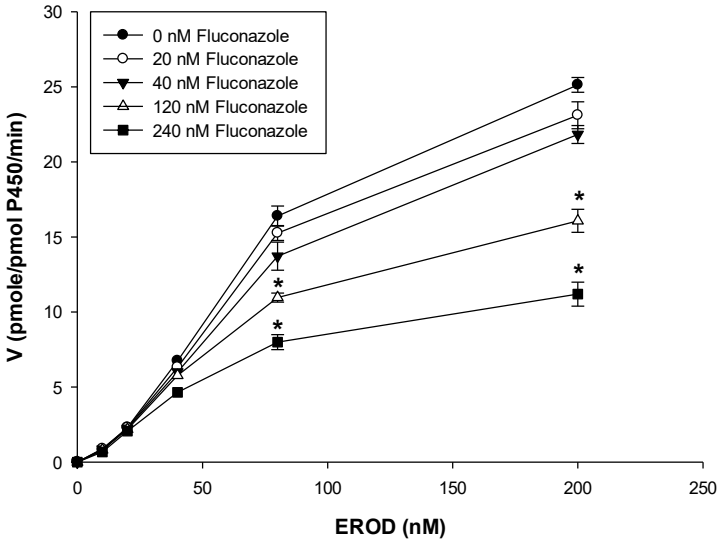

Figure 13: Effect of fluconazole on on EROD activity mediated by human recombinant CYP1B1.

In 96-well solid black polystyrene plates, the reaction mixture containing 100 mM potassium 0phosphate (pH 7.4) buffer supplemented with 5 mM magnesium chloride hexahydrate and 1 pmol of human CYP1B1, was incubated with 10-200 nM of EROD. In addition, 0, 20, 40, 80, 120 or 240 nM of fluconazole was added to the reaction. The reaction was initiated by the addition of 100 µL of 2 mM NADPH, the fluorescent signal related to the formation of resorufin was measured every one minute (excitation and emission wavelengths of 550 and 585 nm, respectively) for 30 min at 37°C using a BioTek Synergy H1 Hybrid Reader (BioTek Instruments, Inc.). The quantity of formed resorufin was measured by the construction of standard curve of 0-200 nM of resorufin dissolved in the same incubation buffer. The values represent mean ± SEM ($n \geq 6$). *$P < 0.05$ compared to control.

Table 2. Effect of Fluconazole on kinetics parameters of resorufin formation by human recombinant CYP1B1.

Km (nM)	Vmax (pmol/pmol P450/min)	Ki (nM)
196.2 ± 44.51	44.51 ± 6.620	130.9 ± 25.36

Data are presented as mean values ± SE based on at least 3 individual experiments.

3.4 Effect of fluconazole on CYP-mediated metabolism in vivo

3.4.1 Effect of fluconazole on the cardiac formation level of AA metabolites

To confirm the modulation of AA metabolites modulation observed in vitro, the effect of fluconazole on the level of AA metabolites mediated by CYPs was investigated in the heart of SD rats. For this purpose, SD rats were randomly segregated into two groups; the first group is control and received normal saline. The second group was injected intraperitonially (i.p) with fluconazole 20 mg/kg for 24 h. Thereafter, the hearts were harvested immediately and followed by microsomes isolation. AA metabolite were measured using LC-ESI-MS as described in materials and methods. Our data showed that fluconazole significantly decreased the formation levels of 15-, 12-, 8 and 5-HETEs by 23%, 23%, 27% and 20%, respectively, compared to control (Figure 14). However, EETs and their correspondent metabolites DHETE levels were not affected by fluconazole. Similarly, 20-HETE level was not altered by fluconazole treatment (Figure 15 A, B and C).

3.4.2 Effect of fluconazole on the cardiac CYPs and sEH genes expression

To determine whether the inhibitory effect of fluconazole on mid-chain HETEs is mediated by CYP and/or sEH in the heart, the gene expression of the CYPs involved in the metabolism of AA in addition to the gene expression of sEH were investigated. SD rats were treated with fluconazole

20mg/kg intraperitonially for 24 h. Thereafter, rat hearts were harvested and mRNA expression of CYP1A2, CYP1B1, CYP2C23, CYP2J3, CYP3A4, CYP4A1, CYP4F1 and sEH were analyzed using real-time PCR as described in the materials and methods. Fluconazole did not show and effect on CYP1A2, CYP2J3, CYP3A4, CYP4A1, CYP4F1 and sEH. Interestingly, fluconazole significantly decreased the gene expression levels of CYP1B1 and CYP2C23 by 36% and 42%, respectively, compared to control (Figure 16). This further confirm the effect of fluconazole observed in vitro.

3.4.3 Effect of fluconazole on the cardiac CYPs protein expression and CYP1B1 enzyme activity

The protein levels of CYP1B1 and CYP2C23 were investigated following the changes observed on the gene expressions. SD rats were treated with fluconazole 20mg/kg intraperitonially for 24 h. Thereafter, hearts were harvested and the protein level was determined using Western blot analysis as described in the materials and methods. Our results showed that fluconazole significantly decreased the protein expression of CYP1B1 and CYP2C23 by 52% and 56%, respectively, compared to control (Figure 17A).

Thereafter, the enzyme activity of CYP1B1 was investigated using selective CYP1B1 enzyme activity substrate, luciferin 6-chloroethyl ether (luciferin-CEE). SD rats were treated with fluconazole 20mg/kg intraperitonially for 24 h. Thereafter, hearts were harvested and the enzyme activity of CYP1B1 was determined using CYP1B1 enzyme activity kit as described in the materials and methods. Our results show that fluconazole significantly decreased CYP1B1 activity by 60% compared to control (Figure 17B).

3.4.4 Effect of fluconazole on the cardiac epoxygenases and sEH enzyme activity

To investigate the effect of fluconazole on CYP epoxygenases and sEH activity, SD rats were randomly segregated into two groups; the first group is control and received normal saline. The second group was injected intraperitonially with fluconazole 20mg/kg for 24 h. Thereafter, the heart was harvested immediately and the microsomes were isolated, AA metabolite were measured using LC-ESI-MS as described in the materials and methods. Our results showed that fluconazole did not have any effect on cardiac epoxygenases (Figure 18A). Also, sEH enzyme activity was not altered by fluconazole treatment (Figure 18B).

3.4.5 Effect of fluconazole on formation level of AA metabolites in the liver

To further investigate whether the effect of fluconazole on AA metabolites is specific to the heart or not, SD rats were randomly segregated into two groups; the first group is control and received normal saline. The second group was injected intraperitonially with fluconazole 20mg/kg for 24 h. Thereafter, the liver was harvested immediately and the microsomes were isolated, AA metabolite were measured using LC-ESI-MS as described in materials and methods. Interestingly, fluconazole only inhibited the formation of 5-HETE by 36% compared to control. Fluconazole showed no effect on 15-, 12-, 11-, 9- and 8-HETEs (Figure 19). Also, fluconazole did not significantly alter the other AA metabolites, EETs and their corresponding DHETEs metabolites as well as the formation level of 20-HETE (Figure 20A, B and C).

3.4.6 Effect of fluconazole on CYP1B1 and CYP2C23 genes and protein expression in the liver

Based on the results that showed inhibitory effect of fluconazole on 5-HETE in the liver, the gene and protein expressions of CYP1B1 and CYP2C23 were investigated. SD rats were treated with fluconazole 20mg/kg intraperitoneally for 24 h. Thereafter liver was harvested and mRNA

expression and protein levels of CYP1B1 and CYP2C23 were analyzed using real-time PCR and Western blot, respectively, as described in the materials and methods. As shown in (Figure 21A), fluconazole significantly inhibited the gene expression level of CYPB1 and CYP2C23 by 58% and 29%, respectively, compared to control. Moreover, fluconazole inhibited the protein expression levels of CYPB1 and CYP2C23 by 51% and 33%, respectively, compared to control (Figure 21B).

3.4.7 Effect of fluconazole on formation level of AA metabolites in the kidneys, lungs and brain

To examine the effect of fluconazole on CYPs-mediated AA metabolism, the levels of AA in the kidneys, lungs and brain were investigated. SD rats were randomly segregated into two groups; the first group is control and received normal saline. The second group was injected intraperitonially with fluconazole 20mg/kg for 24 h. Thereafter, kidneys, lungs and brain were harvested immediately and the microsomes were isolated, AA metabolite were measured using LC-ESI-MS as described in the materials and methods. (Figure 22) shows that fluconazole did not change the levels of mid-chain HETEs metabolites in the kidneys. Similarly, EETs and their corresponding DHETEs and 20-HETE metabolite did not change following fluconazole treatment (Figure 23A, B and C), respectively. Furthermore, the level of mid-chain HETEs, EETs, DHETEs and 20-HETE were not altered following fluconazole treatment in the lungs (Figure 24, 25A, B and C), respectively. Similarly, fluconazole did not alter the levels of mid-chain HETEs, EETs, DHETE and 20-HETE in brain (Figure 26, 27 A, B and C), respectively.

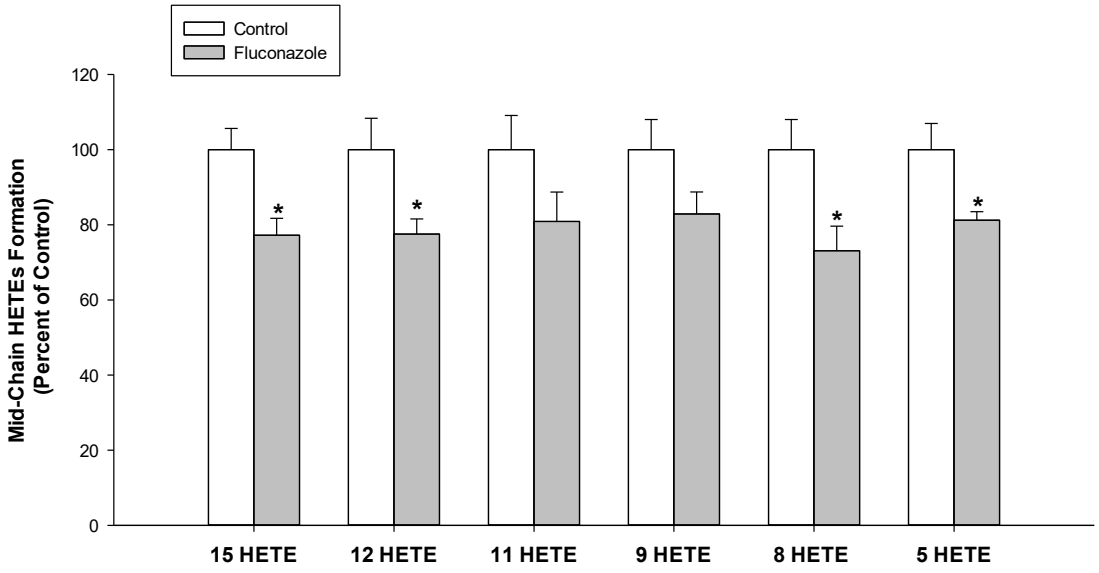

Figure 14: Effect of fluconazole on mid-chain HETEs metabolite levels in the heart.

SD Rats were treated with fluconazole (20mg/kg i.p.) for 24 h. Thereafter, hearts were harvested and heart microsomes of treated rats were incubated with 100 μM AA. The reaction was started by the addition of 1 mM NADPH and lasted for 30 min. The reaction was terminated by the addition of ice-cold acetonitrile. Metabolites were extracted twice by ethyl acetate and dried using speed vacuum. Residues were reconstituted in acetonitrile and injected into an LC-ESI-MS instrument for the determination of mid-chain HETEs. The values represent mean ± SEM (n=6). *$P < 0.05$ compared to control.

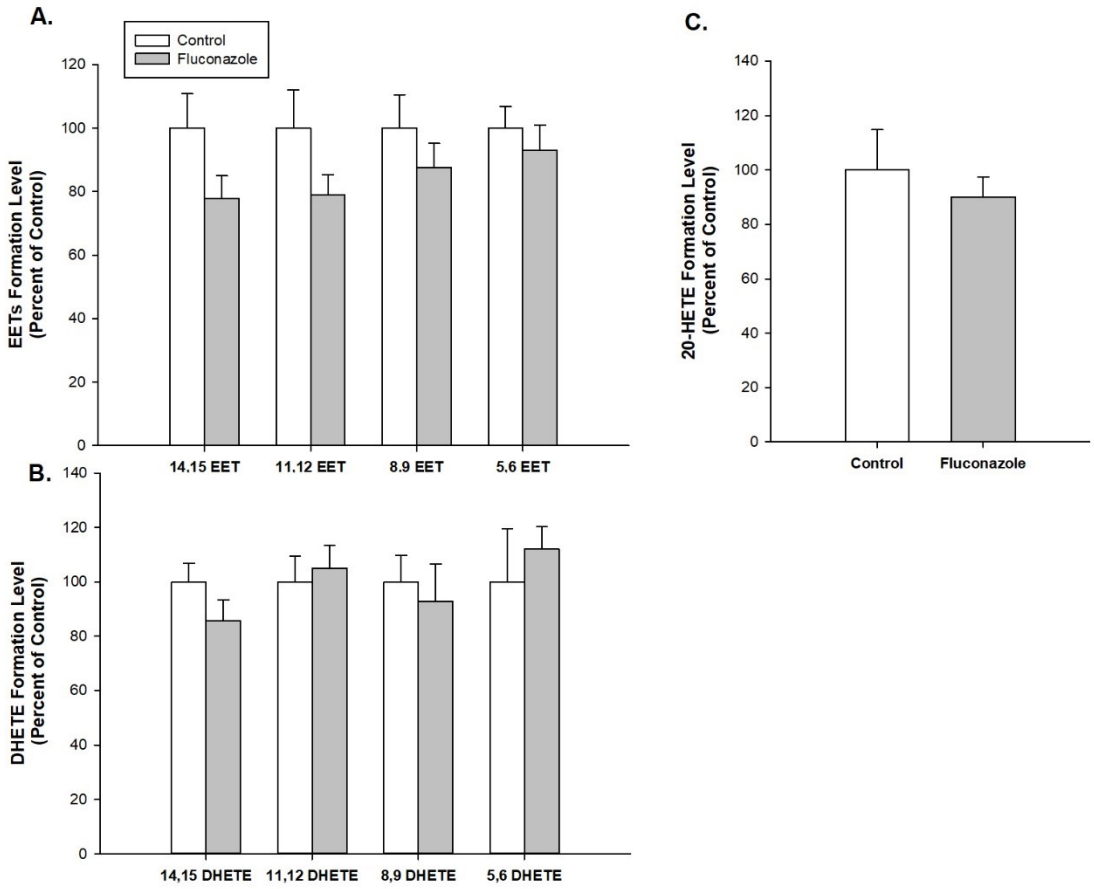

Figure 15: Effect of fluconazole on EETs, DHETE and 20-HETE metabolite levels in the heart.

SD Rats were treated with fluconazole (20mg/kg i.p.) for 24 h. Thereafter, hearts were harvested and heart microsomes of treated rats were incubated with 100 μM AA. The reaction was started by the addition of 1 mM NADPH and lasted for 30 min. The reaction was terminated by the addition of ice-cold acetonitrile. Metabolites were extracted twice by ethyl acetate and dried using speed vacuum. Residues were reconstituted in acetonitrile and injected into an LC-ESI-MS instrument for the determination of (A) EETs, (B) DHETEs and (C) 20-HETE. The values represent mean ± SEM (n=6). *P < 0.05 compared to control. The values represent mean ± SEM (n=6). *P < 0.05 compared to control.

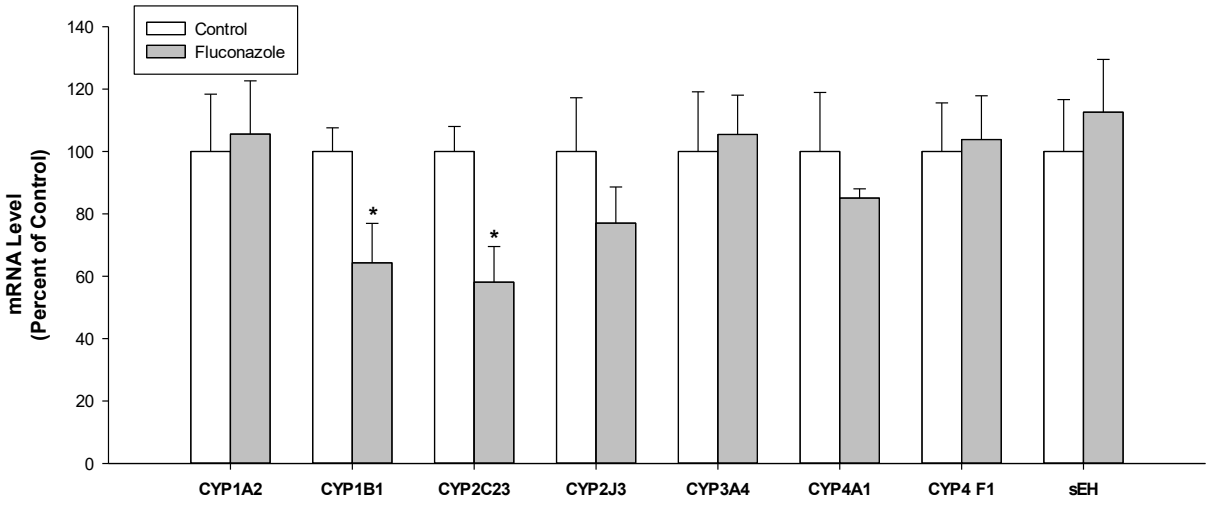

Figure 16: Effect of fluconazole on CYPs and sEH gene expression levels in the heart.

SD rats were treated with fluconazole (20mg/kg i.p.) for 24 h. Thereafter, hearts were harvested and mRNA levels of CYP1A2, CYP1B1, CYP2C23, CYP2J3, CYP3A4, CYP4A1, CYP4F1 and sEH were quantified using real time-PCR and normalized to β-actin. The values represent mean ± SEM (n=6). *P < 0.05 compared to control.

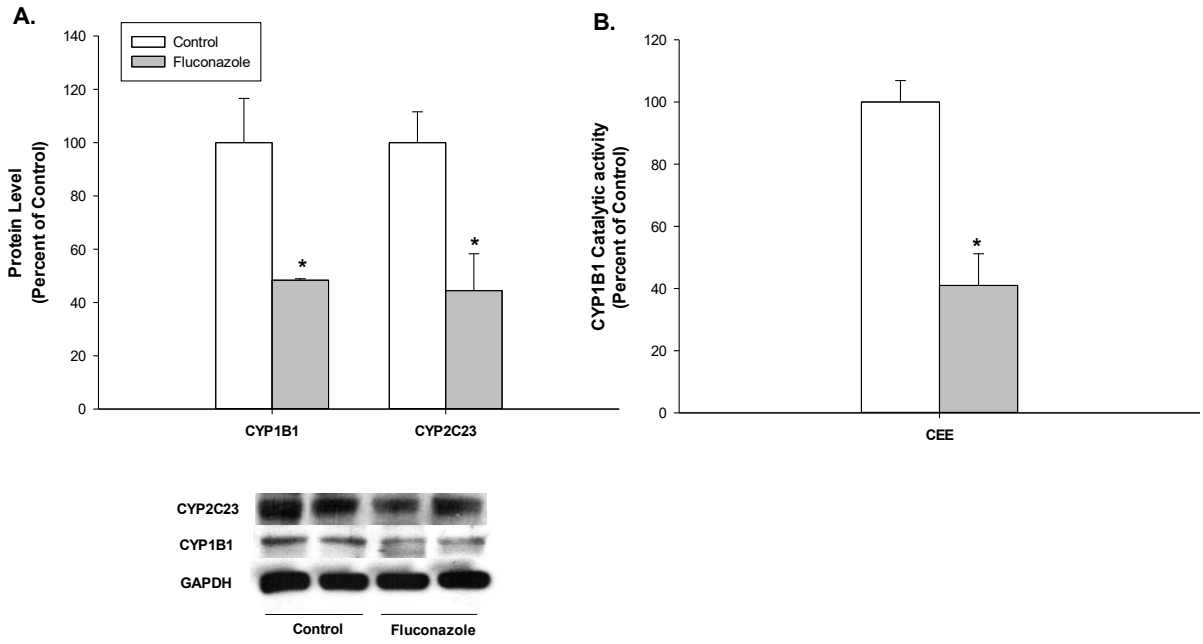

Figure 17: Effect of fluconazole on CYPs protein expression levels and on the catalytic activity of CYP1B1 in the heart.

SD rats were treated with fluconazole (20mg/kg i.p.) for 24 h. Thereafter, (A)protein levels of CYP1B1 and CYP2C23 were determined by Western blot analysis. Protein levels were detected using the enhanced chemiluminescence method. The intensity of the protein band was normalized to the signals obtained for GAPDH protein and quantified using ImageJ. The results are presented as the mean and S.E.M (n=6) of at least three individual experiments. (B) CYP1B1 enzyme activity was determined using specific CEE assay. The values represent mean ± SEM (n=6). *$P < 0.05$ compared to control.

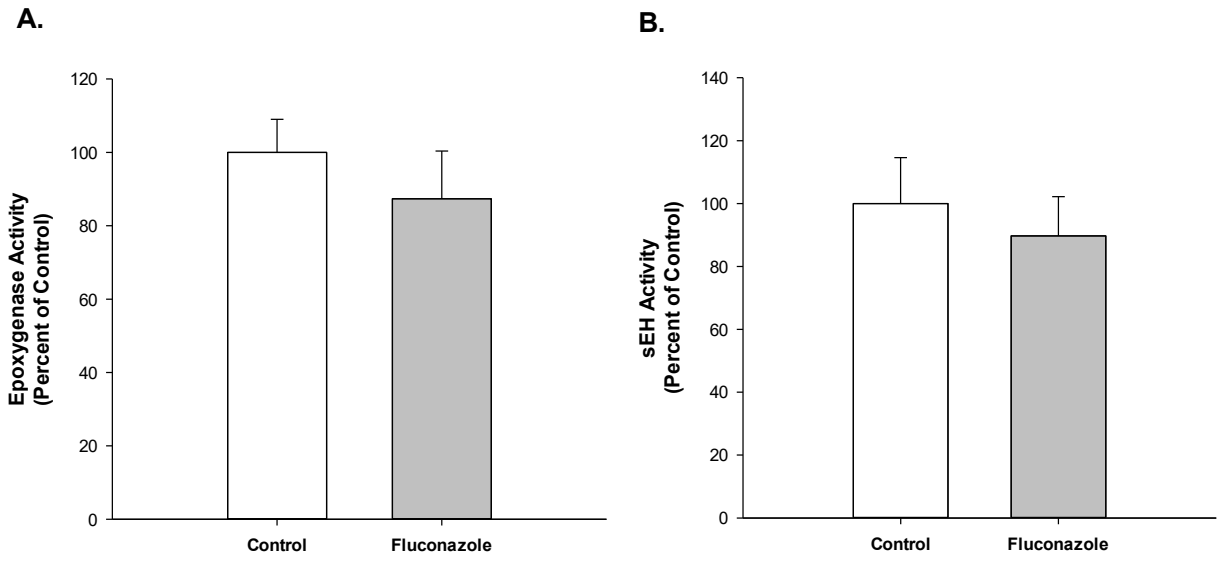

Figure 18: Effect of fluconazole on the cardiac epoxygenases and sEH enzyme activity.

SD Rats were treated with fluconazole (20mg/kg i.p.) for 24 h. Thereafter, hearts were harvested and heart microsomes of treated rats were incubated with 100 μM AA. The reaction was started by the addition of 1 mM NADPH and lasted for 30 min. The reaction was terminated by the addition of ice-cold acetonitrile. Metabolites were extracted twice by ethyl acetate and dried using speed vacuum. Residues were reconstituted in acetonitrile and injected into an LC-ESI-MS instrument for the determination of (A) epoxygenases activity, (B) sEH enzyme activity was was determined by sEH assay. The values represent mean ± SEM (n=6). The values represent mean ± SEM (n=6). *P < 0.05 compared to control.

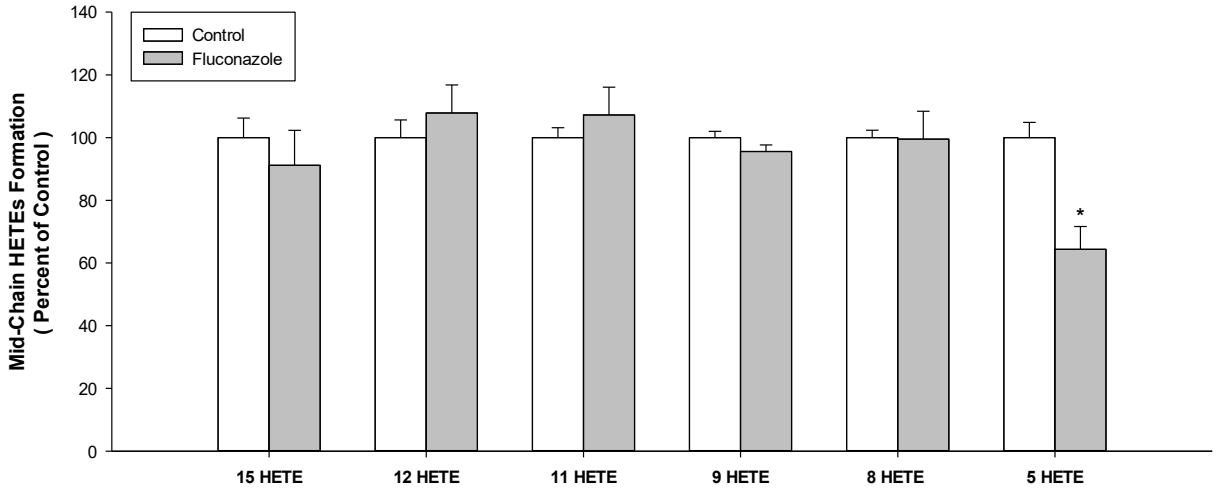

Figure 19: Effect of fluconazole on mid-chain HETEs metabolites level in the Liver.

SD Rats were treated with fluconazole (20mg/kg i.p.) for 24 h. Thereafter, livers were harvested and the microsomes of treated rats were incubated with 100 μM AA. The reaction was started by the addition of 1 mM NADPH and lasted for 30 min. The reaction was terminated by the addition of ice-cold acetonitrile. Metabolites were extracted twice by ethyl acetate and dried using speed vacuum. Residues were reconstituted in acetonitrile and injected into an LC-ESI-MS instrument for the determination of mid-chain HETEs. The values represent mean ± SEM (n=6). *P < 0.05 compared to control.

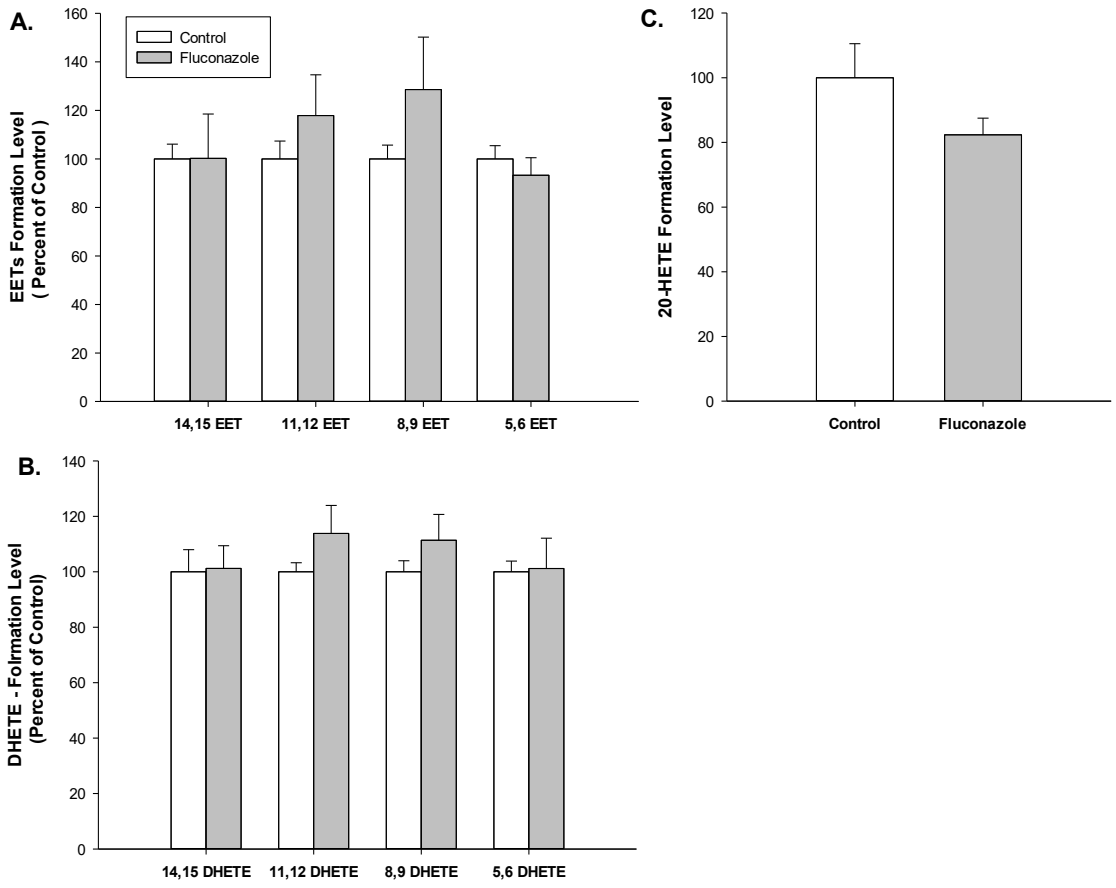

Figure 20: Effect of fluconazole on EETs, DHETE and 20-HETE metabolites level in the Liver.

SD Rats were treated with fluconazole (20mg/kg i.p.) for 24 h. Thereafter, livers were harvested and liver microsomes of treated rats were incubated with 100 µM AA. The reaction was started by the addition of 1 mM NADPH and lasted for 30 min. The reaction was terminated by the addition of ice-cold acetonitrile. Metabolites were extracted twice by ethyl acetate and dried using speed vacuum. Residues were reconstituted in acetonitrile and injected into an LC-ESI-MS instrument for the determination of (A) EETs, (B) DHETEs and (C) 20-HETE. The values represent mean ± SEM (n=6). *P < 0.05 compared to control. The values represent mean ± SEM (n=6). *P < 0.05 compared to control.

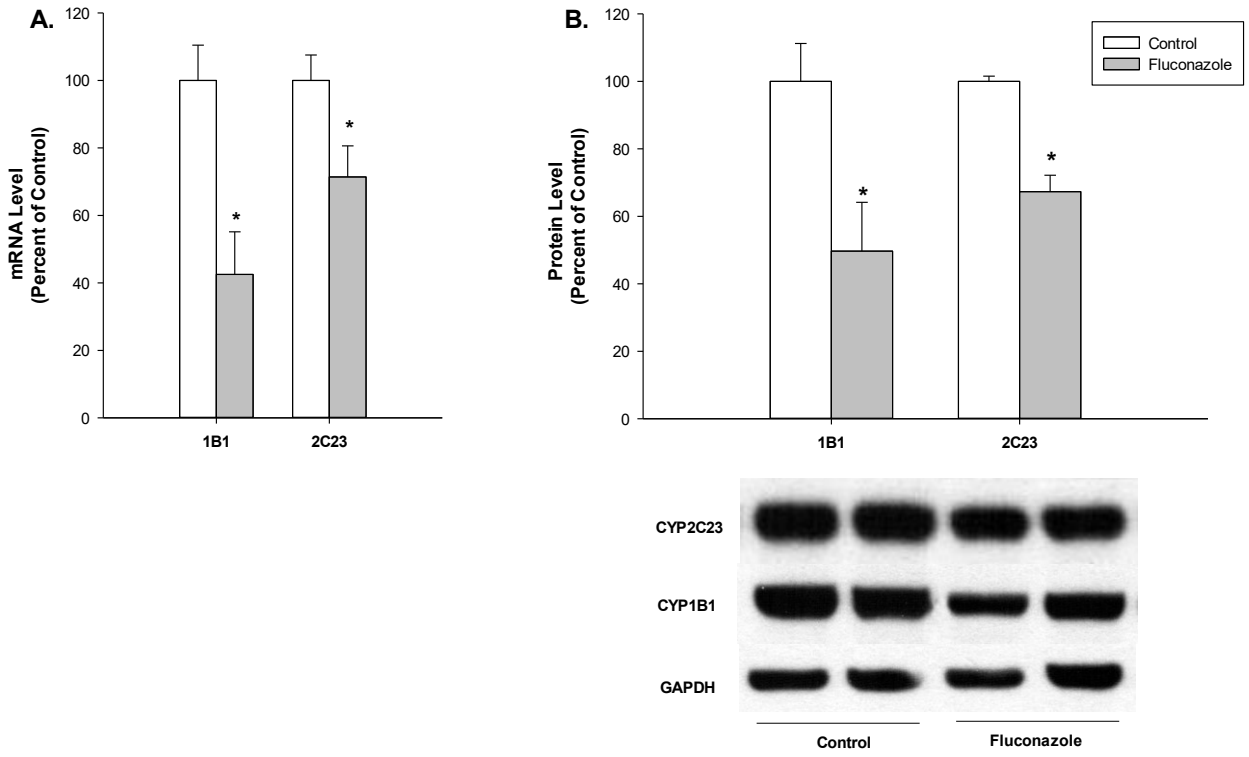

Figure 21: Effect of fluconazole on CYP1B1 and CYP2C23 gene and protein expressions levels in the Liver.

SD rats were treated with fluconazole (20mg/kg i.p.) for 24 h. Thereafter, (A) mRNA levels of CYP1B1 and CYP2C23 were determined by real time PCR and normalized to β-actin. (B) protein levels of CYP1B1 and CYP2C23 were determined by Western blot analysis. Protein levels were detected using the enhanced chemiluminescence method. The intensity of the protein band was normalized to the signals obtained for GAPDH protein and quantified using ImageJ. The results are presented as the mean and S.E.M (n=6) of at least three individual experiments. The values represent mean ± SEM (n=6). *P < 0.05 compared to control.

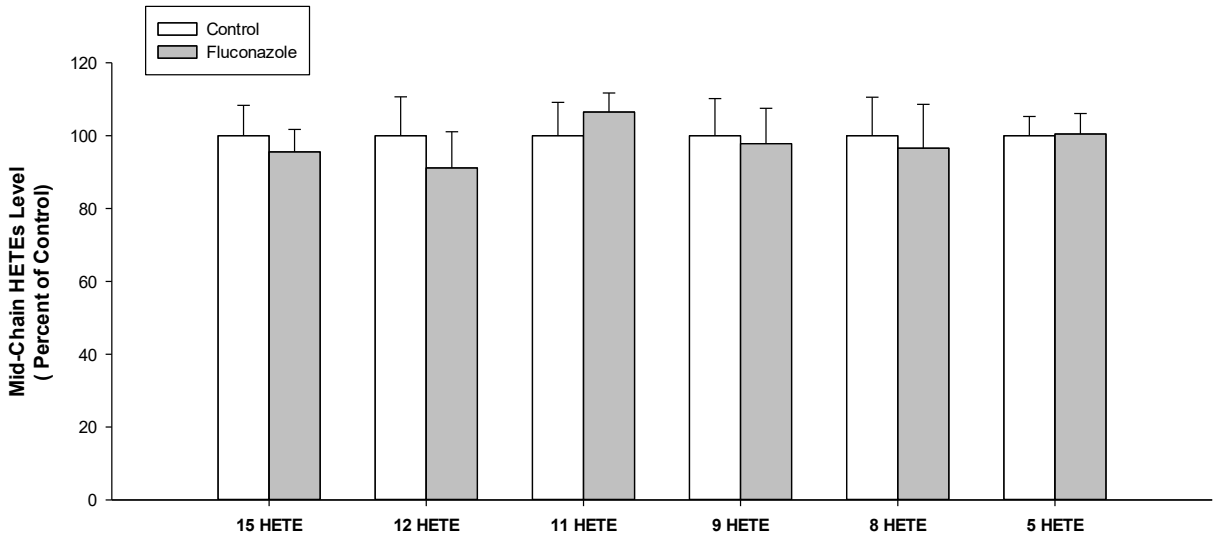

Figure 22: Effect of fluconazole on mid-chain HETEs levels in kidneys.

SD Rats were treated with fluconazole (20mg/kg i.p.) for 24 h. Thereafter, kidneys were harvested and the kidneys microsomes of treated rats were incubated with 100 μM AA. The reaction was started by the addition of 1 mM NADPH and lasted for 30 min. The reaction was terminated by the addition of ice-cold acetonitrile. Metabolites were extracted twice by ethyl acetate and dried using speed vacuum. Residues were reconstituted in acetonitrile and injected into an LC-ESI-MS instrument for the determination of mid-chain HETEs. The values represent mean ± SEM (n=6). *P < 0.05 compared to control.

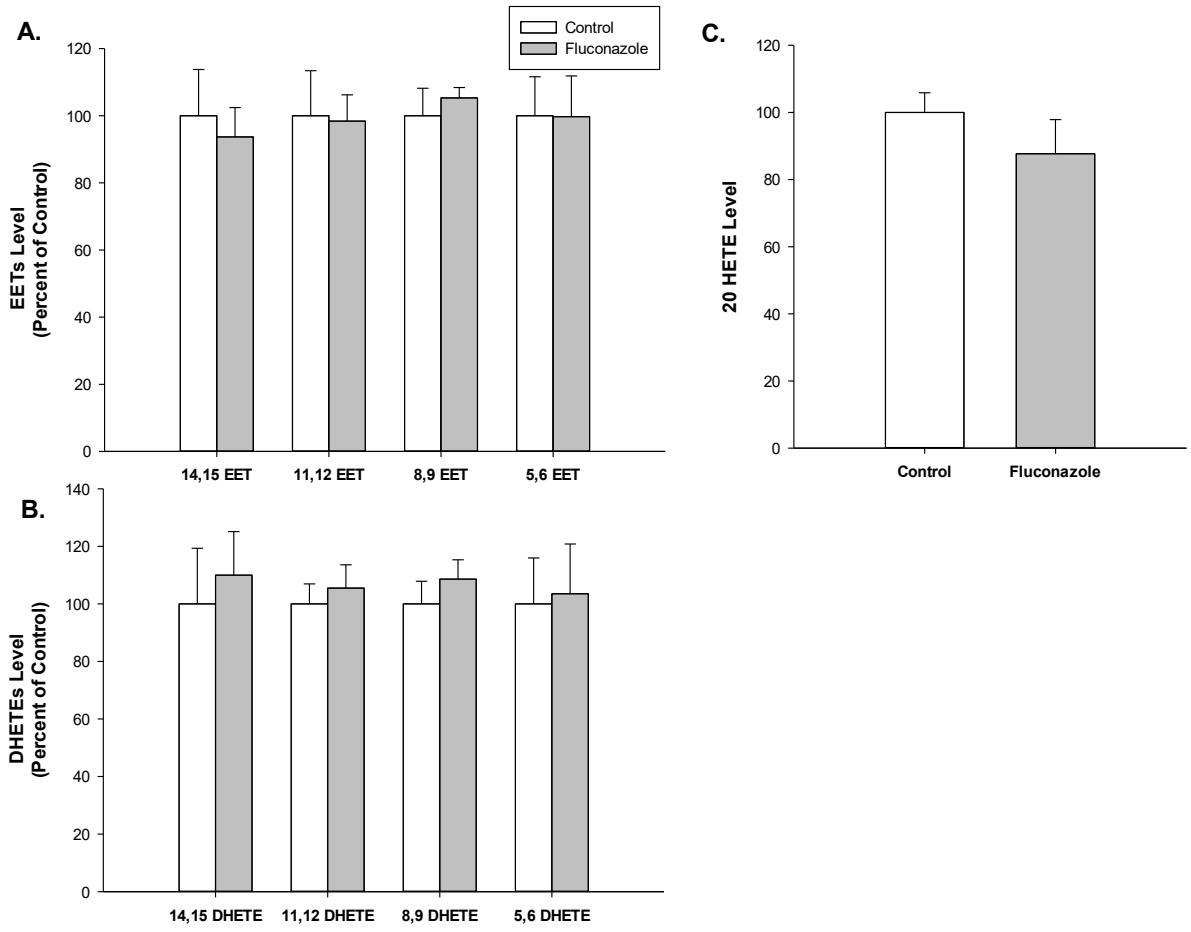

Figure 23: Effect of fluconazole on EETs, DHETEs and 20 HETE levels in kidneys.

SD Rats were treated with fluconazole (20mg/kg i.p.) for 24 h. Thereafter, kidneys were harvested and kidney microsomes of treated rats were incubated with 100 µM AA. The reaction was started by the addition of 1 mM NADPH and lasted for 30 min. The reaction was terminated by the addition of ice-cold acetonitrile. Metabolites were extracted twice by ethyl acetate and dried using speed vacuum. Residues were reconstituted in acetonitrile and injected into an LC-ESI-MS instrument for the determination of (A) EETs, (B) DHETEs and (C) 20-HETE. The values represent mean ± SEM (n=6). *P < 0.05 compared to control. The values represent mean ± SEM (n=6). *P < 0.05 compared to control.

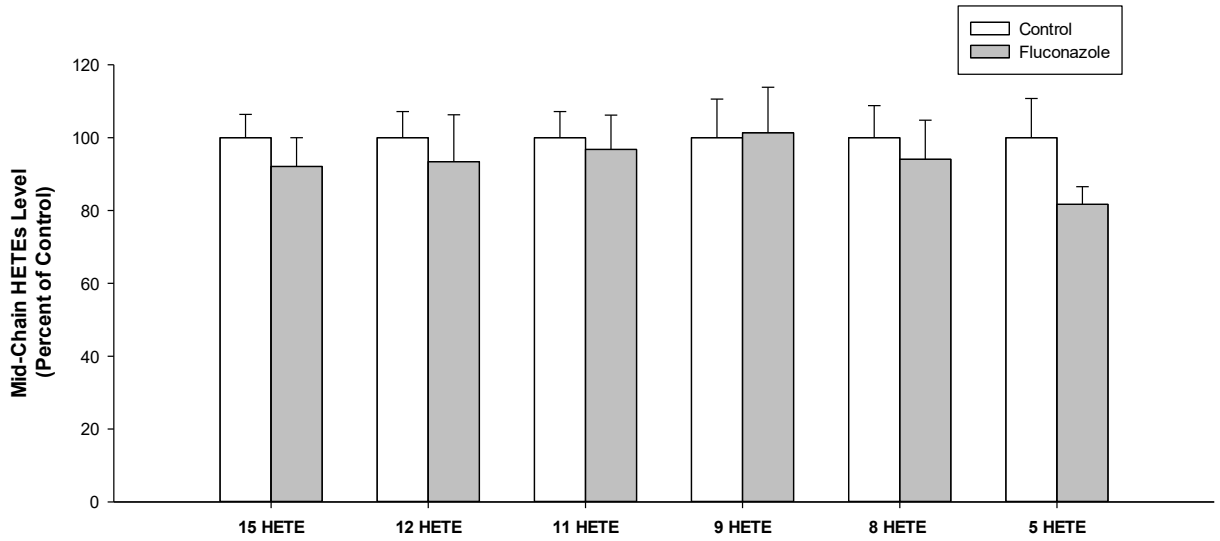

Figure 24: Effect of fluconazole on mid-chain HETEs levels in lungs.

SD Rats were treated with fluconazole (20mg/kg i.p.) for 24 h. Thereafter, lungs were harvested and the lung microsomes of treated rats were incubated with 100 μM AA. The reaction was started by the addition of 1 mM NADPH and lasted for 30 min. The reaction was terminated by the addition of ice-cold acetonitrile. Metabolites were extracted twice by ethyl acetate and dried using speed vacuum. Residues were reconstituted in acetonitrile and injected into an LC-ESI-MS instrument for the determination of mid-chain HETEs. The values represent mean ± SEM (n=6). *$P < 0.05$ compared to control.

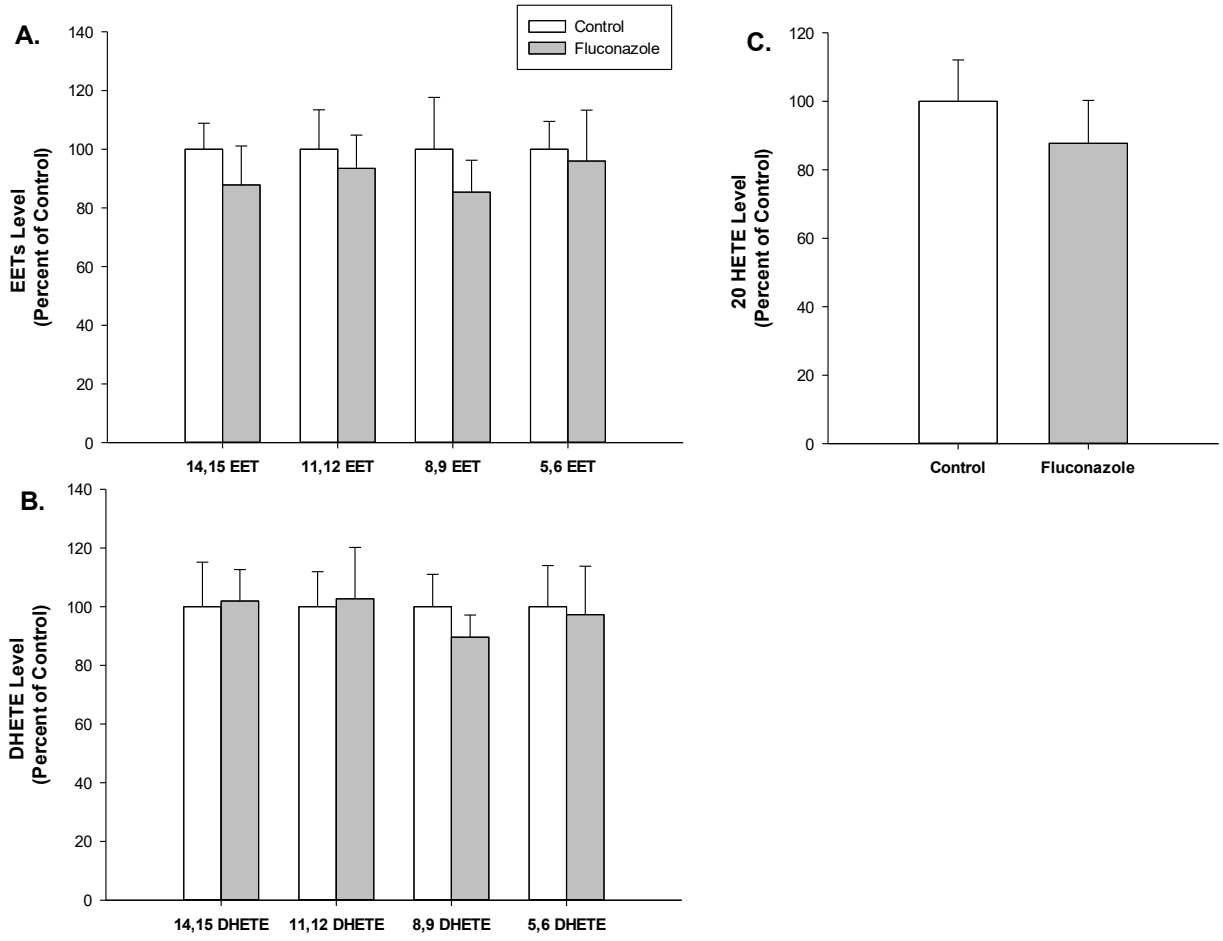

Figure 25: Effect of fluconazole on EETs, DHETEs and 20-HETE levels in lungs.

SD Rats were treated with fluconazole (20mg/kg i.p.) for 24 h. Thereafter, kidneys were harvested and kidney microsomes of treated rats were incubated with 100 µM AA. The reaction was started by the addition of 1 mM NADPH and lasted for 30 min. The reaction was terminated by the addition of ice-cold acetonitrile. Metabolites were extracted twice by ethyl acetate and dried using speed vacuum. Residues were reconstituted in acetonitrile and injected into an LC-ESI-MS instrument for the determination of (A) EETs, (B) DHETEs and (C) 20-HETE. The values represent mean ± SEM (n=6). *P < 0.05 compared to control. The values represent mean ± SEM (n=6). *P < 0.05 compared to control.

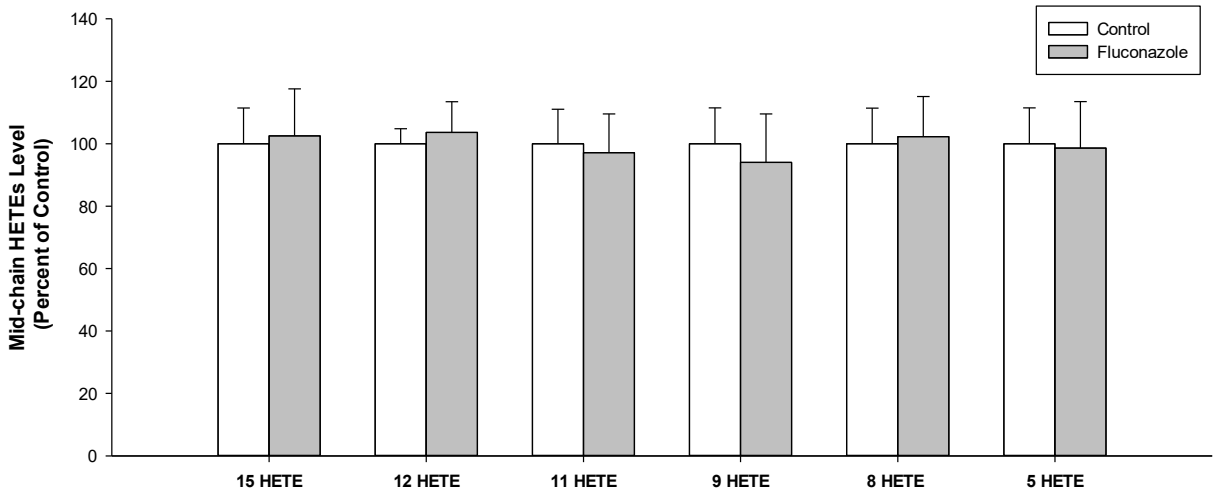

Figure 26: Effect of fluconazole on mid-chain HETEs levels in the brain.

SD Rats were treated with fluconazole (20mg/kg i.p.) for 24 h. Thereafter, brain was harvested and the brain microsomes of treated rats were incubated with 100 μM AA. The reaction was started by the addition of 1 mM NADPH and lasted for 30 min. The reaction was terminated by the addition of ice-cold acetonitrile. Metabolites were extracted twice by ethyl acetate and dried using speed vacuum. Residues were reconstituted in acetonitrile and injected into an LC-ESI-MS instrument for the determination of mid-chain HETEs. The values represent mean ± SEM (n=6). *$P < 0.05$ compared to control.

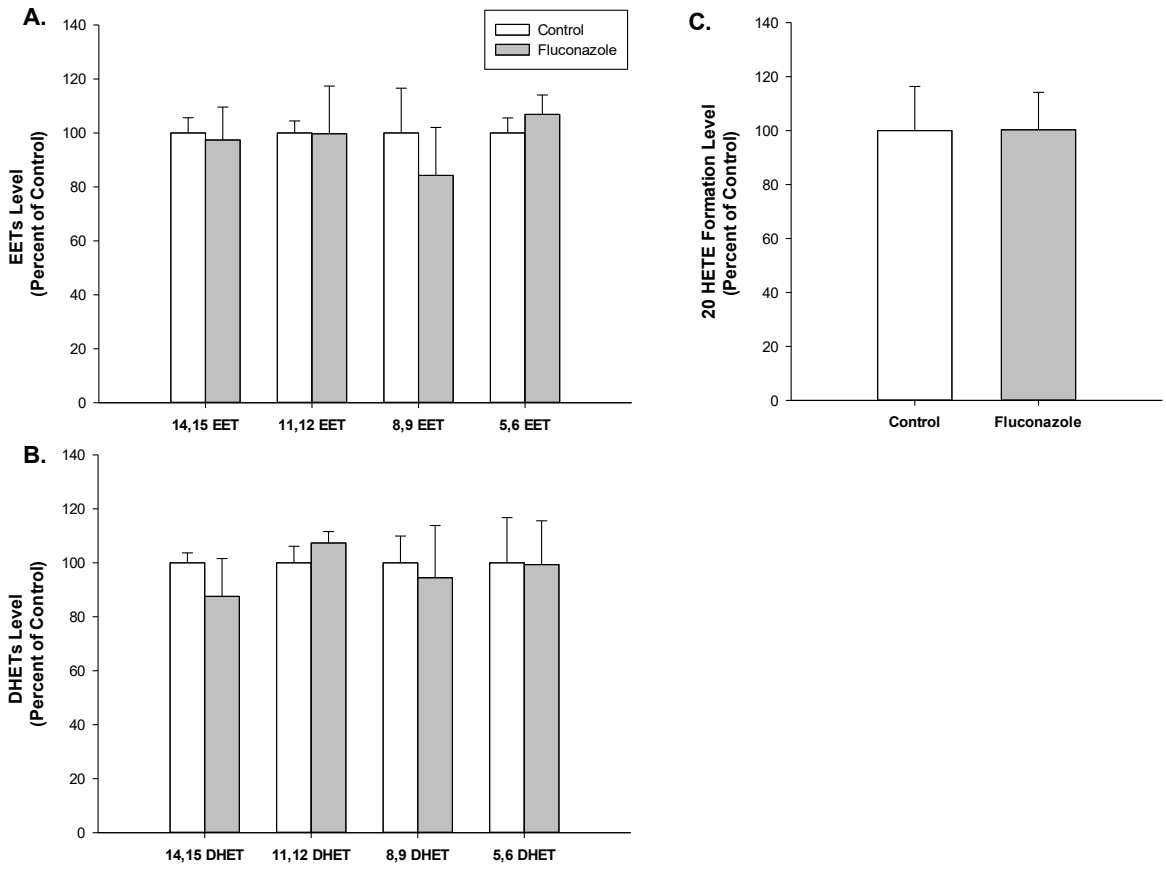

Figure 27: Effect of fluconazole on EETs, DHETEs and 20-HETE levels in the brain.

SD Rats were treated with fluconazole (20mg/kg i.p.) for 24 h. Thereafter, brain was harvested and brain microsomes of treated rats were incubated with 100 μM AA. The reaction was started by the addition of 1 mM NADPH and lasted for 30 min. The reaction was terminated by the addition of ice-cold acetonitrile. Metabolites were extracted twice by ethyl acetate and dried using speed vacuum. Residues were reconstituted in acetonitrile and injected into an LC-ESI-MS instrument for the determination of (A) EETs, (B) DHETEs and (C) 20-HETE. The values represent mean ± SEM (n=6). *P < 0.05 compared to control. The values represent mean ± SEM (n=6). *P < 0.05 compared to control.

Chapter 4: Discussion

Several studies have reported that CYPs enzyme are expressed in cardiovascular tissues and their isoforms have been detected in rat heat and in different regions of human heart (Roman, 2002; Imaoka et al., 2005b; Delozier et al., 2007b). It is been reported that the maintenance of cardiovascular health, including the regulation of vascular tone, extracellular fluid volume, and heart contractility are modulated by the significant role of CYP metabolites (Roman, 2002). One of the major reasons to choose H9c2 and RL-14 cells to study the effect of fluconazole on the expression and activity of CYP enzymes in general instead of isolated cardiomyocyte is the limitations associated with maintaining viable cells to ensure reliable responses. Quantifications of CYP enzymes require a high yield and viability which seems to be difficult to maintain due to the complexity of the isolation procedure as heart muscle cells are firmly connected to each other and it is hard to cleave these connections without injuring the cells (Schlüter and Schreiber, 2005). Rat cardiomyoblast cells, H9c2 cells is a useful tool for cardiovascular research as they can be passaged serially, differentiate, and maintain the characteristics of rat cardiomyocytes (Kimes and Brandt, 1976). However, to investigate the effect of fluconazole on CYP mediated AA metabolites on the human system, incorporating of RL-14 cell in parallel is warranted. RL-14 cells, human fetal ventricular cardiomyocytes, are a commercially available cell line that has been established from non-proliferating primary cultures derived from human fetal heart tissue. Recently (Maayah et al., 2015b), our lab demonstrated that RL-14 cells constitutively express CYP ω-hydroxylases, CYP1A, 1B, 4A and 4F; CYP epoxygenases, CYP2B, 2C and 2J; in addition to soluble epoxide hydrolayse (sEH) at mRNA and protein levels. The basal expression of CYP ω-hydroxylases, epoxygenases and sEH was supported by the ability of RL-14 cells to convert arachidonic acid to its biologically active metabolites, 20-HETEs, 14,15-EET, 11,12-EET, 8,9-EET, 5,6-EET, 14,15-DHET, 11,12-DHET, 8,9-DHET and 5,6-DHET. Furthermore, RL-14 cells express CYP

epoxygenases and ω-hydroxylase at comparable levels to those expressed in adult and fetal human primary cardiomyocytes cells implying the importance of RL-14 cells as a model for studying drug metabolizing enzymes in vitro.

To determine the nontoxic concentration of both fluconazole and Ang II to be used in the current study, we examined the effect of increasing concentrations of both agents alone and in combination on cell viability. Based on MTT assay results and our preciously published reports (El-Sherbeni and El-Kadi, 2016b), a concentration of 50 μM fluconazole was selected for further investigation in H9c2 and RL-14 cells (Figure 3A and B), respectively. As well as for Ang II, we demonestrated (Shoieb and El-Kadi, 2018) that 10 μM was non-toxic and produce a reliable model to investigate cardiac hypertrophy in vitro. Furthermore, the toxicity of the combination of fluconazole and Ang II was determined. Both fluconazole and Ang II alone and in combination are comparable with control (Figure 3C and D), respectevely.

One of the hallmarks of cardiac hypertrophy and heart failure is the increase of β-MHC/α-MHC and BNP expression levels (Barry et al., 2008). The relative ratio of β-MHC to α-MHC has been considered as a good predictor of ventricular dysfunction and was reported to be altered during cardiac hypertrophy (Barry et al., 2008). Disruption of myocardial twitch kinetics is linked to MHC isoform switching from α-MHC to β-MHC leading to decreased in the myosin ATPase enzyme velocity and depletion of the intracellular energy level. This detrimentally affects the systolic function and decreases contractile performances of the cardiomyocytes that significantly contributes to the progression of heart failure (Fatkin et al., 2000; Kiriazis and Kranias, 2000; Locher et al., 2011). On the other hand, natriuretic peptides, such as ANP and BNP are considered as potent endogenous inhibitors of hypertrophy and they are released from cardiomyocytes in response to increased ventricular wall stress (Maayah et al., 2016). BNP has been considered as a

good predictor of heart failure (Maayah and El-Kadi, 2016b) whereas ANP may serve as a marker of cardiac stress but not essentially as a hypertrophic marker, especially at an organ level (Maayah et al., 2015a). Therefore, the protective effect of fluconazole against cellular hypertrophy and its ability to affect the expression of hypertrophic markers was investigated in H9c2 and RL-14 cells. Our results showed that Ang II was able to increase both the ratio of hypertrophic markers β-MHC/α-MHC ratio and BNP mRNA in both cells, H9c2 and RL-14 cells. In agreement with our data, it has been previously reported that Ang II increases both hypertrophic markers (Shoieb and El-Kadi, 2018). Interestingly our data showed that fluconazole was able to protect against Ang II-induced cellular hypertrophy as evidenced by a significant decrease in β-MHC/α-MHC ratio and BNP mRNA expression, in H9c2 and RL-14 and cells, respectively (Figure 4 and 5). Similarly, our data showed that fluconazole was able to restore the increase in cell surface area mediated by Ang II to approximately the normal level (Figure 6A and B) in H9c2 and RL-14 cells, respectively. Taken together, our data demonstrate for the first time that fluconazole confer cardioprotection against Ang II-induced cellular hypertrophy.

The role of CYP1B1 and its associated mid-chain HETE metabolites in the development of cardiac hypertrophy and cardiovascular disease have been reported previously (Korashy and El-Kadi, 2006b; Jenkins et al., 2009; Malik et al., 2012b). Mid-chain HETEs are biologically active eicosanoids resulting from the metabolism of AA by CYP-catalyzed bis-allylic oxidation reaction. The specific role of mid-chain HETEs in the development of cardiovascular events have been reported previously. For example, 5-HETE has been reported to have vasoconstrictive and pro-inflammatory action (Burhop et al., 1988b). 8-HETE has been shown to be detected in cardiac tissue and was reported to have a proliferator and pro-inflammatory action as it directly stimulates human neutrophil chemotaxis in vitro (Burhop et al., 1988b). Furthermore, 12-HETE has been

reported to act as a vasoconstrictor in small renal arteries and induce cellular hypertrophy and fibrosis, while 15-HETE has been proposed to be implicated in heart failure by induction of cardiac fibrosis (Burhop et al., 1988b; El-Sherbeni and El-Kadi, 2014c). Moreover, recent study reported that the rat heart exposed to Ang-II showed an increased expression of CYP1B1 which mediate mid-chain HETEs formation (Jennings et al., 2012). Recently, we demonstrated that CYP1B1 protein expression and the formation of mid-chain HETE metabolites were significantly increased during pressure overload-induced cardiac hypertrophy (El-Sherbeni and El-Kadi, 2014a).

It is worth mentioning that mid-chain HETEs activate both MAPK and NF-κB signaling pathways that are involved in the development of cardiac hypertrophy (Maayah and El-Kadi, 2016a). MAPK are intracellular signal transduction factors that are critically involved in the regulation of signaling pathways, ultimately leading to cardiac hypertrophy and heart failure (Zhang et al., 2003). The three best-characterized MAPK include p38, JNK and ERK1/2. Promoting apoptosis with cardiac dilation and dysfunction are the net result of persistent activation of p38 and JNK. ERK1/2 has been proposed to regulate smooth muscle contraction and to promote cellular hypertrophy (Pearson et al., 2001). Regarding NF-κB, Previous studies have indicated the pathophysiological role of NF-κB the development of cardiac hypertrophy (Hirotani et al., 2002). Activation of NF-κB was reported in failing human heart (Grabellus et al., 2002). Moreover, cardiac hypertrophy induced by to aortic banding and chronic infusion of Ang-II was attenuated by blocking of NF-κB, indicating a mojor role of NF-κB as a signaling pathway in the regulation of cardiac hypertrophy (Kawano et al., 2005).

Taken together, it seems that the inhibition of CYP1B1 and its associated mid-chain HETE metabolites would protect against cardiac hypertrophy induced by Ang II. Based on the evidences mentioned earlier, this protective effect could be mediated through MAPK and NF-κB signaling

pathways. Therefore, we examined the capacity of fluconazole to inhibit CYP1B1 and its associated mid-chain HETEs metabolites in an in vitro model of Ang II-induced cellular hypertrophy.

Our data show, for the first time, that fluconazole significantly decreased the formation levels of mid-chain HETEs namely 15-, 12-, 11-, 9-, 8- and 5-HETEs in H9c2 and RL-14 cells. Interestingly, fluconazole reversed the increase levels of 12- and 5-HETEs mediated by Ang II in H9c2 and 15-, 12- and 5-HETE levels in RL-14 cells (Figure 7 and 8), respectively. This novel finding suggest that fluconazole protect against Ang II-induced cellular hypertrophy by inhibiting the formation level of mid-chain HETEs.

Great deal of evidence supports the role of CYP1B1 enzyme in the formation of mid-chain HETEs and development of cardiac hypertrophy. One of the major metabolic pathways involved in the formation of midchain HETEs is CYP1B1 (Konkel and Schunck, 2011). CYP1B1 is constitutively expressed in the cardiac tissue, and several reports have confirmed the association between this enzyme and several cardiovascular diseases (Zordoky and El-Kadi, 2008b; Chung et al., 2012). For example, Cyp1b1-null mice blood pressure level was reduced in comparison with wild-type animal in Ang II induced hypertension model (Jennings et al., 2010). Protein expression and catalytic activity of CYP1B1 were significantly increased in three different experimental models of cardiac hypertrophy, including pressure overload-induced, isoproterenol-induced, and Ang II-induced cardiac hypertrophy (Jennings et al., 2010; El-Sherbeni and El-Kadi, 2014b; Maayah et al., 2017) Recently, we demonstrated that 2-methoxyestradiol, a selective CYP1B1 inhibitor, protected against pressure overload-induced left ventricular hypertrophy in rats (Maayah et al., 2018). Furthermore, it has been demonstrated previously that the recombinant CYP1B1 enzyme catalyzes the formation of mid-chain HETEs (Choudhary et al., 2004c; El-Sherbeni and El-Kadi,

2014b). The importance of CYP1B1 relies on the fact that the levels of CYP1B1 and mid-chain HETEs were induced at pre-hypertrophic and hypertrophic stages, implying that CYP1B1 as a promising target in the treatment of cardiac hypertrophy (Maayah et al., 2016). Furthermore, it was shown that CYP inhibitors such as SKF-525A persuade a cell cycle delay and inhibit cellular hypertrophy (Nieves and Moreno, 2006). The inhibition of cellular growth in response to SKF-525A was associated with CYP inhibition and the subsequent impairment of synthesis of mid-chain HETEs. Interestingly, exogenous addition of mid-chain HETEs reversed the effects of SKF-525A confirming an important role of CYP in the regulation of mid-chain HETEs (Nieves and Moreno, 2006). Moreover, we recently reported that CRISPR-CYP1B1 delivery led to a significant increase in the formation of 15-, 12- and 8-, 11- and 5-HETE, implying that CYP1B1 is directly involved in the formation of these metabolites (Maayah et al., 2017). Furthermore, CYP1B1-siRNA was able to significantly inhibit the formation of mid-chain HETEs confirming the important role of CYP1B1 in the formation of theses metabolites (Maayah et al., 2017).

Based on the above information, it seems to be important to investigate the effect of CYP1B1 modulator such as fluconazole on the formation of mid-chain HETEs and the cellular hypertrophy mediated by Ang II. We previously reported that Ang II significantly increase the expression of CYP1B1 in hypertrophied rat hearts (Elkhatali et al., 2015). However, the gene and protein expression of CYP1B1 has never been investigated before in an in vitro model of Ang II-induced cellular hypertrophy. For this reason, we investigated the effect of fluconazole on Ang II-induced expression of CYP1B1 at mRNA and protein level. Our data showed that Ang II significantly increase the gene and protein expression of CYP1B1 in H9c2 and RL-14 cells (Figure 9 and 10; Figure 11 A and B), respectively. The novel finding of this study is that fluconazole alone significantly inhibited the gene and protein expression of CYP1B1, suggesting that fluconazole

inhibitory effect on CYP1B1 is at both transcriptional and translational level. Interestingly, fluconazole inhibited the Ang II-mediated induction of CYP1B1 at mRNA and protein expression. It is been previously reported that CYP1B1 is regulated through AhR transcriptional factor (Maayah and El-Kadi, 2016c), which may suggest that fluconazole inhibit CYP1B1 gene expression through AhR-dependent mechanism. This finding strongly suggests that the observed reduction of mid-chain HETEs formation level following fluconazole treatment is mediated through its inhibitory effect on CYP1B1.

To further examine whether the effect obtained at mRNA in response to fluconazole and Ang II treatment is translated into functional catalytic activity, we investigated the effect of fluconazole in the presence and absence of Ang II on CYP1B1. Our data demonstrated for the first time that fluconazole inhibits the catalytic activity of CYP1B1 in H9c2 and RL-14 cells (Figure 12 A and B), respectively. Furthermore, to confirm the inhibitory effect of fluconazole on CYP1B1 catalytic activity observed in H9c2 and RL-14 cells, we examined the direct effect fluconazole on the human recombinant CYP1B1 enzyme activity. Our data showed that fluconazole inhibits the catalytic activity of human recombinant CYP1B1 enzyme in a concentration-dependent manner (Figure 13). This novel finding strongly suggest that fluconazole protect against Ang II induced cellular hypertrophy by decreasing the level of mid-chain HETEs through the inhibition of CYP1B1.

The in vitro effect of fluconazole prompted us to examine whether fluconazole will have the same effect in vivo. For this purpose, SD rats were utilized to answer this important question. The in vivo concentration of fluconazole used in the current study was chosen based on previous study shown that fluconazole in a dose up to 100mg/kg did not show any changes on ALT/ALP levels in the liver (Somchit et al., 2004). Based on this, we have decided to investigate the effect of fluconazole using 20 mg/kg IP as single dose. The dose used in the current study is within both

safety and therapeutic margins that were reported in different in vivo investigations (Martinez et al., 1999; Aoyama et al., 2005; Somchit et al., 2006).

CYPs enzymes and their AA metabolites play differential roles in most cardiac diseases; some of these metabolites are cadiotoxic, others showed cardioprotective effects (Westphal et al., 2015; Zu et al., 2016). We have discussed earlier the protective role of inhibiting mid-chain HETEs in the development of cardiac hypertrophy. Furthermore, we previously reported that fenofibrate-mediated increase of EETs formation is protective against cardiac hypertrophy induced by isoproterenol, suggesting that EETs modulation is an important factor in the development of cardiac hypertrophy (Althurwi et al., 2013a). The cardioprotective metabolites, EETs are metabolized by sEH enzyme to their corresponding non-active metabolites, DHETs. We have previously demonstrated that sEH inhibitor, TUPS protects against isoproterenol-induced cardiac hypertrophy (Althurwi et al., 2013a). This indicates that EETs modulation is significant in the development in cardiac hypertrophy. Moreover, 20-HETE plays a significant role in the development of cardiac hypertrophy (Elshenawy et al., 2013b). In addition, 20-HETE has been shown to activate NF-κB and increase the production of inflammatory cytokines in human endothelial cells (Ishizuka et al., 2008). Recently, 20-HETE has been shown to induce apoptosis in neonatal rat cardiomyocytes which further confirms its detrimental role in the development of cardiac hypertrophy (Bao et al., 2011). Based on the previous information and the fact that fluconazole effect on AA metabolites has never been investigated in vivo before, we examined the effect of fluconazole on these metabolites on SD rats.

One of the most striking finding of the current study is that fluconazole significantly inhibited the formation of mid-chain HETEs in the heart; specifically, 15-, 12-, 8 -and 5-HETEs (Figure 14). These metabolites as discussed earlier play a significant role in the development of cardiac

hypertrophy. Interestingly, the levels of EETs, DHETEs and 20-HETE were not significantly altered by fluconazole treatment (Figure 15 A, B and C). The fact that fluconazole only modulated mid-chain HETEs in vivo is in agreement with our in vitro findings in H9c2 and RL-14 cells and strongly confirm the cardiprotective effect of fluconazole. Furthermore, fluconazole significantly inhibited the gene expression of CYP1B1 and CYP2C23 in rat heart (Figure 16). This is an interesting finding since fluconazole only inhibited the gene expression of CYP1B1 in vitro. Furthermore, to explore whether fluconazole will confer this inhibition on protein expression; as (Figure 17 A) shows, fluconazole significantly inhibits the protein expression of CP1B1 and CYP2C23. This discrepancy could be explained by the lack of other endogenous mediators in cardiac cell lines or the indirect effect of fluconazole. To further explain the lack of change on EETs levels which have been reported to be formed by CYP2C family (Roman, 2002; El-Sherbeni and El-Kadi, 2017b), the epoxygenases activity was assessed and was not altered by fluconazole (Figure 18A) suggesting that the inhibition of CYP2C23 does not affect epoxygenase metabolites in the heart. To further examine whether the effect obtained with CYP1B1 at mRNA and protein levels in response to fluconazole treatment is translated into functional catalytic activity, our data showed that fluconazole significantly inhibited the catalytic activity of CYP1B1 (Figure 17 B) using a specific CYP1B1 substrate; CEE. This indeed is another novel finding that confirm our data with H9c2 and RL-14 cells and strongly suggest that fluconazole inhibition of mid-chain HETEs is mediated by the inhibition of CYP1B1 in the heart at translational, transcriptional and activity levels.

To investigate whether the effect of fluconazole is specific to the heart, we investigated the levels of mid-chain HETEs in the liver, kidney, lung and brain after treatment with fluconazole. Our data showed that fluconazole significantly inhibited the formation level of 5-HETE only and has no

effect on EETs, DHETE and 20-HETE (Figure 19, Figure 20 A, B and C), respectively. Moreover, our data showed that fluconazole significantly inhibited the gene and protein expression of CYP1B1 and CYP2C23 (Figure 21 A and B), respectively. This suggest that inhibition of CYP1B1 at translational and transcriptional level does not translate to functional inhibition on all mid-chain HETEs. This could be explained by the fact that CYP1B1 is highly expressed in the heart in comparison to other organs (Zordoky and El-Kadi, 2008b). Furthermore, the effect of fluconazole on kidneys, lungs ang brain showed for the first time that fluconazole does not affect the mid-chain HETEs, EETs, DHETE and 20-HETE levels in the kidney, lung and brain (Figure 22 ,23 A, B and C; Figure 24, 25A, B and C; Figure 26, 27A, B and C), respectively. This strongly suggest that fluconazole selectively inhibits the formation of mid-chain HETEs through modulation of CYP1B1 dependent mechanism in the heart.

General conclusion

One of the major risk factor of heart failure is cardiac hypertrophy. Heart failure is considered one of the major causes of morbidity and mortality in adults. Thus, a great effort is made toward the management of heart failure. Most of the approaches focus on the management and halting the inevitable outcome of heart failure (Kaye and Krum, 2007). Therefore, there is a need to explore and target the molecular mechanisms involved in the pathogenesis of cardiac hypertrophy. The role of CYPs mediated AA metabolism in the development of cardiac hypertrophy has caught the attention recently and indeed showed a promising finding regarding their role in the development of cardiac hypertrophy (El-Sherbeni and El-Kadi, 2014b). Mid-chain HETEs have been reported to play a major role in the development of cardiac hypertrophy (Maayah and El-Kadi, 2016c). Focusing in targeting these metabolites and the CYPs involved in their formation is a promising approach and need further investigation. Therefore, this work has been focused on targeting

CYP1B1 and its associated mid-chain HETEs metabolites in an effort to explore their role in the prevention of cardiac hypertrophy.

Our results demonstrated for the first time that fluconazole protects against Ang II-induced cellular hypertrophy in H9c2 and RL-14 cells. This protection is manifested by the ability of fluconazole to attenuate the increase in mid-chain HETEs formation-mediated by Ang II. This protective effect was associated with a significant decrease in cell surface area and hypertrophic markers gene expression. Moreover, fluconazole was able to inhibit CYP1B1 at gene, protein and activity level. The other novel finding of this study is that fluconazole protective effect is selective to the heart. Also, our data showed that fluconazole inhibits mid-chain HETEs formation through inhibiting CYP1B1 at gene, protein and activity levels in the heart. These finding strongly suggest a promising role of fluconazole in prevention of the development of cardiac hypertrophy.

Future directions

The results of the present work have highlighted the protective effect fluconazole and the role of AA metabolites in the pathogenesis of cardiac hypertrophy. However, more studies are needed to confirm these findings and to further address the underlying molecular basis of cardiac hypertrophy.

1) To investigate the molecular mechanism by which fluconazole confer cardioprotection
2) To identify and understand the molecular mechanism involved in fluconazole inhibition of CYP1B1.
3) To determine the cardioprotective effect of fluconazole in an in vivo model of cardiac hypertrophy including volume- or pressure-overload induced cardiac hypertrophy.
4) To determine whether fluconazole can reverse an established cardiac hypertrophy.

5. References

Aboutabl, M.E., Zordoky, B.N.M., and El-Kadi, A.O.S. (2009). 3-methylcholanthrene and benzo(a)pyrene modulate cardiac cytochrome P450 gene expression and arachidonic acid metabolism in male Sprague Dawley rats. Br. J. Pharmacol. *158*: 1808–19.

Aguiar, M., Masse, R., and Gibbs, B.F. (2005). Regulation of Cytochrome P450 by Posttranslational Modification. Drug Metab. Rev. *37*: 379–404.

Alsaad, A.M.S., Zordoky, B.N.M., Tse, M.M.Y., and El-Kadi, A.O.S. (2013). Role of cytochrome P450–mediated arachidonic acid metabolites in the pathogenesis of cardiac hypertrophy. Drug Metab. Rev. *45*: 173–195.

Althurwi, H.N., Tse, M.M., Abdelhamid, G., Zordoky, B.N., Hammock, B.D., and El-Kadi, A.O. (2013a). Soluble epoxide hydrolase inhibitor, TUPS, protects against isoprenaline-induced cardiac hypertrophy. Br. J. Pharmacol. *168*: 1794–1807.

Althurwi, H.N., Tse, M.M.Y., Abdelhamid, G., Zordoky, B.N.M., Hammock, B.D., and El-Kadi, A.O.S. (2013b). Soluble epoxide hydrolase inhibitor, TUPS, protects against isoprenaline-induced cardiac hypertrophy. Br. J. Pharmacol. *168*: 1794–807.

Anzenbacher, P., and Anzenbacherová, E. (2001). Cytochromes P450 and metabolism of xenobiotics. Cell. Mol. Life Sci. *58*: 737–47.

Aoyama, T., Ogata, K., Shimizu, M., Hatta, S., Masuhara, K., Shima, Y., et al. (2005). Pharmacokinetics of fluconazole and fosfluconazole after intraperitoneal administration to peritoneal dialysis rats. Drug Metab. Pharmacokinet. *20*: 485–90.

Bao, Y., Wang, X., Li, W., Huo, D., Shen, X., Han, Y., et al. (2011). 20-Hydroxyeicosatetraenoic acid induces apoptosis in neonatal rat cardiomyocytes through mitochondrial-dependent pathways.

J. Cardiovasc. Pharmacol. *57*: 294–301.

Barry, S.P., Davidson, S.M., and Townsend, P.A. (2008). Molecular regulation of cardiac hypertrophy. Int. J. Biochem. Cell Biol. *40*: 2023–39.

Benjamin, E.J., Blaha, M.J., Chiuve, S.E., Cushman, M., Das, S.R., Deo, R., et al. (2017). Heart Disease and Stroke Statistics—2017 Update: A Report From the American Heart Association. Circulation *135*: e146–e603.

Bernardo, B.C., Weeks, K.L., Pretorius, L., and McMullen, J.R. (2010). Molecular distinction between physiological and pathological cardiac hypertrophy: experimental findings and therapeutic strategies. Pharmacol. Ther. *128*: 191–227.

Bertrand-Thiebault, C., Ferrari, L., Boutherin-Falson, O., Kockx, M., Desquand-Billiald, S., Fichelle, J.-M., et al. (2004). Cytochromes P450 are differently expressed in normal and varicose human saphenous veins: linkage with varicosis. Clin. Exp. Pharmacol. Physiol. *31*: 295–301.

Bièche, I., Narjoz, C., Asselah, T., Vacher, S., Marcellin, P., Lidereau, R., et al. (2007). Reverse transcriptase-PCR quantification of mRNA levels from cytochrome (CYP)1, CYP2 and CYP3 families in 22 different human tissues. Pharmacogenet. Genomics *17*: 731–42.

Braunwald, E., and Bristow, M.R. (2000). Congestive heart failure: fifty years of progress. Circulation *102*: IV14-23.

Burhop, K.E., Selig, W.M., and Malik, A.B. (1988a). Monohydroxyeicosatetraenoic acids (5-HETE and 15-HETE) induce pulmonary vasoconstriction and edema. Circ. Res. *62*: 687–98.

Burhop, K.E., Selig, W.M., and Malik, A.B. (1988b). Monohydroxyeicosatetraenoic acids (5-HETE and 15-HETE) induce pulmonary vasoconstriction and edema. Circ. Res. *62*: 687–98.

Carreño, J.E., Apablaza, F., Ocaranza, M.P., and Jalil, J.E. (2006). [Cardiac hypertrophy: molecular and cellular events]. Rev. Esp. Cardiol. *59*: 473–86.

Certíková Chábová, V., Walkowska, A., Kompanowska-Jezierska, E., Sadowski, J., Kujal, P., Vernerová, Z., et al. (2010). Combined inhibition of 20-hydroxyeicosatetraenoic acid formation and of epoxyeicosatrienoic acids degradation attenuates hypertension and hypertension-induced end-organ damage in Ren-2 transgenic rats. Clin. Sci. (Lond). *118*: 617–32.

Chaudhary, K.R., Batchu, S.N., and Seubert, J.M. (2009). Cytochrome P450 enzymes and the heart. IUBMB Life *61*: 954–60.

Choudhary, D., Jansson, I., Stoilov, I., Sarfarazi, M., and Schenkman, J.B. (2004a). Metabolism of retinoids and arachidonic acid by human and mouse cytochrome P450 1b1. Drug Metab. Dispos. *32*: 840–7.

Choudhary, D., Jansson, I., Stoilov, I., Sarfarazi, M., and Schenkman, J.B. (2004b). Metabolism of retinoids and arachidonic acid by human and mouse cytochrome P450 1b1. Drug Metab. Dispos. *32*: 840–7.

Choudhary, D., Jansson, I., Stoilov, I., Sarfarazi, M., and Schenkman, J.B. (2004c). Metabolism of retinoids and arachidonic acid by human and mouse cytochrome P450 1b1. Drug Metab. Dispos. *32*: 840–7.

Chung, E., Heimiller, J., and Leinwand, L.A. (2012). Distinct cardiac transcriptional profiles defining pregnancy and exercise. PLoS One *7*: e42297.

Crowley, S.D., Tharaux, P.-L., Audoly, L.P., and Coffman, T.M. (2004). Exploring type I angiotensin (AT1) receptor functions through gene targeting. Acta Physiol. Scand. *181*: 561–70.

Cyrus, T., Witztum, J.L., Rader, D.J., Tangirala, R., Fazio, S., Linton, M.F., et al. (1999). Disruption of the 12/15-lipoxygenase gene diminishes atherosclerosis in apo E-deficient mice. J. Clin. Invest. *103*: 1597–604.

Debruyne, D. (1997). Clinical Pharmacokinetics of Fluconazole in Superficial and Systemic Mycoses. Clin. Pharmacokinet. *33*: 52–77.

Delozier, T.C., Kissling, G.E., Coulter, S.J., Dai, D., Foley, J.F., Bradbury, J.A., et al. (2007a). Detection of human CYP2C8, CYP2C9, and CYP2J2 in cardiovascular tissues. Drug Metab. Dispos. *35*: 682–8.

Delozier, T.C., Kissling, G.E., Coulter, S.J., Dai, D., Foley, J.F., Bradbury, J.A., et al. (2007b). Detection of human CYP2C8, CYP2C9, and CYP2J2 in cardiovascular tissues. Drug Metab. Dispos. *35*: 682–8.

Dubey, R.K., Jackson, E.K., Gillespie, D.G., Rosselli, M., Barchiesi, F., Krust, A., et al. (2005). Cytochromes 1A1/1B1- and catechol-O-methyltransferase-derived metabolites mediate estradiol-induced antimitogenesis in human cardiac fibroblast. J. Clin. Endocrinol. Metab. *90*: 247–55.

Dubey, R.K., Jackson, E.K., Gillespie, D.G., Zacharia, L.C., and Imthurn, B. (2004). Catecholamines block the antimitogenic effect of estradiol on human coronary artery smooth muscle cells. J. Clin. Endocrinol. Metab. *89*: 3922–31.

Dyck, J.R.B., and Lopaschuk, G.D. (2006). AMPK alterations in cardiac physiology and pathology: enemy or ally? J. Physiol. *574*: 95–112.

El-Sherbeni, A.A., and El-Kadi, A.O.S. (2014a). Alterations in cytochrome P450-derived arachidonic acid metabolism during pressure overload-induced cardiac hypertrophy. Biochem.

Pharmacol. *87*: 456–66.

El-Sherbeni, A.A., and El-Kadi, A.O.S. (2014b). Alterations in cytochrome P450-derived arachidonic acid metabolism during pressure overload-induced cardiac hypertrophy. Biochem. Pharmacol. *87*: 456–66.

El-Sherbeni, A.A., and El-Kadi, A.O.S. (2014c). Characterization of arachidonic acid metabolism by rat cytochrome P450 enzymes: the involvement of CYP1As. Drug Metab. Dispos. *42*: 1498–507.

El-Sherbeni, A.A., and El-Kadi, A.O.S. (2014d). The role of epoxide hydrolases in health and disease. Arch. Toxicol. *88*: 2013–32.

El-Sherbeni, A.A., and El-Kadi, A.O.S. (2016a). Repurposing Resveratrol and Fluconazole To Modulate Human Cytochrome P450-Mediated Arachidonic Acid Metabolism. Mol. Pharm. *13*: 1278–88.

El-Sherbeni, A.A., and El-Kadi, A.O.S. (2016b). Repurposing Resveratrol and Fluconazole To Modulate Human Cytochrome P450-Mediated Arachidonic Acid Metabolism. Mol. Pharm. *13*: 1278–1288.

El-Sherbeni, A.A., and El-Kadi, A.O.S. (2017a). Microsomal cytochrome P450 as a target for drug discovery and repurposing. Drug Metab. Rev. *49*: 1–17.

El-Sherbeni, A.A., and El-Kadi, A.O.S. (2017b). Microsomal cytochrome P450 as a target for drug discovery and repurposing. Drug Metab. Rev. *49*: 1–17.

Elbekai, R.H., and El-Kadi, A.O.S. (2006). Cytochrome P450 enzymes: Central players in cardiovascular health and disease. Pharmacol. Ther. *112*: 564–587.

Elkhatali, S., El-Sherbeni, A.A., Elshenawy, O.H., Abdelhamid, G., and El-Kadi, A.O.S. (2015). 19-Hydroxyeicosatetraenoic acid and isoniazid protect against angiotensin II-induced cardiac hypertrophy. Toxicol. Appl. Pharmacol. *289*: 550–9.

Elkhatali, S., Maayah, Z.H., El-Sherbeni, A.A., Elshenawy, O.H., Abdelhamid, G., Shoieb, S.M., et al. (2017). Inhibition of Mid-chain HETEs Protects Against Angiotensin II-induced Cardiac Hypertrophy. J. Cardiovasc. Pharmacol. *70*: 16–24.

Elshenawy, O.H., Anwar-Mohamed, A., and El-Kadi, A.O.S. (2013a). 20-Hydroxyeicosatetraenoic acid is a potential therapeutic target in cardiovascular diseases. Curr. Drug Metab. *14*: 706–19.

Elshenawy, O.H., Anwar-Mohamed, A., and El-Kadi, A.O.S. (2013b). 20-Hydroxyeicosatetraenoic acid is a potential therapeutic target in cardiovascular diseases. Curr. Drug Metab. *14*: 706–19.

Fagard, R.H. (1997). Impact of different sports and training on cardiac structure and function. Cardiol. Clin. *15*: 397–412.

Fatkin, D., McConnell, B.K., Mudd, J.O., Semsarian, C., Moskowitz, I.G., Schoen, F.J., et al. (2000). An abnormal Ca(2+) response in mutant sarcomere protein-mediated familial hypertrophic cardiomyopathy. J. Clin. Invest. *106*: 1351–9.

Fulton, D., Mahboubi, K., McGiff, J.C., and Quilley, J. (1995). Cytochrome P450-dependent effects of bradykinin in the rat heart. Br. J. Pharmacol. *114*: 99–102.

Fyhrquist, F., Metsärinne, K., and Tikkanen, I. (1995). Role of angiotensin II in blood pressure regulation and in the pathophysiology of cardiovascular disorders. J. Hum. Hypertens. *9 Suppl 5*:

S19-24.

Geetha, A., Marar, T., and Devi, C.S. (1991). Effect of alpha-tocopherol on doxorubicin-induced changes in rat liver and heart microsomes. Indian J. Exp. Biol. *29*: 782–5.

Gerdes, A.M. (2002). Cardiac myocyte remodeling in hypertrophy and progression to failure. J. Card. Fail. *8*: S264–S268.

Grabellus, F., Levkau, B., Sokoll, A., Welp, H., Schmid, C., Deng, M.C., et al. (2002). Reversible activation of nuclear factor-kappaB in human end-stage heart failure after left ventricular mechanical support. Cardiovasc. Res. *53*: 124–30.

Gradman, A.H., and Alfayoumi, F. (2006). From Left Ventricular Hypertrophy to Congestive Heart Failure: Management of Hypertensive Heart Disease. Prog. Cardiovasc. Dis. *48*: 326–341.

Griffin, S.A., Brown, W.C., MacPherson, F., McGrath, J.C., Wilson, V.G., Korsgaard, N., et al. (1991). Angiotensin II causes vascular hypertrophy in part by a non-pressor mechanism. Hypertens. (Dallas, Tex. 1979) *17*: 626–35.

Gross, E.R., Nithipatikom, K., Hsu, A.K., Peart, J.N., Falck, J.R., Campbell, W.B., et al. (2004). Cytochrome P450 omega-hydroxylase inhibition reduces infarct size during reperfusion via the sarcolemmal KATP channel. J. Mol. Cell. Cardiol. *37*: 1245–9.

Guengerich, F.P. (2003). Cytochromes P450, drugs, and diseases. Mol. Interv. *3*: 194–204.

Gutiérrez, S.H., Kuri, M.R., and Castillo, E.R. del (2008). Cardiac role of the transcription factor NF-kappaB. Cardiovasc. Hematol. Disord. Drug Targets *8*: 153–60.

He, Z., Zhang, X., Chen, C., Wen, Z., Hoopes, S.L., Zeldin, D.C., et al. (2015). Cardiomyocyte-specific expression of CYP2J2 prevents development of cardiac remodelling induced by

angiotensin II. Cardiovasc. Res. *105*: 304–17.

Heineke, J., and Molkentin, J.D. (2006). Regulation of cardiac hypertrophy by intracellular signalling pathways. Nat. Rev. Mol. Cell Biol. *7*: 589–600.

Hill-Eubanks, D.C., Gomez, M.F., Stevenson, A.S., and Nelson, M.T. (2003). NFAT regulation in smooth muscle. Trends Cardiovasc. Med. *13*: 56–62.

Hirotani, S., Otsu, K., Nishida, K., Higuchi, Y., Morita, T., Nakayama, H., et al. (2002). Involvement of nuclear factor-kappaB and apoptosis signal-regulating kinase 1 in G-protein-coupled receptor agonist-induced cardiomyocyte hypertrophy. Circulation *105*: 509–15.

Ho, Y.L., Wu, C.C., Lin, L.C., Huang, C.H., Chen, W.J., Chen, M.F., et al. (1998). Assessment of the coronary artery disease and systolic dysfunction in hypertensive patients with the dobutamine-atropine stress echocardiography: effect of the left ventricular hypertrophy. Cardiology *89*: 52–8.

Honn, K. V, Nelson, K.K., Renaud, C., Bazaz, R., Diglio, C.A., and Timar, J. (1992). Fatty acid modulation of tumor cell adhesion to microvessel endothelium and experimental metastasis. Prostaglandins *44*: 413–29.

Hunter, J.A., Finkbeiner, W.E., Nadel, J.A., Goetzl, E.J., and Holtzman, M.J. (1985). Predominant generation of 15-lipoxygenase metabolites of arachidonic acid by epithelial cells from human trachea. Proc. Natl. Acad. Sci. U. S. A. *82*: 4633–7.

Ichihara, S., Senbonmatsu, T., Price, E., Ichiki, T., Gaffney, F.A., and Inagami, T. (2001). Angiotensin II type 2 receptor is essential for left ventricular hypertrophy and cardiac fibrosis in chronic angiotensin II-induced hypertension. Circulation *104*: 346–51.

Ikeda, Y., Aihara, K.-I., Sato, T., Akaike, M., Yoshizumi, M., Suzaki, Y., et al. (2005). Androgen

receptor gene knockout male mice exhibit impaired cardiac growth and exacerbation of angiotensin II-induced cardiac fibrosis. J. Biol. Chem. *280*: 29661–6.

Imaoka, S., Hashizume, T., and Funae, Y. (2005a). Localization of rat cytochrome P450 in various tissues and comparison of arachidonic acid metabolism by rat P450 with that by human P450 orthologs. Drug Metab. Pharmacokinet. *20*: 478–84.

Imaoka, S., Hashizume, T., and Funae, Y. (2005b). Localization of rat cytochrome P450 in various tissues and comparison of arachidonic acid metabolism by rat P450 with that by human P450 orthologs. Drug Metab. Pharmacokinet. *20*: 478–84.

Imig, J.D. (2012). Epoxides and Soluble Epoxide Hydrolase in Cardiovascular Physiology. Physiol. Rev. *92*: 101–130.

Ishizuka, T., Cheng, J., Singh, H., Vitto, M.D., Manthati, V.L., Falck, J.R., et al. (2008). 20-Hydroxyeicosatetraenoic acid stimulates nuclear factor-kappaB activation and the production of inflammatory cytokines in human endothelial cells. J. Pharmacol. Exp. Ther. *324*: 103–10.

Ito, T., Suzuki, T., Tamura, K., Nezu, T., Honda, K., and Kobayashi, T. (2008). Examination of mRNA expression in rat hearts and lungs for analysis of effects of exposure to concentrated ambient particles on cardiovascular function. Toxicology *243*: 271–83.

Jenkins, C.M., Cedars, A., and Gross, R.W. (2009). Eicosanoid signalling pathways in the heart. Cardiovasc. Res. *82*: 240–9.

Jennings, B.L., Anderson, L.J., Estes, A.M., Yaghini, F.A., Fang, X.R., Porter, J., et al. (2012). Cytochrome P450 1B1 Contributes to Renal Dysfunction and Damage Caused by Angiotensin II in Mice. Hypertension *59*: 348–354.

Jennings, B.L., Sahan-Firat, S., Estes, A.M., Das, K., Farjana, N., Fang, X.R., et al. (2010). Cytochrome P450 1B1 Contributes to Angiotensin II-Induced Hypertension and Associated Pathophysiology. Hypertension *56*: 667–674.

Kabe, Y., Ando, K., Hirao, S., Yoshida, M., and Handa, H. (2005). Redox Regulation of NF-κB Activation: Distinct Redox Regulation Between the Cytoplasm and the Nucleus. Antioxid. Redox Signal. *7*: 395–403.

Kawano, S., Kubota, T., Monden, Y., Kawamura, N., Tsutsui, H., Takeshita, A., et al. (2005). Blockade of NF-kappaB ameliorates myocardial hypertrophy in response to chronic infusion of angiotensin II. Cardiovasc. Res. *67*: 689–98.

Kayama, Y., Minamino, T., Toko, H., Sakamoto, M., Shimizu, I., Takahashi, H., et al. (2009). Cardiac 12/15 lipoxygenase–induced inflammation is involved in heart failure. J. Exp. Med. *206*: 1565–1574.

Kaye, D.M., and Krum, H. (2007). Drug discovery for heart failure: a new era or the end of the pipeline? Nat. Rev. Drug Discov. *6*: 127–139.

Kennedy, S.W., Lorenzen, A., James, C.A., and Collins, B.T. (1993). Ethoxyresorufin-O-deethylase and porphyrin analysis in chicken embryo hepatocyte cultures with a fluorescence multiwell plate reader. Anal. Biochem. *211*: 102–12.

Kerzee, J.K., and Ramos, K.S. (2001). Constitutive and inducible expression of Cyp1a1 and Cyp1b1 in vascular smooth muscle cells: role of the Ahr bHLH/PAS transcription factor. Circ. Res. *89*: 573–82.

Kimes, B.W., and Brandt, B.L. (1976). Properties of a clonal muscle cell line from rat heart. Exp.

Cell Res. *98*: 367–81.

Kiriazis, H., and Kranias, E.G. (2000). Genetically Engineered Models with Alterations in Cardiac Membrane Calcium-Handling Proteins. Annu. Rev. Physiol. *62*: 321–351.

Konkel, A., and Schunck, W.-H. (2011). Role of cytochrome P450 enzymes in the bioactivation of polyunsaturated fatty acids. Biochim. Biophys. Acta - Proteins Proteomics *1814*: 210–222.

Korashy, H.M., and El-Kadi, A.O.S. (2006a). The Role of Aryl Hydrocarbon Receptor in the Pathogenesis of Cardiovascular Diseases. Drug Metab. Rev. *38*: 411–450.

Korashy, H.M., and El-Kadi, A.O.S. (2006b). The Role of Aryl Hydrocarbon Receptor in the Pathogenesis of Cardiovascular Diseases. Drug Metab. Rev. *38*: 411–450.

Lemieux, H., and Hoppel, C.L. (2009). Mitochondria in the human heart. J. Bioenerg. Biomembr. *41*: 99–106.

Levick, S.P., Loch, D.C., Taylor, S.M., and Janicki, J.S. (2007). Arachidonic acid metabolism as a potential mediator of cardiac fibrosis associated with inflammation. J. Immunol. *178*: 641–6.

Liu, Y., Peterson, D.A., Kimura, H., and Schubert, D. (1997). Mechanism of cellular 3-(4,5-dimethylthiazol-2-yl)-2,5-diphenyltetrazolium bromide (MTT) reduction. J. Neurochem. *69*: 581–93.

Livak, K.J., and Schmittgen, T.D. (2001). Analysis of relative gene expression data using real-time quantitative PCR and the 2(-Delta Delta C(T)) Method. Methods *25*: 402–8.

Lo, S.-N., Chang, Y.-P., Tsai, K.-C., Chang, C.-Y., Wu, T.-S., and Ueng, Y.-F. (2013). Inhibition of CYP1 by berberine, palmatine, and jatrorrhizine: selectivity, kinetic characterization, and molecular modeling. Toxicol. Appl. Pharmacol. *272*: 671–80.

Locher, M.R., Razumova, M. V, Stelzer, J.E., Norman, H.S., and Moss, R.L. (2011). Effects of low-level α-myosin heavy chain expression on contractile kinetics in porcine myocardium. Am. J. Physiol. Heart Circ. Physiol. *300*: H869-78.

LOWRY, O.H., ROSEBROUGH, N.J., FARR, A.L., and RANDALL, R.J. (1951). Protein measurement with the Folin phenol reagent. J. Biol. Chem. *193*: 265–75.

Maayah, Z.H., Abdelhamid, G., and El-Kadi, A.O.S. (2015a). Development of cellular hypertrophy by 8-hydroxyeicosatetraenoic acid in the human ventricular cardiomyocyte, RL-14 cell line, is implicated by MAPK and NF-κB. Cell Biol. Toxicol. *31*: 241–59.

Maayah, Z.H., Althurwi, H.N., Abdelhamid, G., Lesyk, G., Jurasz, P., and El-Kadi, A.O.S. (2016). CYP1B1 inhibition attenuates doxorubicin-induced cardiotoxicity through a mid-chain HETEs-dependent mechanism. Pharmacol. Res. *105*: 28–43.

Maayah, Z.H., Althurwi, H.N., El-Sherbeni, A.A., Abdelhamid, G., Siraki, A.G., and El-Kadi, A.O.S. (2017). The role of cytochrome P450 1B1 and its associated mid-chain hydroxyeicosatetraenoic acid metabolites in the development of cardiac hypertrophy induced by isoproterenol. Mol. Cell. Biochem. *429*: 151–165.

Maayah, Z.H., and El-Kadi, A.O.S. (2016a). 5-, 12- and 15-Hydroxyeicosatetraenoic acids induce cellular hypertrophy in the human ventricular cardiomyocyte, RL-14 cell line, through MAPK- and NF-κB-dependent mechanism. Arch. Toxicol. *90*: 359–373.

Maayah, Z.H., and El-Kadi, A.O.S. (2016b). The role of mid-chain hydroxyeicosatetraenoic acids in the pathogenesis of hypertension and cardiac hypertrophy. Arch. Toxicol. *90*: 119–36.

Maayah, Z.H., and El-Kadi, A.O.S. (2016c). The role of mid-chain hydroxyeicosatetraenoic acids

in the pathogenesis of hypertension and cardiac hypertrophy. Arch. Toxicol. *90*: 119–136.

Maayah, Z.H., Elshenawy, O.H., Althurwi, H.N., Abdelhamid, G., and El-Kadi, A.O.S. (2015b). Human fetal ventricular cardiomyocyte, RL-14 cell line, is a promising model to study drug metabolizing enzymes and their associated arachidonic acid metabolites. J. Pharmacol. Toxicol. Methods *71*: 33–41.

Maayah, Z.H., Levasseur, J., Siva Piragasam, R., Abdelhamid, G., Dyck, J.R.B., Fahlman, R.P., et al. (2018). 2-Methoxyestradiol protects against pressure overload-induced left ventricular hypertrophy. Sci. Rep. *8*: 2780.

Malik, K.U., Jennings, B.L., Yaghini, F.A., Sahan-Firat, S., Song, C.Y., Estes, A.M., et al. (2012a). Contribution of cytochrome P450 1B1 to hypertension and associated pathophysiology: A novel target for antihypertensive agents. Prostaglandins Other Lipid Mediat. *98*: 69–74.

Malik, K.U., Jennings, B.L., Yaghini, F.A., Sahan-Firat, S., Song, C.Y., Estes, A.M., et al. (2012b). Contribution of cytochrome P450 1B1 to hypertension and associated pathophysiology: A novel target for antihypertensive agents. Prostaglandins Other Lipid Mediat. *98*: 69–74.

Martínez-Jiménez, C.P., Jover, R., Donato, M.T., Castell, J. V, and Gómez-Lechón, M.J. (2007). Transcriptional regulation and expression of CYP3A4 in hepatocytes. Curr. Drug Metab. *8*: 185–94.

Martinez, R., Malta, M.H., Verceze, A. V, and Arantes, M.R. (1999). Comparative efficacy of fluconazole and amphotericin B in the parenteral treatment of experimental paracoccidioidomycosis in the rat. Mycopathologia *146*: 131–4.

McCallum, G.P., Horton, J.E., Falkner, K.C., and Bend, J.R. (1993). Microsomal cytochrome P450

1A1 dependent monooxygenase activity in guinea pig heart: induction, inhibition, and increased activity by addition of exogenous NADPH-cytochrome P450 reductase. Can. J. Physiol. Pharmacol. *71*: 151–6.

Michaud, V., Frappier, M., Dumas, M.-C., and Turgeon, J. (2010). Metabolic activity and mRNA levels of human cardiac CYP450s involved in drug metabolism. PLoS One *5*: e15666.

Minamiyama, Y., Takemura, S., Akiyama, T., Imaoka, S., Inoue, M., Funae, Y., et al. (1999). Isoforms of cytochrome P450 on organic nitrate-derived nitric oxide release in human heart vessels. FEBS Lett. *452*: 165–9.

Molkentin, J.D. (2004). Calcineurin-NFAT signaling regulates the cardiac hypertrophic response in coordination with the MAPKs. Cardiovasc. Res. *63*: 467–75.

Molkentin, J.D., Lu, J.R., Antos, C.L., Markham, B., Richardson, J., Robbins, J., et al. (1998). A calcineurin-dependent transcriptional pathway for cardiac hypertrophy. Cell *93*: 215–28.

Morisseau, C., and Hammock, B.D. (2007). Measurement of Soluble Epoxide Hydrolase (sEH) Activity. In Current Protocols in Toxicology, (Hoboken, NJ, USA: John Wiley & Sons, Inc.), p Unit 4.23.

Muslin, A.J. (2005). Role of Raf Proteins in Cardiac Hypertrophy and Cardiomyocyte Survival. Trends Cardiovasc. Med. *15*: 225–229.

Nadal-Ginard, B., Kajstura, J., Leri, A., and Anversa, P. (2003). Myocyte death, growth, and regeneration in cardiac hypertrophy and failure. Circ. Res. *92*: 139–50.

Nakamura, K., Fushimi, K., Kouchi, H., Mihara, K., Miyazaki, M., Ohe, T., et al. (1998). Inhibitory effects of antioxidants on neonatal rat cardiac myocyte hypertrophy induced by tumor

necrosis factor-alpha and angiotensin II. Circulation *98*: 794–9.

Nieves, D., and Moreno, J.J. (2006). Hydroxyeicosatetraenoic acids released through the cytochrome P-450 pathway regulate 3T6 fibroblast growth. J. Lipid Res. *47*: 2681–9.

Nithipatikom, K., Grall, A.J., Holmes, B.B., Harder, D.R., Falck, J.R., and Campbell, W.B. (2001). Liquid chromatographic-electrospray ionization-mass spectrometric analysis of cytochrome P450 metabolites of arachidonic acid. Anal. Biochem. *298*: 327–36.

Nozawa, K., Tuck, M.L., Golub, M., Eggena, P., Nadler, J.L., and Stern, N. (1990). Inhibition of lipoxygenase pathway reduces blood pressure in renovascular hypertensive rats. Am. J. Physiol. *259*: H1774-80.

Okita, R.T., and Okita, J.R. (2001). Cytochrome P450 4A fatty acid omega hydroxylases. Curr. Drug Metab. *2*: 265–81.

Parmentier, J.H., Muthalif, M.M., Saeed, A.E., and Malik, K.U. (2001). Phospholipase D activation by norepinephrine is mediated by 12(s)-, 15(s)-, and 20-hydroxyeicosatetraenoic acids generated by stimulation of cytosolic phospholipase a2. tyrosine phosphorylation of phospholipase d2 in response to norepinephrine. J. Biol. Chem. *276*: 15704–11.

Pearson, G., Robinson, F., Beers Gibson, T., Xu, B., Karandikar, M., Berman, K., et al. (2001). Mitogen-Activated Protein (MAP) Kinase Pathways: Regulation and Physiological Functions [1]. Endocr. Rev. *22*: 153–183.

Poulos, T.L. (2005). Intermediates in P450 catalysis. Philos. Trans. A. Math. Phys. Eng. Sci. *363*: 793-806; discussion 1035–40.

Public Health Agency of Canada (2018). No Title.

Purcell, N.H., Tang, G., Yu, C., Mercurio, F., DiDonato, J.A., and Lin, A. (2001). Activation of NF-kappa B is required for hypertrophic growth of primary rat neonatal ventricular cardiomyocytes. Proc. Natl. Acad. Sci. U. S. A. *98*: 6668–73.

Revermann, M., Mieth, A., Popescu, L., Paulke, A., Wurglics, M., Pellowska, M., et al. (2011). A pirinixic acid derivative (LP105) inhibits murine 5-lipoxygenase activity and attenuates vascular remodelling in a murine model of aortic aneurysm. Br. J. Pharmacol. *163*: 1721–32.

Roger, V.L. (2013). Epidemiology of heart failure. Circ. Res. *113*: 646–59.

Rohini, A., Agrawal, N., Koyani, C.N., and Singh, R. (2010a). Molecular targets and regulators of cardiac hypertrophy. Pharmacol. Res. *61*: 269–280.

Rohini, A., Agrawal, N., Koyani, C.N., and Singh, R. (2010b). Molecular targets and regulators of cardiac hypertrophy. Pharmacol. Res. *61*: 269–280.

Roman, R.J. (2002). *P* -450 Metabolites of Arachidonic Acid in the Control of Cardiovascular Function. Physiol. Rev. *82*: 131–185.

Rose, B.A., Force, T., and Wang, Y. (2010). Mitogen-activated protein kinase signaling in the heart: angels versus demons in a heart-breaking tale. Physiol. Rev. *90*: 1507–46.

Sanna, B., Bueno, O.F., Dai, Y.-S., Wilkins, B.J., and Molkentin, J.D. (2005). Direct and indirect interactions between calcineurin-NFAT and MEK1-extracellular signal-regulated kinase 1/2 signaling pathways regulate cardiac gene expression and cellular growth. Mol. Cell. Biol. *25*: 865–78.

Schlüter, K.-D., and Schreiber, D. (2005). Adult ventricular cardiomyocytes: isolation and culture. Methods Mol. Biol. *290*: 305–14.

See, F., Thomas, W., Way, K., Tzanidis, A., Kompa, A., Lewis, D., et al. (2004). p38 mitogen-activated protein kinase inhibition improves cardiac function and attenuates left ventricular remodeling following myocardial infarction in the rat. J. Am. Coll. Cardiol. *44*: 1679–1689.

Shimada, T., Sugie, A., Shindo, M., Nakajima, T., Azuma, E., Hashimoto, M., et al. (2003). Tissue-specific induction of cytochromes P450 1A1 and 1B1 by polycyclic aromatic hydrocarbons and polychlorinated biphenyls in engineered C57BL/6J mice of arylhydrocarbon receptor gene. Toxicol. Appl. Pharmacol. *187*: 1–10.

Shoieb, S.M., and El-Kadi, A.O.S. (2018). S-Enantiomer of 19-Hydroxyeicosatetraenoic Acid Preferentially Protects Against Angiotensin II-Induced Cardiac Hypertrophy. Drug Metab. Dispos. *46*: 1157–1168.

Somchit, N., Norshahida, A.R., Hasiah, A.H., Zuraini, A., Sulaiman, M.R., and Noordin, M.M. (2004). Hepatotoxicity induced by antifungal drugs itraconazole and fluconazole in rats: a comparative in vivo study. Hum. Exp. Toxicol. *23*: 519–25.

Somchit, N., Wong, C.W., Zuraini, A., Ahmad Bustamam, A., Hasiah, A.H., Khairi, H.M., et al. (2006). Involvement of phenobarbital and SKF 525A in the hepatotoxicity of antifungal drugs itraconazole and fluconazole in rats. Drug Chem. Toxicol. *29*: 237–53.

Sun, G., Thai, S.-F., Lambert, G.R., Wolf, D.C., Tully, D.B., Goetz, A.K., et al. (2006). Fluconazole-induced hepatic cytochrome P450 gene expression and enzymatic activities in rats and mice. Toxicol. Lett. *164*: 44–53.

Tacconelli, S., and Patrignani, P. (2014). Inside epoxyeicosatrienoic acids and cardiovascular disease. Front. Pharmacol. *5*: 239.

Thannickal, V.J., and Fanburg, B.L. (2000). Reactive oxygen species in cell signaling. Am. J. Physiol. Lung Cell. Mol. Physiol. *279*: L1005-28.

Thum, T., and Borlak, J. (2000). Cytochrome P450 mono-oxygenase gene expression and protein activity in cultures of adult cardiomyocytes of the rat. Br. J. Pharmacol. *130*: 1745–52.

Thum, T., and Borlak, J. (2002). Testosterone, cytochrome P450, and cardiac hypertrophy. FASEB J. *16*: 1537–49.

Tran, D.T., Ohinmaa, A., Thanh, N.X., Howlett, J.G., Ezekowitz, J.A., McAlister, F.A., et al. (2016). The current and future financial burden of hospital admissions for heart failure in Canada: a cost analysis. C. Open *4*: E365–E370.

Tse, M.M.Y., Aboutabl, M.E., Althurwi, H.N., Elshenawy, O.H., Abdelhamid, G., and El-Kadi, A.O.S. (2013a). Cytochrome P450 epoxygenase metabolite, 14,15-EET, protects against isoproterenol-induced cellular hypertrophy in H9c2 rat cell line. Vascul. Pharmacol. *58*: 363–73.

Tse, M.M.Y., Aboutabl, M.E., Althurwi, H.N., Elshenawy, O.H., Abdelhamid, G., and El-Kadi, A.O.S. (2013b). Cytochrome P450 epoxygenase metabolite, 14,15-EET, protects against isoproterenol-induced cellular hypertrophy in H9c2 rat cell line. Vascul. Pharmacol. *58*: 363–73.

Urano, F., Wang, X., Bertolotti, A., Zhang, Y., Chung, P., Harding, H.P., et al. (2000). Coupling of stress in the ER to activation of JNK protein kinases by transmembrane protein kinase IRE1. Science *287*: 664–6.

USFDA (2013). Guidance for Industry Drug interaction studies—study design, data analysis, implications for dosing, and labeling recommendation.

Wang, X., Ni, L., Yang, L., Duan, Q., Chen, C., Edin, M.L., et al. (2014). CYP2J2-derived

epoxyeicosatrienoic acids suppress endoplasmic reticulum stress in heart failure. Mol. Pharmacol. *85*: 105–15.

Wassmann, S., Laufs, U., Bäumer, A.T., Müller, K., Konkol, C., Sauer, H., et al. (2001). Inhibition of geranylgeranylation reduces angiotensin II-mediated free radical production in vascular smooth muscle cells: involvement of angiotensin AT1 receptor expression and Rac1 GTPase. Mol. Pharmacol. *59*: 646–54.

Weber, K.T., and Brilla, C.G. (1991). Pathological hypertrophy and cardiac interstitium. Fibrosis and renin-angiotensin-aldosterone system. Circulation *83*: 1849–65.

Weber, K.T., and Brilla, C.G. (1993). Structural basis for pathologic left ventricular hypertrophy. Clin. Cardiol. *16*: II10-4.

Welch, W.J. (2008). Angiotensin II-Dependent Superoxide: Effects on Hypertension and Vascular Dysfunction. Hypertension *52*: 51–56.

Wen, Y., Gu, J., Peng, X., Zhang, G., and Nadler, J. (2003). Overexpression of 12-lipoxygenase and cardiac fibroblast hypertrophy. Trends Cardiovasc. Med. *13*: 129–36.

Westphal, C., Konkel, A., and Schunck, W.-H. (2015). Cytochrome P450 Enzymes in the Bioactivation of Polyunsaturated Fatty Acids and Their Role in Cardiovascular Disease. In Advances in Experimental Medicine and Biology, pp 151–187.

Westphal, C., Spallek, B., Konkel, A., Marko, L., Qadri, F., DeGraff, L.M., et al. (2013). CYP2J2 overexpression protects against arrhythmia susceptibility in cardiac hypertrophy. PLoS One *8*: e73490.

Wilkins, B.J., and Molkentin, J.D. (2004). Calcium–calcineurin signaling in the regulation of

cardiac hypertrophy. Biochem. Biophys. Res. Commun. *322*: 1178–1191.

Wong, E.T., and Tergaonkar, V. (2009). Roles of NF-κB in health and disease: mechanisms and therapeutic potential. Clin. Sci. *116*: 451–465.

Xu, D., Li, N., He, Y., Timofeyev, V., Lu, L., Tsai, H.-J., et al. (2006). Prevention and reversal of cardiac hypertrophy by soluble epoxide hydrolase inhibitors. Proc. Natl. Acad. Sci. U. S. A. *103*: 18733–8.

Zafari, A.M., Ushio-Fukai, M., Minieri, C.A., Akers, M., Lassègue, B., and Griendling, K.K. (1999). Arachidonic acid metabolites mediate angiotensin II-induced NADH/NADPH oxidase activity and hypertrophy in vascular smooth muscle cells. Antioxid. Redox Signal. *1*: 167–79.

Zhang, L., Li, Y., Chen, M., Su, X., Yi, D., Lu, P., et al. (2014). 15-LO/15-HETE mediated vascular adventitia fibrosis via p38 MAPK-dependent TGF-β. J. Cell. Physiol. *229*: 245–57.

Zhang, W., Elimban, V., Nijjar, M.S., Gupta, S.K., and Dhalla, N.S. (2003). Role of mitogen-activated protein kinase in cardiac hypertrophy and heart failure. Exp. Clin. Cardiol. *8*: 173–83.

Zhao, Z., Geng, J., Ge, Z., Wang, W., Zhang, Y., and Kang, W. (2009). Activation of ERK5 in angiotensin II-induced hypertrophy of human aortic smooth muscle cells. Mol. Cell. Biochem. *322*: 171–178.

Zordoky, B.N.M., Aboutabl, M.E., and El-Kadi, A.O.S. (2008). Modulation of Cytochrome P450 Gene Expression and Arachidonic Acid Metabolism during Isoproterenol-Induced Cardiac Hypertrophy in Rats. Drug Metab. Dispos. *36*: 2277–2286.

Zordoky, B.N.M., and El-Kadi, A.O.S. (2007). H9c2 cell line is a valuable in vitro model to study the drug metabolizing enzymes in the heart. J. Pharmacol. Toxicol. Methods *56*: 317–22.

Zordoky, B.N.M., and El-Kadi, A.O.S. (2008a). Modulation of cardiac and hepatic cytochrome P450 enzymes during heart failure. Curr. Drug Metab. *9*: 122–8.

Zordoky, B.N.M., and El-Kadi, A.O.S. (2008b). Modulation of cardiac and hepatic cytochrome P450 enzymes during heart failure. Curr. Drug Metab. *9*: 122–8.

Zu, L., Guo, G., Zhou, B., and Gao, W. (2016). Relationship between metabolites of arachidonic acid and prognosis in patients with acute coronary syndrome. Thromb. Res. *144*: 192–201.